Economic Geology, v. 105, pp. 1191–1241

Evolution of Calc-Alkaline Volcanism and Associated Hydrothermal Gold Deposits at Yanacocha, Peru**

Anthony A. Longo,†,1,* John H. Dilles,2 Anita L. Grunder,2 and Robert Duncan3

[1]*Department of Geosciences, Oregon State University, Corvallis, Oregon 97370 and Minera Yanacocha and Newmont Mining Corporation, Cajamarca, Peru*

[2]*Department of Geosciences, Oregon State University, Corvallis, Oregon 97370*

[3]*College of Oceanic and Atmospheric Sciences, Oregon State University Corvallis, Oregon 97370*

Abstract

Clusters of high-sulfidation epithermal deposits containing more than 50 Moz of gold are hosted by advanced argillic-altered Miocene volcanic rocks in the Yanacocha district, northern Peru (lat. 6°59'30" S, long. 78°30'45" W). We describe the nature of the volcanism and its relation to the gold ores on the basis of new district-scale geologic mapping, 69 $^{40}Ar/^{39}Ar$ ages on igneous rocks and hydrothermal alunite, and petrologic and geochemical investigations.

Volcanic rocks of the Calipuy Group are the oldest Cenozoic rocks at Yanacocha, and include the Huambo Cancha andesite, andesitic lahars of Tual and Chaupiloma (19.5–15.9 Ma), and the dacitic Cerro Fraile pyroclastics (15.5–15.1 Ma). The younger Yanacocha Volcanics (14.5–8.4 Ma) form a cogenetic series of lavas and pyroclastic rocks with a cumulative volume of ~88 km^3 that represents eruption from a moderate-size volcanic center. Early pyroxene>hornblende-bearing lavas of the Atazaico Andesite (14.5–13.3 Ma) erupted from small stratovolcanoes progressively younger from southwest to northeast. Dacitic dikes followed that are spatially associated with gold deposits at Quilish and Cerro Negro (~7 Moz Au) and stage 1 alunite (13.6–12.6 Ma). The Colorado Pyroclastics erupted in the center of the district and include the hornblende- and biotite-bearing andesitic to dacitic Cori Coshpa (12.6 Ma) and Maqui Maqui (12.5–12.4 Ma) ignimbrites. The Colorado Pyroclastics are overlain by hornblende>pyroxene-bearing andesitic to dacitic lavas, flow-domes, and minor pyroclastic rocks of the Azufre Andesite (12.1–11.6 Ma). Widespread stage 2 alunite (11.5 Ma) and minor gold deposition (~0.5 Moz) closely follow. The San Jose Ignimbrite (11.5–11.2 Ma) overlies the Azufre Andesite and stage 2 alunite and includes three members of hornblende-pyroxene (biotite) dacite and andesite that erupted in the center of the district and flowed southward. Mineralogically similar domes were emplaced into the inferred vents.

The Coriwachay Dacite (10.8–8.4 Ma) forms the youngest and most silica rich igneous rocks in the district, and includes intrusions and flow domes of dacite to rhyolite at Corimayo (10.8 Ma), Cerro Yanacocha (9.9 Ma), and Yanacocha Lake (8.4 Ma). Most of the gold (>47 Moz) was deposited at Yanacocha during intrusion of the late Coriwachay Dacite. These late dacites are volumetrically smallest (~2% of the total volume of erupted magma) and are temporally associated with stage 3 to 5 alunites. Stage 3 alunite (11.0–10.7 Ma) developed along a northeast trend for 9 km that includes the gold deposits of Corimayo, San Jose, Carachugo, and Maqui Maqui. The deeper Kupfertal Cu-Au porphyry has an age of 10.7 Ma on hydrothermal biotite and underlies zones of stage 4 and 5 quartz-alunite alternation that are 0.8 and 1.5 m.y. younger, respectively. Stage 4 alunite ranges in age from 10.2 to 10.3 Ma at the Tapado and Chaquicocha Sur gold deposits to Cerro Sugares east of the Maqui Maqui deposit. Stage 4 also includes a younger alunite age of 9.9 Ma from the San Jose gold deposit. Stage 5 alunite ranges from ~9.3 to ~8.2 Ma at Cerro Yanacocha, the largest gold deposit in the district. All these deposits contain massive and vuggy quartz, quartz-alunite, and quartz-pyrophyllite alteration associated with pyrite±enargite-tennantite-covellite.

Magmatism in the Yanacocha district lasted for ~11 m.y. The Yanacocha Volcanics spanned the last ~6 m.y. of this period and were associated with long-lived magmatic-hydrothermal activity and episodic gold mineralization. The Yanacocha calc-alkaline suite was oxidized, water and sulfate rich, and evolved from early pyroxene>hornblende andesite to late titanite-bearing dacite and minor rhyolite. Several dacites contain populations of both high- and low-aluminum hornblendes that crystallized in the middle and upper crust, respectively. The variation of Mg, Ti, P, Sr, and Ba contents in these rocks is consistent with a complex magmatic origin via both cooling, fractional crystallization, periodic recharge of deeply derived hydrous basaltic or andesitic melts, and mixing with silicic melts derived by crustal melting. Low eruption rates, high phenocryst contents of the volcanic rocks, and widespread hydrothermal alteration are consistent with the hypothesis that most of the magmas at Yanacocha crystallized in shallow chambers as granitoids that passively degassed ore fluids. The compositional diversity of the volcanic rocks together with an extended magmatic-hydrothermal history reflect complex magmatic processes that were optimum for producing the world-class gold deposits at Yanacocha.

*Present address: Department of Geoscience, University of Nevada Las Vegas, Las Vegas, Nevada 89154.

† Corresponding author: e-mail, longotal@gmail.com

**This paper contains an Appendix, found at the end of the paper, and a digital supplement. Appendix Table and Figure numbers are preceded by the letter A; digital figures and table are preceded by SD. The digital supplement is available at <http://www.geoscienceworld.org/> or, for subscribers, on the SEG website, <http://www.segweb.org>.

0361-0128/10/3919/1191-51

Submitted: February 22, 2010
Accepted: July 21, 2010

Introduction

SUBDUCTION-RELATED calc-alkaline volcanism or plutonism in a given area along continental margins globally is well documented for a duration of up to 5 m.y. and, in some cases, 11 m.y. (Marsh et al., 1997; Coleman et al., 2004; Grunder et al., 2008). Protracted magmatism leads to a self-organization of widespread magma batches that become more spatially focused, hydrous, oxidized, and silica-rich through time. Extensive hydrothermal alteration associated with porphyry and epithermal mineral deposits coincides broadly with late-stage, more centralized and more evolved magmatic activity (Dilles, 1987; Casselman et al., 1995).

The Yanacocha district is located in the northern Andes of Peru centered on lat. 6°59' 30" S and long. 78°30' 45" W, between 3,400 and 4,200 m in elevation, and 600 km north of Lima and 125 km east of the Pacific Ocean in the Department of Cajamarca (Fig. 1). The district is characterized by andesitic and dacitic volcanic rocks and subvolcanic intrusions that are broadly contemporaneous with genetically related epithermal high-sulfidation gold deposits hosted by advanced argillic alteration. Yanacocha belongs to the global association of high-sulfidation ore deposits with hydrous, calc-alkaline magmatism characterized by oxidized magnetite-series dacites (Deen et al., 1994; Arribas, 1995). Intermediate-composition magmas in this association are the source of magmatic-hydrothermal fluids that cause acidic alteration of rock and subsequent gold and copper-iron sulfide mineralization (Ransome, 1907; Steven and Ratté, 1960; Stoffregen, 1987; Arribas et al., 1995). High-sulfidation epithermal deposits worldwide are commonly characterized by alteration zones of vuggy residual quartz containing ore mineral assemblages with relatively high sulfur contents and sulfidation states within broad zones of alunite + quartz ± pyrophyllite ± diaspore ± dickite alteration. This alteration characterizes hypogene advanced argillic alteration that formed at relatively low temperature (~150°–350°C) from highly acidic, oxidized, and sulfur-rich hydrothermal fluids (Arribas, 1995; Hedenquist et al., 1998). These early acidic fluids enhanced the permeability and fluid-flow pathways prior to gold deposition by developing large stratiform and subvertical zones of residual quartz alteration (Sillitoe, 1999).

At Yanacocha, the magmatic record is well preserved in a volcanic field associated with numerous subvolcanic intrusions,

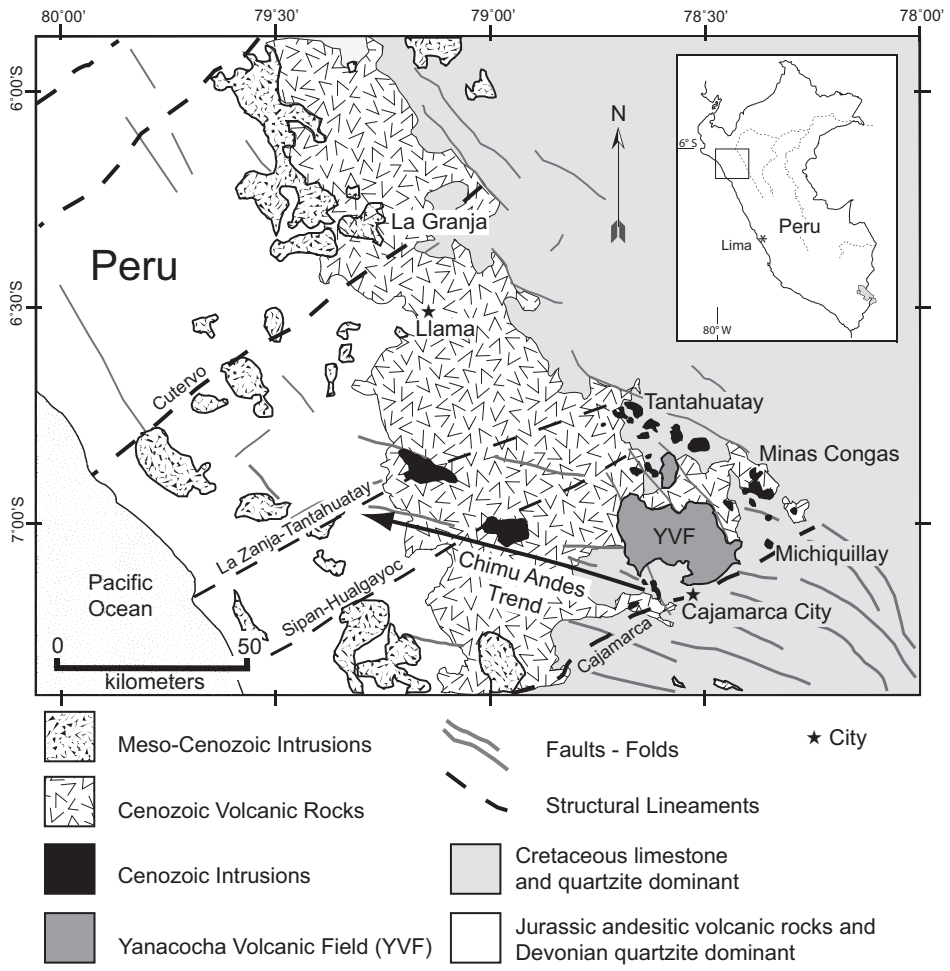

FIG. 1. Location map of the Yanacocha mining district in the Yanacocha Volcanic Field (YVF), northern Peru, showing key locations. Note the porphyry Cu-Au and other Au and base metal deposits that define a northwest trend from the Michiquillay and Minas Congas porphyry Cu-Au deposits, to the Tantahuatay high-sulfidation gold deposit and possibly to the La Granja porphyry Cu deposit.

and characterized by amphibole-bearing andesitic to dacitic magmas that were water rich and anhydrite bearing (Chambefort et al., 2008). On the basis of previous work, Miocene volcanism at Yanacocha spanned several million years, and was punctuated by several spatially and temporally distinct pulses of hydrothermal activity (Turner, 1997; Longo, 2005; Longo and Teal, 2005).

This paper presents the following: (1) the volcanic stratigraphy of the Yanacocha district based on new geologic mapping of ~1,000 km^2 exposures, (2) 69 $^{40}Ar/^{39}Ar$ ages from igneous and hydrothermal minerals and rocks, (3) the petrology of the igneous rocks based on major and trace element chemistry as well as mineralogy, and (4) the distribution and age of hydrothermally altered rocks in the district. We conclude the paper with a geologic model that identifies the spatial and temporal relationships of the volcanism and hydrothermal activity, and comment on the role of magmatic processes in forming giant magmatic-hydrothermal gold deposits. Teal and Benavides (2010) present geologic maps and interpretations developed independently of this study.

History of the Yanacocha mining district

Yanacocha is a world-class mining district with combined reserves, resources, and production that amount to >50 Moz of gold in oxidized ore from eight high-sulfidation epithermal deposits (Table 1). These deposits overlie a large, poorly measured gold and copper resource in sulfidic rocks that includes a Cu-Au porphyry (Myers and Williams, 2000; Teal et al., 2002; Bell et al., 2004). From the beginning of mining in 1993 until the end of 2009, the total ounces of gold from ore tons mined has exceeded 38 Moz (Table 1), making Yanacocha the most productive group of epithermal gold deposits in the world.

The district was first mined by native Peruvians during pre-Incan time (E. Maynard, pers. commun., 1998), and ancient pits were found at nearly every site where modern exploration discovered a gold deposit. In addition to mining native gold and cinnabar, pre-Inca and Inca peoples fashioned a technology for extracting clays and quartz for ceramics. The district was forgotten until 1968 when Nippon Mining explored three years for porphyry copper deposits by drilling 13 diamond drill holes at the site of the Kupfertal porphyry-style Cu-Au deposit near Cerro Yanacocha (Plate I). The British Geological Survey (1969–1971) subsequently detected metal anomalies at Yanacocha in a regional drainage geochemical survey, and in 1981, the CEDIMIN branch of the French government agency BRGM claimed the area and continued exploration (A.D. Quiroz, writ. commun., 1994; Benavides and Vidal, 1999).

Yanacocha was then explored by Newmont Peru Limited (NPL) (Table 1). Newmont geologists first visited the district in September 1983 and recommended acquisition. In 1984, CEDIMIN signed a joint venture agreement with Newmont and Buenaventura, and exploration directed by NPL began (Table 1). At this time, Yanacocha was classified as a volcanic-hosted, low-grade silver deposit and was considered a low priority. Drilling targeted two silver anomalies near Cerro Yanacocha and gold-bearing quartz-alunite veins at Yanacocha Norte. The drilling resulted in discovery of a non-economic silver deposit, and, more importantly, an interesting drill intercept with gold (7 m @ 9.6 g/t Au) at Yanacocha Norte. Exploration drilling continued, and by 1986, two zones rich in gold (1–17 g/t Au) were delineated at Yanacocha Norte and Sur. Systematic rock-chip geochemical surveys identified several gold anomalies throughout the district that included Cerro Quilish, San Jose, Carachugo, and Maqui Maqui. Drilling resulted in discovery of gold deposits at Carachugo in 1988 and Maqui Maqui in 1989–1990. Gold mining operations began in 1993 at Carachugo Sur. The first gold reserve of 1.3 Moz was announced by Minera Yanacocha, S.A. in 1992 (Table 1), and by the end of 1994 the combined reserve and resource increased to 8.1 Moz. The gold reserve and combined resource dramatically increased during the next five years, and peaked in 2000 at 36.6 Moz as geologists discovered 13 new gold deposits with >25 Moz in resource (Table 1). Annual gold production increased from 73,700 oz in 1993 to a peak of 3.33 Moz in 2005, and by 2010 cumulative gold production was 38.1 Moz (Table 1).

Local concern about contamination from the mining operation, fueled by the Choropampa mercury spill in 2000, led to numerous protests and road closures that forced Minera Yanacocha to relinquish all permits for exploration and development of the Quilish gold deposit. Exploration has been in steady decline since the spill, and restricted to areas nearby the active mines. The gold reserve and resource decreased to 10.5 Moz in 2010. The total gold mined (38.1 Moz) combined with the 2010 reserve and resource (10.5 Moz), and with the nonminable resources at Quilish and elsewhere (~6.5 Moz), provide the basis for our estimate of ~55 Moz for the total gold endowment of Yanacocha (Table 1).

Regional Geology

Structural setting

The Andean Cordillera displays a characteristic northwest structural trend in the Department of Cajamarca, but a major bend in the Cordillera, referred to as the Chimu Andes trend or Cajamarca Curvature (Benavides-Caceres, 1999), deflects the Mesozoic strata into a series of west- and west-northwest–trending fold axes and faults that project beneath the Yanacocha Volcanics (Figs. 1, 2; Reyes, 1980; Wilson, 1984). Prominent northeast-striking faults and fractures, oriented transverse to the Cordillera, define the Cutervo-Cajamarca structural zone and include the four major lineaments named Cajamarca, La Zanja-Tantahuatay, Sipan-Hualgayoc, and Cutervo (Fig. 1). The lineaments are associated with several significant metal deposits, of which the most southerly and important is Yanacocha. It lies within the Chicama-Yanacocha structural corridor (Quiroz, 1997; Turner, 1999). Approximately 20 km northeast of the Yanacocha district is a northwest-trending belt of eight porphyry Cu-Au deposits that appears to extend 100 km from Michiquillay to La Granja (Figs. 1, 2; Llosa et al., 1999; Diaz et al., 1997).

Tectonics and magmatism of northern Peru

Tectonic episodes of the Andean Cycle in Peru (Cobbing et al., 1981; Megard, 1984) began with the subduction of the Farallon plate in the early Mesozoic and have lasted for >200 m.y. (Petford and Atherton, 1995). Several episodes of compression and uplift, followed by various magmatic events and extension, shaped the Andes of northern Peru (Noble et al., 1990; Benavides-Caceres, 1999).

TABLE 1. Summary of Newmont's Exploration and Discovery History of the Yanacocha District from 1981 to 2009

Year	Significant events	Exploration	Discovery	Production[1]/ total gold[2] (Year-Moz Au)	Gold reserve[3] (year ending Moz Au)
1981	Newmont and Compania de Minas Buenaventura, S.A (BV) begin their association (A. Benavides, M. Nabighian, A. Pavard)	Newmont begins reviews of BV properties in central Peru			
1982	Newmont begins association with French government Bureau de Recherches Geologiques et Minieres (BRGM)[4] (A. Pavard, J. Claveau, J. Boulanger)	Newmont begins reviews of BRGM properties in Peru			
1983	BRGM suggests Newmont visit Yanacocha; Newmont geologist A. Bowerman visits and recommends acquisition				
1984	Newmont - BRGM decide to include the Peruvian mining company Buenaventura for political expediency, and sign a joint venture agreement: Newmont (40%), BRGM (40%), BV (20%)	Exploration begins with soil and trench samples near CerroYanacocha	Ag anomaly 260 g/t Ag, 2.5 g/t Au		
1985	Exploration around Cerro Yanacocha directed by A. Bowerman and A. Pavard	Systematic rock chip sampling begins. 21 reverse circulation (RC) drill holes in Ag anomaly and 6 diamond drill holes (DDH) in Yanacocha Norte	Non-economic silver deposit: 3.1 Mt @ 87 g/t Ag, 0.4 g/t Au Interesting drill intercept: 7 m @ 9.6 g/t Au at Yanacocha Norte		
1986-1987	Exploration at Cerro Yanacocha, San Jose, Carachugo, Maqui Maqui (A. Bowerman, A. Pavard, and M. Cardoso)	Systematic rock chip sampling expanded to Carachugo, San Jose, Maqui Maqui; 7 DDHs at Yanacocha Norte and Sur	Gold-rich (1–17 g/t Au) zones at Yanacocha Norte; DDH results: 122 m of 1.36 g/t Au (Yanacocha Norte); 297 m of 2.76 g/t Au (Yanacocha Sur).	A gold resource in massive quartz at Yanacocha Norte-Sur was considered non-leachable; exploration was abandoned until 1995	
1988-1989	Exploration at Carachugo and Maqui Maqui (A. Bowerman, M. Cardoso, A. Pavard)	9 DDHs at Carachugo Sur and Norte; Systematic rock chip sampling at Maqui Maqui	Carachugo Sur deposit, High grade found at Maqui Maqui Sur in rock chip samples		0.45
1990-1994	Mining operations began at Carachugo Sur, Exploration directed by M. Cardoso. Minera Yanacocha, S.A.[5] joint venture created in 1992: Newmont (38%), BV (32.3%), BRGM (24.7%), and the International Finance Corporation (5%)	District-wide systematic rock chip sampling continued; RC scout drilling at Cerro Quilish, San Jose Norte, Cerro Negro, Carachugo Este, Maqui Maqui Norte; resource drilling at Maqui Maqui Sur and Carachugo Norte	Deposits: Maqui Maqui Sur, Carachugo Norte Anomalies: Chaquicocha Norte, Cerro Quilish, Cerro Negro, San Jose, Maqui Maqui Norte, and Encajon	1993: 0.074/0.127 1994: 0.305/0.468	1992: 1.28 1994: 3.97 1994: 8.144
1995-1997	Systematic district wide exploration begins directed by B. Harvey, who utilizes "geologic folio" approach; focus on peer-reviewed field geology	Pre-1994 anomalies revisited, extensive geologic mapping, rock chip sampling and core drilling; gold found in alluvium at La Quinua; moraine exploration began district-wide	Deposits: Yanacocha Norte, Yanacocha Sur, Encajon, Chaquicocha Norte, San Jose Sur, Cerro Negro, Tapado, La Quinua gravels; anomalies: Maqui Maqui and Sacsha gravels (200–300 Koz), Colorado	1995: 0.552/0.81 1996: 0.811/1.08 1997: 1.05/1.27	1997: 8.98 Reserve+resource 1997 ~20

TABLE 1. *(Cont.)*

Year	Significant events	Exploration	Discovery	Production[1]/ total gold[2] (Year-Moz Au)	Gold reserve[3] (year ending Moz Au)
1998-2000	District-wide geologic reinterpretation, geologic modeling, and exploration directed by S. Myers; BRGM loses a 4-year legal battle in the Peruvian Supreme Court resulting in the current ownership of Minera Yanacocha: Newmont (51.35%), BV (43.65%), International Finance Corporation (5%); Choropampa mercury spill	Systematic district-wide, folio-driven exploration continues using new exploration models and target concepts; drilling begins at Corimayo and Quecher, and continues at Cerro Quilish and Chaquicocha Sur	Deposits: Chaquicocha Sur, Corimayo, Quecher, Arnacocha, and bonanza gold at Chaquicocha Alta Anomaly: Kupfertal porphyry, Antonio	1998–1.36/1.90 1999–1.67/2.27 2000–1.80/2.57	2000: ~8.0 Reserve+resource 2000 36.55
2001-2009	Permits for exploration and development of the Cerro Quilish deposit are relinquished because of local concerns and protests of contamination (fueled by the mercury spill); Antonio deposit downgraded from probable to indicated resource	Exploration activity declines due to increased protest by the local communities	Deposit: Antonio, small discoveries (100–200 Koz) Sacsha gravels at San Jose (200 Koz increased to >1 Moz)	2001: 1.90/2.54 2002–2005: 13.39/14.78 2006–2009: 8.04/10.24 2010[6]: 1.13/1.34	Reserve+resource 2001: 34.17 2009: 10.50

Notes: Production data presented in Table 1 were obtained from the published operating statistics in Newmont Mining Corporation, Form 10K, annual reports; production data from 1993 to 1998 were obtained from L. Leng, writ. commun., 1999; and D. Hall, writ. commun., 2000; references for exploration and discovery history: 1981–1993; A. Pavard and A. Bowerman, writ. commun., 1994; and 1994–2009; Harvey et al., 1999; Myers and Williams, 2000; S. Myers, pers. commun., 2009; B. Arkell, pers. commun., 2009; cf. Teal and Benavides, 2010

[1]Production is the total annual production as a function of gold grades for oxide and refractory ore and their recoveries as reported by Newmont, Form 10K annual reports; oxide gold grades ranged from 0.018 to 0.039 opt Au (avg ~0.03 opt Au), refractory gold grades were 0.08 to 0.12 opt Au, and recoveries ranged from 67 to 90%

[2]Total gold is reported as total ounces of contained gold in the ore tons mined, and calculated as the sum of the products of the annual mined ore tonnage (Mt, million dry short tons processed for leach and mill) to their respective average gold grade (oz/ton); this calculation is not a function of gold recoveries and, therefore, is the preferred estimate for the total gold endowment at Yanacocha; a total of 38.1 Moz gold in ore tons was mined from 1993 to 2009, and combined with the 2009 reserve+resource of 10.5 Moz and an estimated 6 Moz reserve+resource for the Quilish deposit (taken out of reserve in 2001), is the basis for the total gold endowment for Yanacocha of ~55 Moz (as presented in Table 6 and Fig. 17)

[3]Gold reserves are the proven and probable reserves reported by Newmont, Form 10-K, 1993–2010, Greenwood Village, Colorado; these calculations are based on economics that range from a pre-2004 gold price of $300/oz to $800/oz gold price used for 2009; reserve + resource include the proven and probable reserve combined with the indicated and inferred mineral resource

[4]In Peru, BRGM operated as CEDIMIN (Compania de Exploraciones, Desarrollo e Inversiones de Mineria), the Peruvian branch of the Bureau de Recherches Geologiques et Minieres

[5]Minera Yanacocha, S.A. was created in 1992 from a joint venture composed of Newmont (38%), Compania de Minas Buenaventura, S.A. (32.3%), BRGM (24.7%), and the International Finance Corporation (5%); in 1994, BRGM announced a plan to sell a portion of Yanacocha to the Australian company Normandy Mining; Newmont and Buenaventura immediately filed a law suit to stop the sale, launching the largest commercial litigation in Peruvian history (PBS Frontline/World, 2005); in 1998, BRGM lost a 4-year legal battle in the Peruvian Supreme Court, resulting in the current ownership of Minera Yanacocha, S.A. composed of Newmont (51.35%), Buenaventura (43.65%), and the International Finance Corporation (5%)

[6]Newmont 3rd quarter 2010 update, Regional Operating Statistics

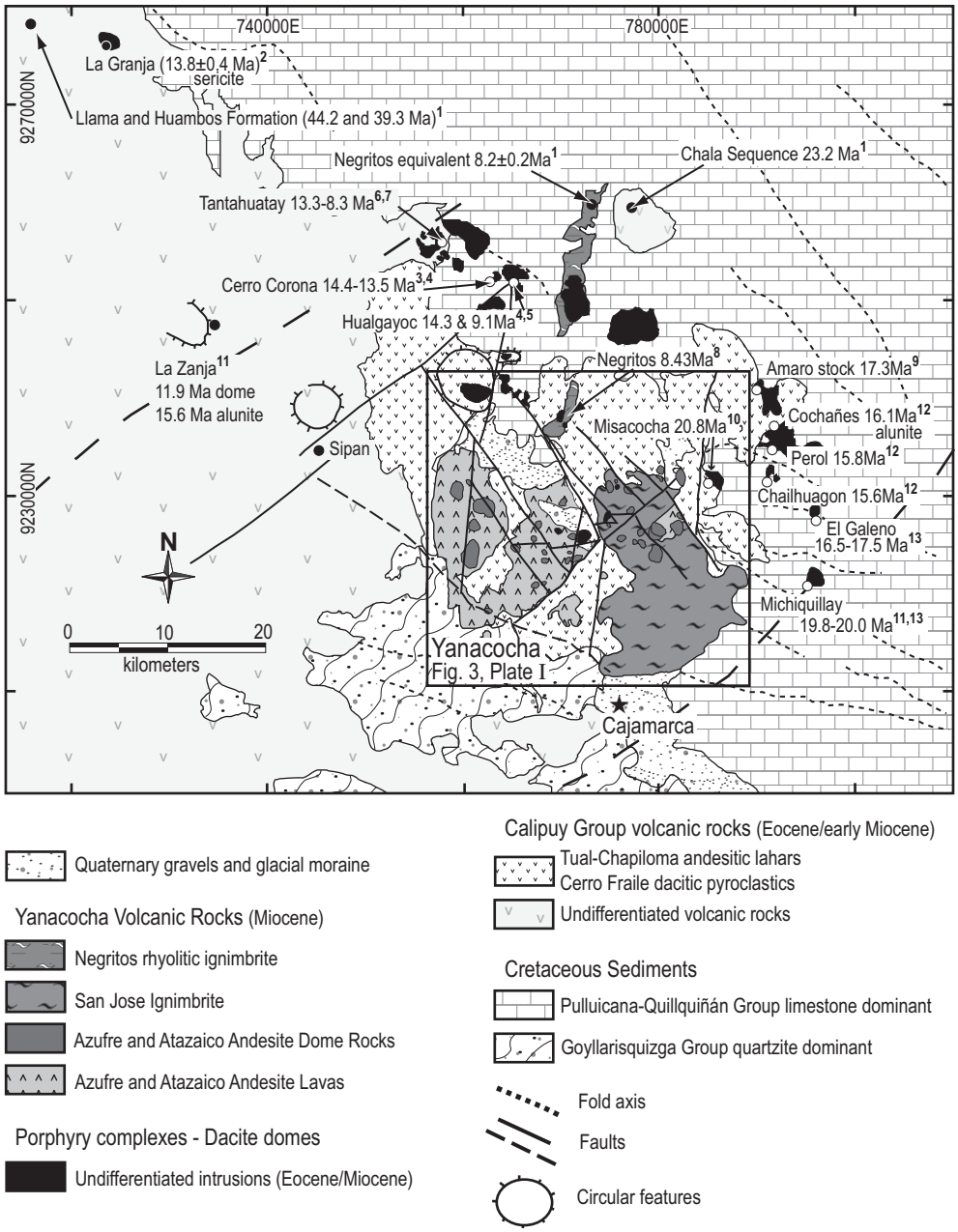

FIG. 2. Simplified geology map of northern Peru surrounding Yanacocha and Minas Congas, modified after Cobbing et al. (1981), with geology from Longo (2005). Locations and ages of (1) ores from mineral districts in the the structural corridor defined by the Cajamarca and La Zanja-Tantahuatay lineaments (gray dots) and (2) Cenozoic volcanic formations (black dots) are keyed by number 1 through 13 to sources in App. Table A1.

Cenozoic volcanism in northern Peru is marked by four episodes that began in the early Eocene (55 Ma) and ended in the late Miocene (8.4 Ma), based on $^{40}Ar/^{39}Ar$ and K-Ar ages (App. Table A1). Each magmatic episode was separated by a period of erosion marked by an unconformity. Volcanism in northern Peru began after the Incaic I orogeny in the early Eocene at ~ 55 Ma with eruptions of silicic ash-flow tuffs of the Llama Formation (Cobbing et al., 1981; Noble et al., 1990; Benavides-Caceres, 1999). Volcanism flared up again after the Incaic II orogeny (~44 Ma) with eruptions of volcanic rocks of the Porculla Formation and silicic ash-flow tuffs of the Huambos Formation (39-35 Ma; Noble et al., 1990; Fig. 2). Diorite stocks that crop out in the Minas Congas and Michiquillay districts span 4 m.y. in the middle Eocene, and may be roots of stratovolcanoes that erupted these volcanic rocks (Fig. 2; Table A1). During the Oligocene, northern Peru experienced volcanic quiescence that culminated in the Quechua I orogeny at ~23 Ma (Noble et al., 1974; McKee and Noble, 1982).

Arc volcanism reinitiated near Yanacocha following Quechua I deformation. Conglomerates, volcaniclastic rocks, and air-fall tuffs of the Chala sequence (23.2 Ma; Fig. 2) were

deposited in angular unconformity atop the Huambos Formation (Noble et al., 1990). Miocene volcanism near Yanacocha includes older andesites and dacites of the Calipuy Group volcanic rocks (19.5–15.5 Ma; this study) that are overlain by younger andesites and dacites of the Yanacocha Volcanics (14.5–8.4 Ma; this study). At ~8.4 Ma arc volcanism ceased near Yanacocha and is correlated with initiation of flat-slab tectonics and development of a volcanic gap between lat. 2° and 15° S in northern Peru (Gutscher et al., 1999).

Timing of regional magmatism and mineralization

Mineralization is broadly associated with Miocene magmatism in the Department of Cajamarca (Fig. 2; Table A1). Early to middle Miocene granitoid stocks, 20 km northeast of Yanacocha, span a ~5 m.y. interval (20.8–15.9 Ma). Stocks associated with Cu-Au porphyry ores have ages of potassium silicate alteration ranging from 20.6 to 15.4 Ma at Misacocha, Amaro, Perol, Chailhuagon, Galeno, and Michiquillay, and an age of alunite at Cochañes of 16.1 Ma. Middle Miocene magmatism in a ~25-km-long belt from Chailhuagon northwest to the Tantahuatay district is recorded by igneous ages from 14.4 to 8.3 Ma in the Tantahuatay, Cerro Corona, Hualgayoc, and La Zanja mineral districts, and by ages of hydrothermal activity that range from 15.6 to 11.0 Ma. High-sulfidation epithermal deposits in the Tantahuatay district overlap the magmatism and span a 2.3 m.y. interval from 13.3 to 11.0 Ma, ~0.2 m.y. younger than the porphyry Cu-Au mineralization ~6 km southeast at Cerro Corona (13.5 Ma).

Previous ages from Yanacocha

Previously reported isotopic ages partly outline the magmatic and hydrothermal events at Yanacocha (Table A1). Three K/Ar (Noble et al., 1990; D.C. Noble, pers. commun., 1997), three U/Pb zircon ages (Chariadia et al., 2009), and eight $^{40}Ar/^{39}Ar$ ages (n = 6; Turner, 1997; n = 2; Chariadia et al., 2009) range from 15.8 to 8.4 Ma for early to late Miocene volcanic rocks and intrusions. These data suggested a 3.4 m.y. gap in magmatic activity between 15.8 and 12.4 Ma. Previous ages of hydrothermal alunite were obtained only from the gold deposits in the northeastern part of the district (e.g., Carachugo, Fig. 3), and span 11.5 to 10.9 Ma (Turner, 1997; Harvey et al., 1999). Previous ages on late dacitic and rhyodacitic dikes range from 9.9 to 8.4 Ma (Turner, 1997; Chariadia et al., 2009). Turner (1997) proposed that early volcanic activity at Yanacocha spanned ~1 m.y., hydrothermal activity and gold deposition overlapped with the early volcanism and continued for another 0.5 m.y., and, after a ~1 m.y. gap, postmineral dacitic magmatism lasted an additional 1.5 m.y.

Yanacocha Geology, Ores, and Hydrothermal Alteration

Pre-Cenozoic rocks

Cenozoic volcanic rocks overlie Cretaceous limestone and marl of the Pulluicana-Quillquiñan Group and Cajamarca Formation, and older quartzite and argillite from the Goyllarisquizga Group on the margins of the Yanacocha district (Benavides, 1956; Cobbing et al., 1981; Wilson, 1984). Quartzite, black hornfels and argillite fragments found in the intrusions, pyroclastic rocks, and pebble dikes in the Yanacocha district suggest that these rocks lie at depth. Thick-bedded micritic limestone crops out northeast of the Maqui Maqui deposit and along the La Quinua fault in the central part of the district (Fig. 3, Plate I).

Cenozoic volcanic rocks

Miocene andesitic and dacitic volcanic rocks are up to 1,800 m thick, based on exposures, drill hole intercepts, and geophysical data (Goldie, 2000, 2002) in a 25 km diameter area centered on Yanacocha (Fig. 3, Plate I). Early to middle Miocene volcanic rocks, classified as the Calipuy Group (Reyes, 1980; Cobbing et al., 1981; Wilson, 1984), overlie the Pulluicana and Goyllarisquizga Group sedimentary units with angular unconformity (Fig. 4). The younger and more centrally focused Yanacocha Volcanics of middle Miocene age cover an area of ~350 km^2 that is slightly elongated in a northeast-southwest direction for 20 km (Figs. 1, 3; Plate I). The Yanacocha Volcanics are composed of andesitic and dacitic lavas, domes, ignimbrites, and minor subvolcanic intrusions, dikes, and breccias

Quaternary glaciation

Pleistocene glaciers extensively scoured and reshaped the volcanic geomorphology above 3,900 m elevation in the eastern parts of the Yanacocha district and produced polished and striated quartz-rich altered rocks on the highest peaks and in U-shaped valleys up to 300 m deep (Klein et al., 1999; Harvey et al., 1999; Longo, 2000, 2005). Moraines crop out at >3,700 m elevation and contain cobbles of advanced argillic altered volcanic rocks. Massive quartz and quartz alunite boulders are common. Detrital gold ore in the La Quinua gravel deposit (>10 Moz Au) was sourced from an eroded portion of Cerro Yanacocha (Williams and Vicuña, 2000; Mallette et al., 2004). Up to 300 m of rock was removed from the original paleosurface in the eastern parts of the Yanacocha district so that the present exposures represent deeper levels of the high-sulfidation epithermal systems.

Hydrothermal alteration and gold ores

The Yanacocha district consists of clusters of high-sulfidation epithermal gold deposits that occur in a N 50° E-trending zone of intense hydrothermal alteration 15 km long by up to 8 km wide and >100 km^2 in area (Plate I). The intense hydrothermal alteration hosts the gold ore and makes protolith identification and stratigraphic correlation extremely difficult (cf. Teal and Benavides, 2010).

In the center of the district, a corridor ~10 km^2 in area extends from Cerro Yanacocha through the San Jose, Carachugo, and Chaquicocha deposits (Figs. 3, 5A) and consists of rock that is nearly 100 percent altered to quartz (Longo, 2000, 2005). Quartz-rich rock at Yancocha, formed by intense hypogene acidic leaching of original igneous rocks (Steven and Ratté, 1960), displays a variety of textures that include massive quartz, vuggy quartz, granular quartz, and vuggy quartz partly replaced by granular quartz (Table 2; Supplementary data (SD) Figs. 1A-C). Quartz-rich rock occurs largely as gently dipping, tabular bodies 100 to 200 m thick that are broadly conformable to the volcanic stratigraphy (Harvey et al., 1999; Longo, 2000; Bell et al., 2004), but is also present as structurally controlled subvertical bodies, locally >450 m thick, that crosscut the stratigraphy (i.e., Chaquicocha Norte;

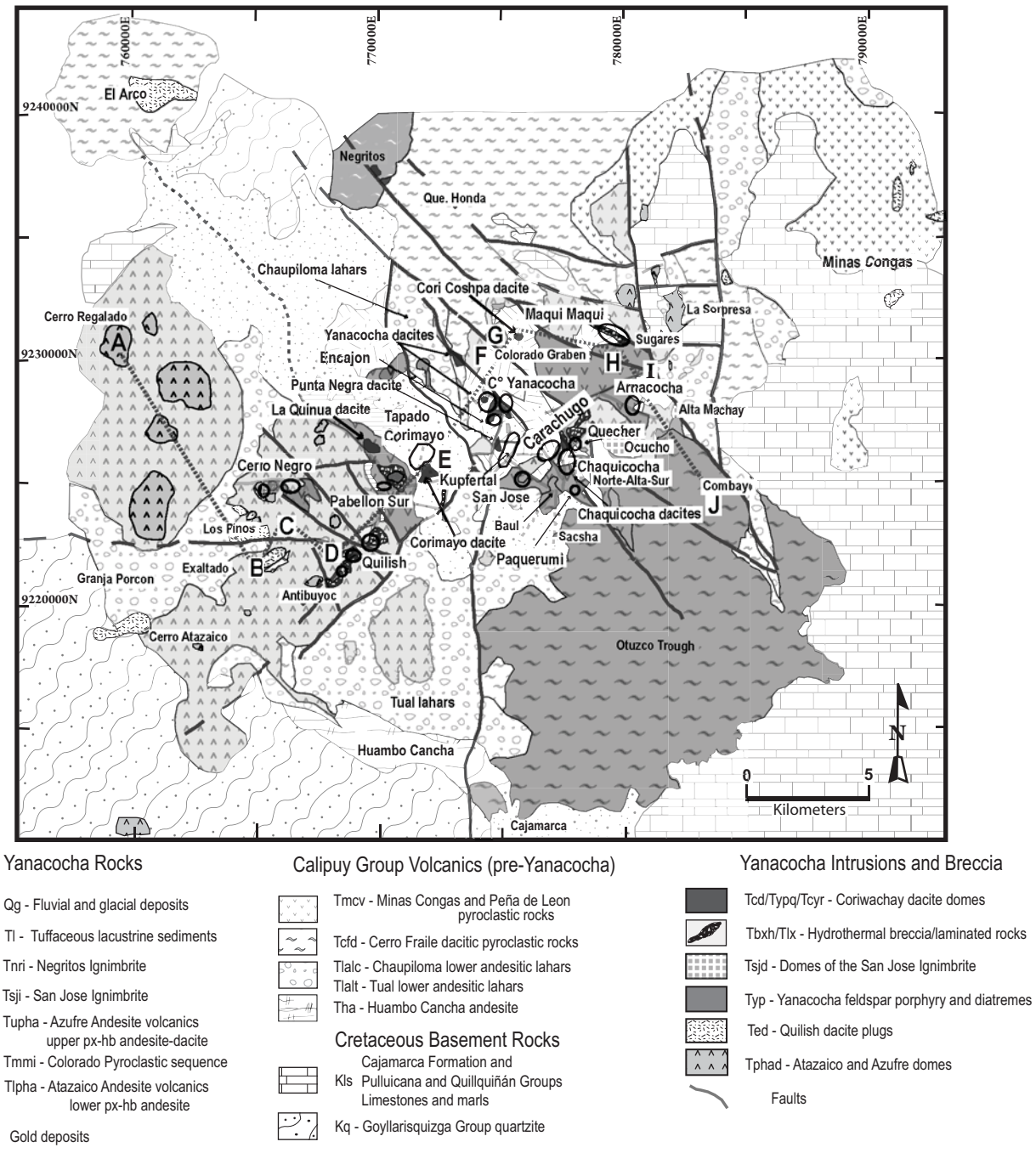

FIG. 3. Simplified geologic map of the Yanacocha district showing the locations of the gold deposits and names of selected localities discussed in the text. Pseudo-section line A-J shows the location of the stratigraphic columns in Figure 7.

Longo, 2000; Goldie, 2000). The quartz-rich rocks define a central alteration zone that is progressively enveloped by ~10- to 100-m-wide alteration zones of quartz-alunite ± pyrophyllite ± diaspore ± dickite ± kaolinite (advanced argillic), illite-smectite±pyrite (intermediate argillic), and a distal and weakly developed zone of chlorite-illite-smectite-calcite (propylitic) (Table 2; Harvey et al., 1999; Myers and Williams, 2000; Bell et al., 2004).

Gold ore commonly contains higher grades (>2 g/t Au) in steeply dipping structural zones of fractured massive and vuggy quartz that are enclosed within larger tabular zones of quartz-rich alteration with lower gold grades (~0.2–1 g/t Au; Harvey et al., 1999; Longo, 2000; Myers and Williams, 2000; Teal et al., 2002). Gold ore with typical grades of 1 to 2 g/t is hosted in quartz-rich altered rocks that originally contained hypogene sulfides (Table 2), subsequently oxidized by supergene processes. Supergene oxidation within some structural zones reached depths of >400 m (Harvey et al., 1999; Goldie, 2000, 2002; Myers and Williams, 2000; Longo, 2000; Bell et al., 2004). The central oxidized, quartz-rich zones generally

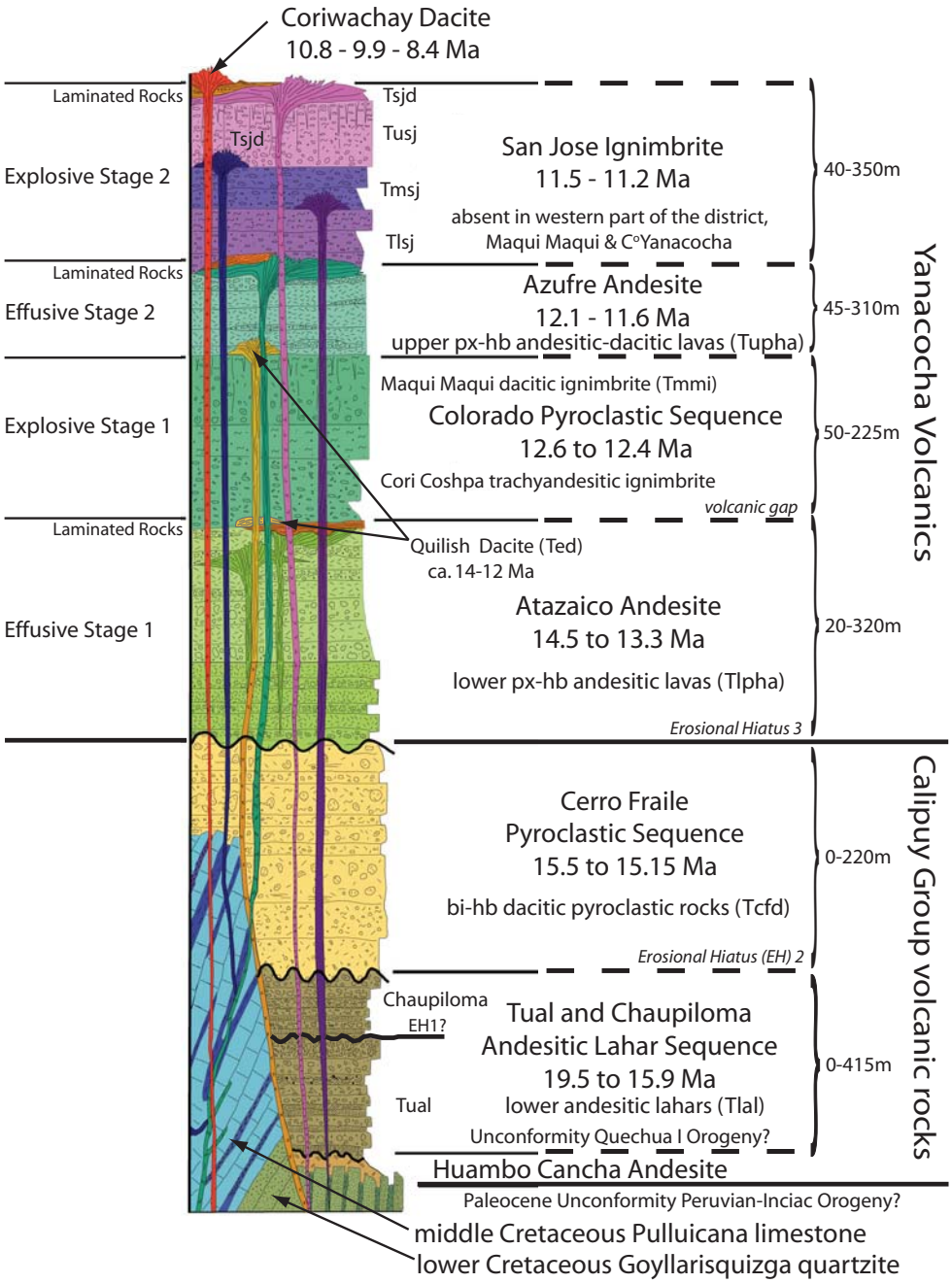

FIG. 4. Generalized stratigraphic column for the Yanacocha district showing lithologic units of Miocene Calipuy Group volcanics and Yanacocha Volcanics, their age range based on $^{40}Ar/^{39}Ar$ determinations, and range of thicknesses. Dikes and domes are shown schematically in correct stratigraphic or age position. Abbreviations: bi = biotite, hb = hornblende, px = pyroxene.

have the highest average gold grades (>2.5 g/t) and host local bonanza-grade gold ore (up to 540 g/t), where paragenetically late, coarse visible gold is intergrown with barite or quartz in vugs and along high-angle fractures that crosscuts quartz-rich rock. It is also associated with massive botryoidal limonite, rare Sn-rich hydrous iron oxide, and locally cream-colored porcellaneous chalcedony with rutile.[1]

[1] Creamy chalcedony at Rodalquilar is interpreted as an oxidation product of chalcedony containing fine-grained hypogene sulfides and bonanza gold (Arribas et al., 1995), and at Yanacocha it is termed *silice pardo* (Gomez, 2002; Bell et al., 2004).

At depths below supergene oxidation, sulfide ore zones contain covellite-enargite-pyrite ± chalcocite (Harvey et al., 1999; Goldie, 2000; Bell et al., 2004). Higher gold grades (>5 g/t) are associated with pyrite-tennantite-covellite-gold ± barite ± orpiment ± native sulfur, and apparently formed during the last stage of hydrothermal mineralization (Longo, 2000). Grains of coarse visible gold (up to 1 mm in size) are adjacent to pyrite veinlets replaced with tennantite in zones grading >25 g/t Au. The ore-related minerals discussed above commonly also fill cavities and fractures in the quartz-rich zones, and therefore, locally postdate the principal wall-rock alteration.

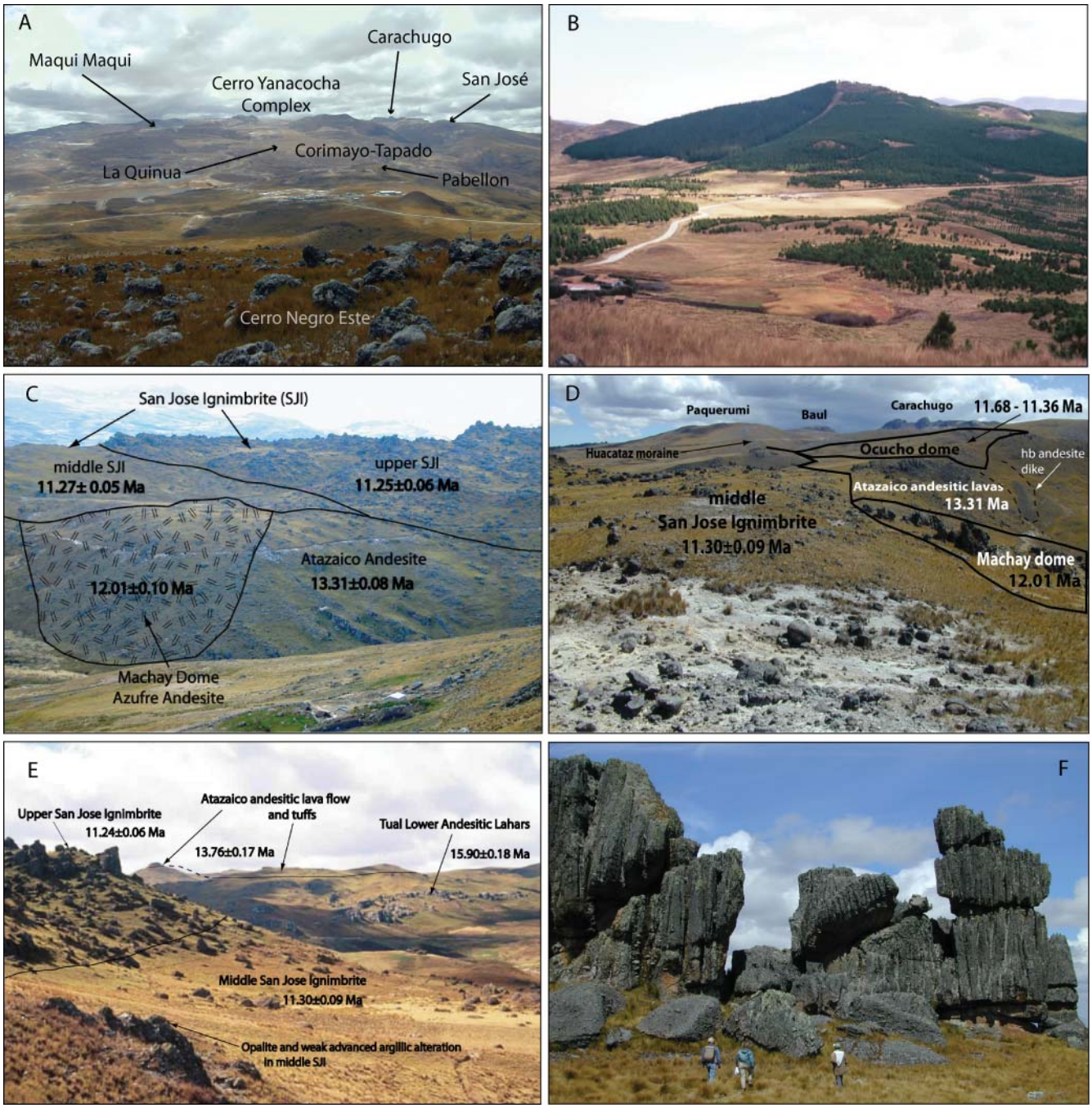

FIG. 5. Photographs of volcanic, stratigraphic, and intrusive relationships in the Yanacocha district annotated with $^{40}Ar/^{39}Ar$ ages. (A) View northeast from Cerro Negro Este showing locations of some of the gold deposits and the topographic high characteristic of the central part of the district. (B) The Cerro Atazaico stratovolcano (14.21 Ma) and vent for Atazaico Andesite lavas in the western district. (C) View southeast of the middle and upper members of the San Jose Ignimbrite (SJI) overlying in angular unconformity with lavas of the Atazaico Andesite and the Machay dome, which intrudes the Atazaico lavas. (D) The base of the middle SJI is marked by a concentration of coarse lithics (bottom left) that are predominantly accidental fragments of hydrothermally altered rock. The San Jose Ignimbrite unconformably overlies the Machay dome and lavas of Atazaico Andesite. In the background, the composite-age Ocucho dome intruded lavas of Atazaico Andesite. (E) View looking northwest in the Alta Machay area of middle and upper SJI (foreground) to Atazaico Andesite, overlying the Chaupiloma (Tual) andesitic lahars (background). (F) Exposures: characteristic of fluted columnar exposures of the upper SJI.

Hydrothermal breccias

Many varieties of hydrothermal breccia (Sillitoe, 1985; Davies et al., 2008) are spatially associated with gold ore in quartz-rich rock and include the following: (1) early matrix-supported, heterolithic and monolithic breccias with dense quartz cement; (2) heterolithic and monolithic breccias with alunite cement; and (3) heterolithic, matrix- to clast-supported breccias with a granular quartz matrix, referred to as phreatic breccias

TABLE 2. Alteration Mineral Assemblages, Breccia, and Mineralization at Yanacocha

Alteration	Minerals	Texture	Related breccia	Mineralization	Comments and interpretation
Quartz-rich rock (silicic alteration)					
Vuggy quartz	~90-100% Quartz (rt-jar±lim ±py±sf)	Fine-grained quartz with open-space voids (vugs); original rock texture is partly preserved; texures are very porous with abundant vugs that represent sites of phenocrysts, pumice, and lithic rock fragments in the original igneous rock; three textural types of groundmass quartz: (1) dense fine-grained (<0.1 mm diam) quartz grains in aggregates with planar boundaries (2) fine-grained quartz as in (1) overprinted with slightly coarser (~0.1 mm diam) granular-textured quartz (3) fine-grained quartz is recrystallized to 0.3 mm diam quartz and drusy quartz line vugs	Vuggy quartz matrix-supported, fragmental rocks are common in zones dominated by quartz-rich rocks; some with 2–5-cm-size flattened to rounded cavities; fragments are both massive and vuggy quartz; these fragmental rocks are interpreted by Minera Yanacocha geologists as having a prevuggy quartz, pyroclastic origin and are termed ignimbrite or tuff	Sulfide zones[1]: py, en, tn, cv, sf, late cc. Rare ac, ga, sl, orp; found in vugs and fractures Oxide ore: poorly cemented, highly fractured, vuggy quartz with jar, he, go or lim cement (crackle breccias, silica-iron oxide breccias of Harvey et al., 1999); bonanza-grade gold ore (up to 540 g/t) with coarse visible gold associated with go, rt, cas, ba, and rare Sn-rich Fe hydroxides	Quartz is largely residual and is produced by intense base cation leaching from acidic hydrothermal fluids; grades into dense massive quartz where vugs are infilled with quartz; vugs and late fractures host the gold-bearing sulfide and oxide ore; >400-m of oxide in fracture-dominated structural zones Interpretation: Vuggy quartz developed in the crystal-rich volcanic rocks and provided fluid-flow pathways with high porosity and permeability; subsequent acidic hydrothermal fluids from later hydrothermal activity (i.e., stages 3–5) channeled into the early vuggy quartz and laterally into the volcanic stratigraphy; silicic alteration progressively expanded outward as strataform bodies of vuggy quartz; less original igneous wall rock remained and the buffering capacity from fluid-rock reactions decreased; fluids remained acidic for longer periods
Massive quartz		Dense massive microcrystalline (generally <0.05 mm diam, but in rare cases up to 0.2 mm) quartz with the grains in aggregates of interlocking crystals with very low porosity and permeability; original rock textures were obliterated	Heterolithic, fragmental rocks, angular to subrounded clasts in dense quartz cement, typically subvertical, but also as subhorizontal bodies (e.g., San Jose Sur) Cream-colored,[2] dense microcrystalline quartz cement in highly fractured zones, monolithic; contains rt	Sulfide zones[1]: py, en, tn, cv, sf, coarse native gold, late cc; trace gold (30–350 ppb) in dense massive quartz rock with disseminated py; oxide ore: 1–5 g/t gold in highly fractured, poorly cemented, massive quartz (crackle breccias) with jar, sf, he, go or lim cement (silica-iron oxide breccias of Harvey et al., 1999). High grade Au (>5 g/t) associated creamy microcrystalline quartz (<0.3 mm diam) with rt (<5 μm)	Stacked, tabular bodies >300 m thick, hydrofractured massive quartz is common adjacent dense quartz cemented fragmental rocks Interpretation: Silica solubility decreased as the fluid compositions changed, cooled, and pH increased through fluid-rock reactions and mixing; amorphous silica was deposited at the water table and later recrystallized to microcrystalline quartz; stacked, tabular bodies suggest fluctuations of the elevation of the water table and silica deposition through time with each consecutive stage
Granular quartz		Granular quartz ranges from lithified (compact) to unconsolidated (i.e., from sandstone to beach sand) with subrounded quartz grains (0.1–0.5 mm diam); grain contacts range from tangential, planar, to interlocking quartz overgrowths as pore space decreases and compaction increases; original rock textures are obliterated, but open cavities that resemble eutaxitic-texture were observed at San Jose Sur; many granular quartz zones are 100% quartz	Granular-quartz matrix, heterolithic, clast to matrix supported fragmental rocks; termed "phreatic" by geologists at Minera Yanacocha[3]	Generally barren, but hosts gold ore (~1.0 g/t) at Chaquicocha Norte and 5–10 g/t at San Jose Sur; locally Hg-enriched No ore in breccias	Tabular stratiform and subvertical bodies of residual quartz from intense acid leaching; stratiform bodies may overlie (Cerro Norte Este), underlie vuggy and massive quartz (Chaquicocha Sur, Yanacocha Norte, Chaquicocha Norte), underlie quartz alunite (Chaquicocha Norte), or underlie a layer of smectite clay below weakly altered San Jose Ignimbrite (San Jose Sur)

TABLE 2. *(Cont.)*

Alteration	Minerals	Texture	Related breccia	Mineralization	Comments and interpretation
Quartz-alunite	Qt-alun (pyr-dick±dia)	Original rock texture is commonly preserved; found as fragments in hydrothermal breccias, and matrix to some hydrothermal breccias	Alunite-matrix, heterolithic and monolithic, fragmental rocks are both tabular and subvertical with angular to subrounded clasts of massive quartz and quartz-alunite	Low grade 0.2–1.0 g/t gold, deeper zones at Cerro Yanacocha	Hypogene, magmatic-hydrothermal advanced argillic alteration assemblages; sometimes pyrophyllite-dominant (Quilish and deep Cerro Yanacocha); zoned outward to quartz+alunite+dickite to quartz+alunite+kaolinite to quartz+kaolinite
Opaline silica	Amorphous silica (opal)	Opaline silica replacement that preserved the original rock textures		Barren; may contain anomalous Hg	Rootless pods of opal occur near quartz-kaolinite and montmorillonite at the margins of and ~200 m above gold ore; supergene or steam-heated?
Argillic	Ill-smec-kao±qt	Original rock textures preserved	Clay-matrix, heterolithic, fragmental rocks; termed "diatreme" by geologists at Minera Yanacocha	Barren	Generally clay dominant, but can contain quartz: generally grades outward to fresh rock; kaolinite may be supergene
Propylitic	Chl, mont, ill, ca	Original rock textures preserved		Barren	Rare and commonly not present Grades outward to fresh rock

After Sillitoe, 1993, 1999; (Klein, writ. commun., 1997; San Jose Sur); Harvey et al., 1999; Longo, 2000; Loayza-Tam, 2002. Bell et al., 2004

Alteration abbreviations: alun = alunite, ca = calcite, chl = chlorite, dia = diaspore, dick = dickite, ill = illite, kao = kaolinite, mont = montmerillonite, pyr = pyrophillite, qt = quartz, smec = smectite.

Sulfide zone abbreviations: ac = acanthite (rare), cc = chalcocite, cv = covellite, en = enargite, ga = galena (rare), orp = orpiment (rare), py = pyrite, sl = sphalerite (rare), tn = tennantite, sf = native sulfur

Oxide zone abbreviations: beud = beudantite, ba - barite, go = goethite, he = powdery hematite, jar = jarosite, lim = miscellaneous hydrous Fe oxides, rt = rutile, cas = cassiterite (rare).

[1] Sulfide-bearing zones: Au-Cu rich: covellite-enargite-pyrite ± chalcocite; Au-rich: pyrite-tennantite-covellite-electrum ±barite±orpiment ±native sulfur

[2] Cream-colored microcrystalline quartz cement at Rodquilar is considered an oxidation product of chalcedony with fine hypogene sulfides and bonanza gold (Arribas et al., 1995).

[3] Abarca and Harvey, 1997; Turner, 1997; Harvey et al., 1999; Longo, 2000; Velasco et al., 2000; Gomez, 2002; Loayza-Tam, 2002; Bell et al., 2004

at Yanacocha (Table 2). Early hydrothermal breccias with dense quartz cement are hosted in a variety of quartz-rich and quartz alunite alteration (Abarca and Harvey, 1997; SD Fig. 4). They appear to predate gold ore, because they commonly grade <0.03 g/t Au and are only locally cut by fractures containing barite and coarse native gold, e.g., at Chaquicocha Alta (Fig. 3, Plate I). Later hydrothermal breccias with quartz-alunite matrices contain fragments of massive quartz and early quartz-cemented breccia, and locally have high gold grades >25 g/t.

Phreatic breccias are chaotic, poorly sorted, matrix- to clast-supported breccias that resulted from eruptions of superheated ground waters at a shallow depth. These breccias crosscut all lithologies and alteration types, and contain fragments of nearly all rock types found at Yanacocha (SD Fig. 5). There are no juvenile fragments. Fine-grained granular quartz forms the matrix of these breccias. Multiple steeply and gently dipping fluidized pebble dikes and sills are a late component of the phreatic event that crosscuts the main body of phreatic breccia. They have a characteristic core of coarse, well-sorted, rounded pebbles (2–6 mm in size) of massive quartz that grade outward to sand-sized (<1 mm) particles that show both planar and crossbedded features (SD Fig. 6).

Diatreme breccias

Diatreme breccias are rare and intrude the volcanic section. These breccias widen upward and are spatially associated with feldspar and quartz porphyry intrusions. A clay-rich matrix supports clasts (SD Fig. 7), which are heterolithic and include quartz-rich rock, clay-altered Yanacocha porphyry, volcanic and porphyritic rocks, and basement quartzite and black argillite. Rare juvenile fragments of the Yanacocha porphyries are plastically deformed and suggest contemporaneous intrusion and brecciation (Abarca and Harvey, 1997; Turner, 1997; Longo, 2000; Loayza-Tam, 2002). Common quartz- and clay-altered fragments indicate hydrothermal activity prior to breccia emplacement. The clay-dominated breccias are not strongly mineralized themselves, but gold ore commonly occurs along their margins, suggesting the ore fluids took advantage of the permeable breccia margin (Changanaqui, 1995; Abarca and Harvey, 1997; Turner, 1997; Rota, 1997; Harvey et al., 1999; Longo, 2000). Rota (1997, 1998) defined irregular but distinct, cone-shaped bodies of clay-rich matrix supported breccia at Carachugo and Cerro Yanacocha that widen toward the surface and narrow to a cylindrical-shaped root at depth, similar to the diatremes described by Lorenz (1986).

Mapping and Sampling for $^{40}Ar/^{39}Ar$ Geochronology

Geologic mapping was integrated with $^{40}Ar/^{39}Ar$ age determinations, geochemistry, and petrography to establish the volcanic stratigraphy and temporal framework of volcanism and mineralization within the district (SD Table 1). We present 69 new $^{40}Ar/^{39}Ar$ ages of volcanic rocks and hydrothermal alunite and biotite (App. Tables A2, A3) to complement the mapping centered on Yanacocha (Plate I). Geologic mapping at 1:25,000 scale covered an area ~1,000 km^2 within and surrounding the Yanacocha mining district, augmented by detailed core logging of diamond drill holes from the center of the district. The least altered volcanic and intrusive rocks beyond the limits of the hydrothermal alteration were sampled for radiometric dating and petrologic studies. These rocks were then correlated with hydrothermally altered rocks in the center of the district, based on stratigraphic relationships, petrography, and isotopic ages.

Of the 69 samples selected for $^{40}Ar/^{39}Ar$ geochronology, 48 were fresh to very weakly altered igneous rocks, of which 37 were from volcanic units and 11 were from intrusions and domes (Table A2). Petrographic analysis of each sample confirmed that 85 percent of these rocks sampled for dating are fresh and show no hydrothermal alteration; the remaining rocks contain trace to minor amounts of alteration minerals.

The remaining 21 samples were from hydrothermally altered rocks that include hydrothermal alunite (n = 20) and biotite (n = 1). These samples were dated to determine the age of the mineralization events (Table A3). All alunite-bearing samples were collected from stratiform horizons or breccia zones of quartz-alunite alteration within or adjacent to each major gold deposit, and contain from trace to >3 g/t Au (Table A3; Longo, 2005). Most of the mapped alunite is relatively coarse grained (>100 μm) natroalunite or alunite associated with quartz, and in many cases also occurs with pyrophyllite, kaolinite, diaspore, and pyrite (Longo, 2005; SD Figs. 8, 9). Isotopic analyses of sulfur from 22 alunites, including all the samples dated, yielded $\delta^{34}S_{CDT}$ values from 11.4 to 25.9 per mil (Table A3). Two samples of pyrite yielded $\delta^{34}S_{CDT}$ compositions of –2.4 and –14.5 per mil (Longo, 2005). The high $\delta^{34}S$ values for alunite and low values for pyrite indicate formation of magmatic-hydrothermal alunite rather than steam-heated or supergene alunite (cf. Rye et al., 1992). The alunites ages provide a maximum age of gold deposition at each locality, given that gold crosscuts quartz-alunite alteration, as previously discussed.

$^{40}Ar/^{39}Ar$ Results and Interpretation

Results of the age determinations are summarized and preferred ages listed in Table 3, Figure 6, and Tables A2 and A3. The Appendix provides details of the analytical methods and representative examples of the age spectra (App. Figs. A1–A4). The age spectra of the 69 experiments are mostly simple, and 62 of the age determinations meet all the criteria for a reliable estimate of the crystallization age (Table A2; see Longo, 2005). That is, plateau ages are the weighted means of three or more heating step ages comprising over 50% of the total $^{39}Ar_K$ gas released and are concordant with isochrons with initial $^{40}Ar/^{36}Ar$ intercepts calculated from Ar compositions of the same steps. In these cases, the plateau age is taken as the preferred age because the analytical uncertainty is generally less than the uncertainty of the isochron age, owing to the often small dispersion in step Ar composition.

Some of the plateaus are bordered by heating step ages that reveal the effects of minor argon loss, excess argon, or argon recoil. These effects do not compromise the interpretion of crystallization ages (Duncan et al., 1997; McDougall and Harrison, 1999; Longo, 2005). Interpretations of the ages of a few problematic samples are discussed below. All additional age spectra are available in online Supplementary Data (or see Longo, 2005).

TABLE 3. Textural and Petrographic Characteristics of

Rock name (symbol) no. samples	Previous names[1]	Composition rock type	SiO_2 (wt %)	Phenocryst proportions	Phenocryst abundance and size (mm)
Tual(t) and Chaupiloma(c) lower andesite lahars (Tlal) Tual Tlalt 4 Chaupiloma Tlalc 11	San Pablo, Porculla, Llama; Lower Andesite Lahars (LAL)	Andesite, principally lahars, rare lavas	t59–62 c57–62	Pl>Hb>Px>Opq Cpx>Opx	Pl: A 0.75–2 Hb: A 0.75–3(R 3–5) Px: C 0.5–1.5
Cerro Fraile pyroclastics Tcfd 23	Frailones, Huambos	Dacite, pyroclastic rocks	61–69	Pl>Bi >Qz>Hb> Opq>Af	Qz: C 0.7–2.7 Pl: A 1–2.5 Hb: C 0.7–2.5 Bi: A 2–5 coarse (0.5 cm dia.)
Atazaico Andesite Tlpha 28	Porculla, Regalado, Lower Yanacocha Volcanics (LPHA)	Andesite, principally lavas	59–61.5	Pl>Px>Hb >Opq Rare Qz, 2% in domes/int	Qz: C in domes/Int Pl: A 1–3 intrusions up to 6 Hb: C 1–2.5 domes/Int up to 5 Px: C 0.5–2 Cpx>Opx twin Cpx common
Quilish Dacite Ted 8	Early dacite	Dacite (intrusions)	63–64	Pl>Hb>Qz>Af > Bi> Opq	Pl: A 3–6 Hb: A 2–5 Bi: R 1–2 Qz: C Em 1.5–2.5
Colorado Pyroclastics Cori Coshpa CC Maqui Maqui MM Tmmi 22	Maqui Maqui Ignimbrite or Pyroclastic Sequence (MMI)	Trachyandesite To dacite, ignimbrite	60–66	Pl>Hb>Opq>Bi rare Qz+Af trace Cpx in MM	Pl: A 1.5–3.5 Hb: A 0.75–3 Bi: R 0.5–1.5 CC R 4 Cpx: T <0.35 Qz: R 0.5
Yanacocha porphyry Yp and Cp	Yp and Cp plugs, sills, diatremes	Andesite to dacite porphyry dikes, plugs, lavas	61–63.6	Pl≥Hb>Af Trace Qz+Bi +Ap±Cpx	Pl: A 0.2–6 Hb: A 0.5–8 Kfs: R 0.25–0.35 Bi: T 0.25–0.5 Px: T 0.35 to absent Qz: T 0.25–1.5 Em
Azufre Andesite Tupha 33	Porculla, Regalado, Upper Yanacocha Volcanics (UPHA)	Trachyandesite, trachydacite, silicic andesite, and low-silica dacite; lavas-domes	61–65	Pl>Hb>Px>Opq no Qz-Af-Bi-Tit	Pl: A 2.5–5 domes to 6.5 Hb: C 1–2.5 Oxyhb(Poikilitic) R 3–5 Int to 10 Bimodal Hb ac<0.75 pr>1.0, Px: C 1–2.5 Cpx>Opx
Lower San Jose Ignimbrite Tlsj 19	Huambos, Frailones, Otuzco	Dacite, andesite, minor trachydacite, trachyandesite; Ignimbrite	62–64.2	Pl>Hb>Cpx >Opq>Bi rare Opx	Pl: A 1.5–4 Hb: A 1.5–5 +1 mm are poikilitic Px: C 0.5–0.75 R2.0 Bi: R 0.6–2 Qz: T 0.15
Middle San Jose Ignimbrite Tmsj 24	Huambos, Frailones, Otuzco *White Tuff*	Dacite, trachydacite, trachyandesite; ignimbrite *White Tuff* trachydacite, ignimbrite	61–63.4	Pl>Hb>Opq >Bi >Px.	Pl: A 1.5–3.5 Hb: C 1–2.5 R 4 (T +1cm Cz) Px: T–R 0.3–1.0 Cpx Bi: R 0.25–2.5 Qz: T 0.5–0.8
Upper San Jose Ignimbrite *Spatter Ign* Tusj 11	Frailones, Huambos, Upper San Jose Spatter Ignimbrite	Andesite to dacite, minor trachydacite and trachyandesite; ignimbrite	62.2–65	Pl>Hb>Cpx>Opx > Opq>Bi Spatter blobs Px>Hb	Pl: A 1–3 Hb: A 1–6 (T +1cm Cz) Oxyhb(Poikilitic) Px: A 0.5 – 3 Bi: T 1.3

Volcanic Rocks and Related Intrusions, Yanacocha District

Total phenocrysts (vol %)	Total mafics[2] (vol %)	Accessory minerals (size mm)	Textures	Fragments (accidental and juvenile)	Extent (km^2)	Ar-Ar age(s)
14 lavas 60 lahars	9–13t 6–13c	Ap Detrital qz	Pyroclastic breccia, broken phenocrysts, clast-supported epiclastic	Contaminated with basement, porphyritic, trachytic lava, and white pumice fragments, generally poorly sorted and heterolithic	430 Tlalt~35 Tlalc>350	19.53±0.13t 15.90±0.18c 15.41±0.36c
20–50 Qz 1–9 Avg 4.5	4–18 Bi 2–10 avg 4.3 Hb 2–5 avg 3.5	Zr	Nonwelded to eutaxitic, poorly-sorted and ash-rich pyroclastic breccias and tuff breccias, the ignimbrites contain remnant elutriation pipes	Heterolithic with porphyritic dacite, basement rocks, and abundant white pumice (2–5mm), abundant broken phenocrysts, rare charred wood	340+ dips 12°–40° NNE to 8°–25° E	15.51±0.05 to 15.15±0.06
26–58 Avg ~50	6–29 15 avg Domes 13–26	Ap	Two types of flow-foliated lavas[3]: (1) Fine-grained pilotaxitic, (2) medium-grained (1–5 mm) porphyritic, pyroclastic rocks are monolithic, poorly-sorted and clast-supported	Rare mafic enclaves of diorite	West district: 157 East district: 80 District-wide est.: 340	14.52±0.13 to 13.31±0.08
19–44 34 common	5–12	T Ap+Zr No Tit	Porphyry, glomero-porphyritic	na	na	no radiometric age
CC: 40–58 Pm: 10–30 MM: 40–68 55 common Pm: 10–25	5–14 biotite CC: 1.5–2 MM: T–1.5	Large Ap striated cloudy cores (0.7 in MM).	Eutaxitic, fines depleted, abundant broken phenocrysts, Seriate pl w/ Int	Basement Qz and Arg fragments common, rare porphyritic, nonwelded white pumice in CC, Pm 5–10-cm-size, 20-25 vol %	89 eroded: minimum	12.63±0.05 to 12.40±0.10
20–39 R 43 Avg. 32 Qz <1 Lava: 10–38	10–12.5	Ap	Int are coarsely porphyritic (e.g., DN-77, SLT-2); Lavas are trachytic-textured, and flow-foliated (e.g., YS-370); commonly clay altered (Cp)	na	na	12.39±0.12 to 11.90±0.11 12.26±0.12[4]
22–55 C 31	4–19 C~10	Ap>Zr	Flow foliated, pilotaxitic, porphyritic (bimodal), rare glomero-porphyritic	Rare mafic enclaves of diorite	125	*West district* 12.09±0.10 to 11.91±0.08 *East district* 12.09±0.08 to 11.68±0.07
32–63 C 46 Pm 5–20	4–13	large Ap striated cloudy cores (0.3-0.75), Zr 0.2.	Eutaxitic to non-welded, broken phenocrysts, fines depleted	Hetero- to monolithithic, trachytic andesite and basement argillite fragments, pumice 1–4cm rare altered accidental fragments of SM, Large (up to 1 m diam) patchy- and wormy-textured quartz-alunite accidental fragments at Cerro Baul	134	11.79±0.14 11.54±0.09 to 11.43±0.06 11.58±0.18[4]
37–71 Avg 66	3–12	Trace Tit,Ap,Zr *White Tuff* Ap (0.25) Zr (0.2)	Devitrified, eutaxitic to nonwelded, broken phenocrysts, fines depleted *White Tuff:* devitrified	Heterolithic porphyry and basement fragments, abundant accidental fragments of Mq, Vq, qA, and qz-andalusite-Af pumice lapilli AR-2/1 fiamme AR-10/1 White tuff: rare porphyry altered fragments, pumice	100 ?	11.43±0.11 to 11.29±0.08 *White Tuff* 11.22±0.08
37–74 Avg. 54 Mtx 50–74 Blobs 40–45	3–10 Green Cpx up to 7	C Ap, T Zr	Fines-depleted, eutaxitic, dominated by broken phenocrysts and small blobs and blocks <5 cm, clast size grades downward from 10–50 to 1–5 cm	Rare fiamme (AR 10/1); rare previously altered accidental fragments, abundant spatter blobs 20–50 vol % (AR 7:1, pvAR 2-1), and equant sub-angular blocks with laminated to thin-bedded tuff that resemble base-surge deposits	16.5 175 Cumulative areal extent 3 members	11.25±0.07 and 11.24±0.10

TABLE 3.

Rock name (symbol) no. samples	Previous names[1]	Composition rock type	SiO_2 (wt %)	Phenocryst proportions	Phenocryst abundance and size (mm)
Domes of San Jose Ignimbrite Tsjd 6	Regalado	Dacite, andesite, and minor trachydacite to trachyandesite Emplaced into vents of TSJ	62–64	Pl>Hb>Cpx>Opx > Opq>Qz>Af	Pl: A 2–3 Hb: A 2.5 Px: A 0.5–1.5 Qz: T 0.1 Af: T 0.5
Coriwachay Dacite 19	Upper (late) dacite	Dacite to rhyolite	67–71	Pl>Hb>Qz>Af>Bi> Opq>Tit	Pl: A 2.5–7 Hb: A 0.5–2.5 Bi: C 0.8–2 Qz: C Em 0.8-3.5 Tit C to 1.2 mm
Members					
Corimayo dacite Tcd 11		Dacite	67–69	R Bi>Hb	Pl: A 1-7 Hb A 1–2.5 Bi: C <2 Qz: C Em <2.0 Tit: C <1.0
Co. Yanacocha dacite porphyry Typq 7	Yanacocha quartz porphyry	Dacite	68		Pl: A <4 Hb A <3 Bi: C <2 Qz: C Em <4 Tit: C <1.2
Yanacocha Lake rhyolite dikes Tcyr 1		Rhyolite	70.6		Pl: A <4 Hb A <2 Bi: C <1 Qz: C slEm <1 Tit: C <0.4
Negritos ignimbrite Tnr 1		Rhyolite	71	Bi>Hb	Pl: A <2 Hb C <0.5 Bi: A <2 Qz A <2 Tit: C <0.4

[1] Previous names of Ryes, 1980; Cobbing et al., 1981; Wilson, 1984; Turner, 1997; Longo, 2005
[2] Ferromagnesian minerals (applied to the mafic minerals hb+cpx+opx)
[3] Edwards, 2000
[4] Ages from Turner, 1997
[5] Ages from Chiaradia et al., 2009

The relative abundance and maximum size in mm are reported for each mineral: A = abundant, C = common, R = rare, T = trace, N = none; rock abbreviations: Arg = Argillite, Qtz = quartzite, Int = intrusion, P = porphyritic, Ign = ignimbrite, Int = intrusion

Mineral abbreviations: Af = alkali feldspar, Ap = apatite, Bi = biotite, Cpx = clinopyroxene, Hb = hornblende, Opq = Fe-Ti oxides, Opx = orthopyroxene, Pl = plagioclase, Px = pyroxene, Qz = quartz, Rt = rutile, Tit = titanite (sphene), Zr = zircon. Other abbreviations: AR = cross sectional aspect ratio (pv-planar view), Bimodal Hb = ac-acicular lath and pr-prismatic, Cz = concentrically zoned = large 1-cm-size Hb with *onion-skin* zonation that is visible in hand samples (for details on Hb zoning see Chambefort et al., in press), Em = embayed, Eu = euhedral, Mtx = matrix, Oxyhb = oxyhornblende, Pm = pumice, Mq = massive quartz, Vq = vuggy quartz, qA = quartz alunite, Avg = average, na = not applicable; Colorado Pyroclastics: CC = Cori Coshpa ignimbrite, MM = Maqui Maqui ignimbrite

Volcanic Stratigraphy and Geochronology

The geologic mapping, core logging, petrography, and radiometric ages from this study allow revisions to and improved understanding of the Miocene volcanic stratigraphy (Figs. 3, 4, 6, 7, 8; Plate I). The Miocene stratigraphy is divided into eight major volcanic units of which the first three are assigned to the older Calipuy Group volcanic rocks (after Cobbing et al., 1981; Wilson; 1984), and the last five are here named the Yanacocha Volcanics (Fig. 4, Tables 3, 4).

Calipuy Group

Volcanic rocks of the Calipuy Group are up to 600 m thick and erupted from numerous centers over a wide area from ~20 and ~15 Ma (Reyes, 1980; Wilson, 1984; Turner, 1997; Davies, 2002; Longo, 2005). These rocks include, from oldest to youngest, the following: (1) the Huambo Cancha andesite, (2) the lower andesitic lahars of the Tual and Chaupiloma sequences, and (3) the Cerro Fraile dacitic pyroclastic sequence.

Huambo Cancha andesite (Tha): Porphyritic andesite and volcaniclastic rocks at Huambo Cancha and Rio Porcon overlie Cretaceous quartzite at an angular unconformity and are the oldest Cenozoic volcanic rocks exposed in the study area (Figs. 3, 4, Plate I). Trachytic- and coarsely porphyritic-textured andesitic lavas are interbedded with thin-bedded volcaniclastic siltstones. The Huambo Cancha andesite is locally tightly folded from compressional deformation not recognized in the overlying rocks. The andesite is typically hydrothermally altered to clay with disseminated pyrite or indigenous limonite after pyrite. The undated Huambo Cancha andesite is older than the overlying 19.5 Ma Tual andesite (Table A2; SD Table 1).

Lower andesitic lahars of Tual (Tlalt) and Chaupiloma (Tlalc): These coarsely porphyritic hornblende and horn-

(Cont.)

Total phenocrysts (vol %)	Total mafics[2] (vol %)	Accessory minerals (size mm)	Textures	Fragments (accidental and juvenile)	Extent (km^2)	Ar-Ar age(s)
28–60 44 avg.	3–25	Ap (0.1)	Porphyritic, pilotaxitic, flow foliated, seriate Pl	Rare mafic enclaves of diorite with Pl and Cpx dominant	~5	12.01±0.10 to 11.23±0.07
24–43 35 avg.	4–16	Zr, Ap, Rt, Tit	Porphyry texture, R flow foliations, seriate Pl		~15	
>24–43 Qz ~3	10–15	C Tit, R Ap, T Zr	Broken phenocrysts with tuff	Porphyritic dacite (3-4 mm-diam)	~7	10.78±0.05 11.06±0.02 to 10.62±0.155
30 Qz ~5	4–8	C Tit, T Rt, T Ap	R Eu Qt		~2	9.91±0.04 9.90±0.05[4]
30 Qz ~5	~10	C Tit	R Eu Qt		~1	8.40±0.06[4] 8.59±0.14[5]
43 Qz 15	~5	T Ap, T Tit	Broken phenocrysts	Dacite porphyry, Hb-Bi feldspar porphyry, rare granular-textured quartz	~5	8.43±0.04

blende-pyroxene andesites are divided in two sequences; the Tual and the Chaupiloma (Figs. 3, 4; Table 3; Plate I; SD Fig. 10). The andesites, up to 415 m thick, filled paleochannels cut into the Huambo Cancha andesite and the Cretaceous basement rocks (Figs. 4, 7; Table 4).

Both of these units are dominated by lahar and hyperconcentrated flow deposits. The Tual andesite crops out only in the southwestern and western parts of the district, north of Cajamarca (Fig. 3, Plate I), where it forms distinctly stratified yellow, poorly reworked epiclastic rocks, pumice-rich debris-flow and lahar deposits, and volcaniclastic sandstones and pebble conglomerates. The Chaupiloma andesite overlies the Tual andesite along a disconformity (see Figs. 4, 7, erosional hiatus 1). The Chaupiloma is characterized by thick gray lahar deposits of hornblende-pyroxene andesite that are interbedded with rare ash-fall tephra and volcaniclastic sedimentary rocks ranging from pebble conglomerates to laminated siltstone (SD Fig. 10). The lower 80 m consists of 1- to 3-m-thick beds of lahar flows with large fragments of andesite and basement rock (<2 m diam) that are interbedded with 1- to 2-m-thick beds of massive lahars with small fragments (<3 cm diam, SD Fig. 11). Above the basal lahars are 20 m of thin (~1 m) beds of fine-grained and pumice-rich mudflows. Thick lahar deposits that are interbedded with laminated siltstone, ash-fall tephra, and andesitic lavas dominate the upper 40 to 80 m.

Plagioclase from pumice in a basal lahar of the Tual andesite east of Huambo Cancha yielded an early Miocene age of 19.53 ± 0.13 Ma, and plagioclase from glomeroporphyritic andesitic lava near the top of the Chaupiloma andesite at Maqui Maqui Norte yielded a middle Miocene age of 15.90 ± 0.18 Ma (Table A2). These ages suggest there may be a significant time gap between the Tual and Chaupiloma andesites.

Cerro Fraile dacitic pyroclastics (Tcfd): The Cerro Fraile dacitic pyroclastic deposits are characterized by distinctive outcrops of large, irregular, free-standing columns. These pyroclastic rocks have been previously classified as the Huambos Formation (Table 3; Wilson, 1984; Turner, 1997). The Cerro Fraile pyroclastic rocks overlie both the Chaupiloma and Tual andesites with erosional disconformity (Fig. 4, erosional hiatus 2), and crop out in an area of >300 km^2. They reach a thickness of 220 m in the northeast part of the district where they fill a north- to northwest-trending paleobasin 10 by 20 km (Figs. 3, 4, 7; Table 4; Plate I). These rocks were gently folded prior to eruption of the Yanacocha Volcanics.

The Cerro Fraile pyroclastic rocks display a characteristic columnar jointing and consist of a series of 1- to 10-m-thick ignimbrites and unwelded, poorly bedded pyroclastic deposits interlayered with thin-bedded (<1 m) tuff (Tables 3, 4,

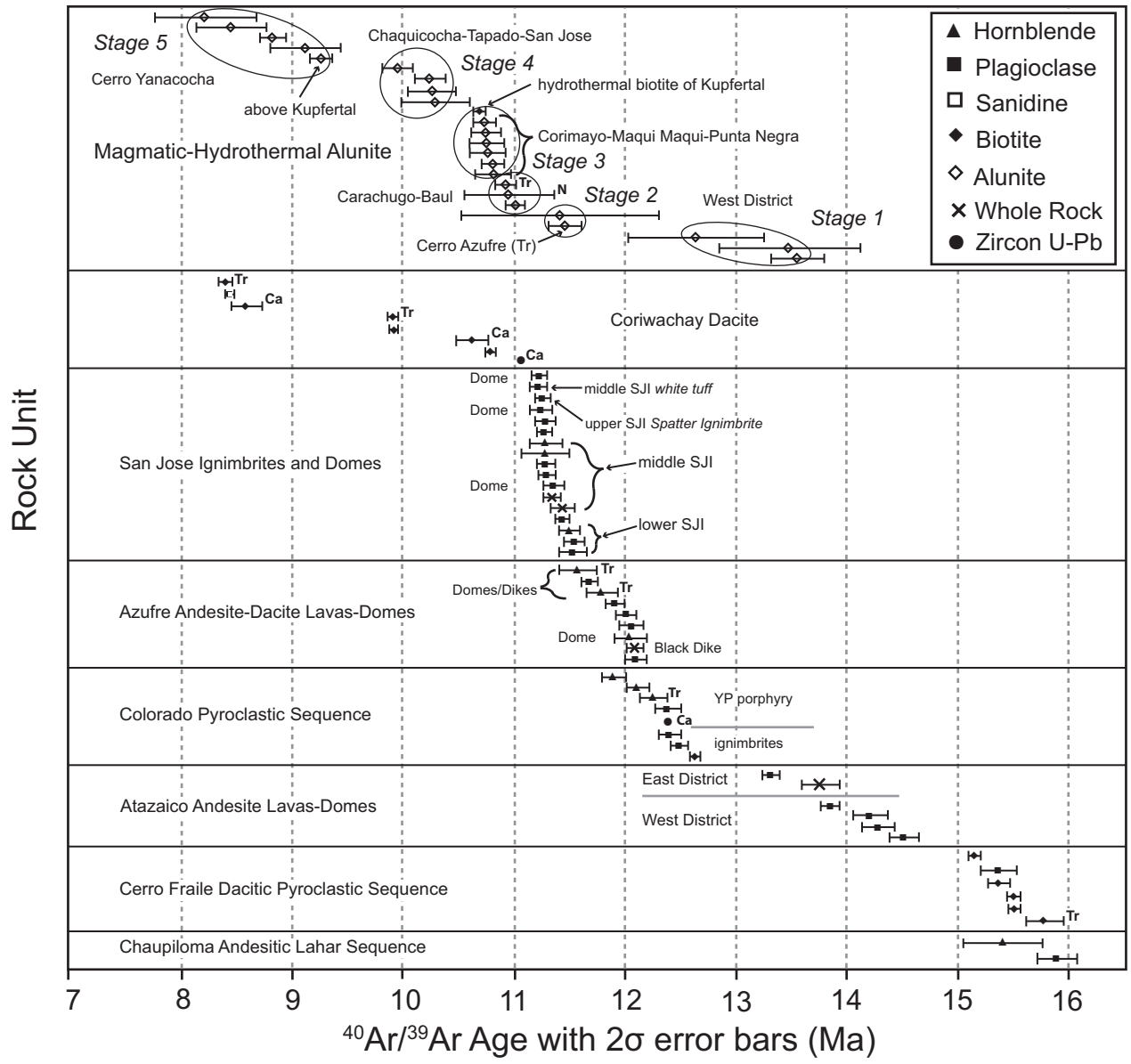

FIG. 6. $^{40}Ar/^{39}Ar$ ages of Miocene igneous rocks as a function of stratigraphic position and of hydrothermal minerals by age groups (stages 1-5) and locations. The preferred ages with 2σ error bars are plotted for all samples from this study including eight ages (1 alunite and 10 fresh igneous rocks) from Turner (1997; Tr) and Chiaradia et al. (2009; Ca, the 2σ error (±0.02) for the U-Pb ages are less than the size of the symbol), and one K/Ar age on alunite from Carachugo Sur (D.C. Noble, pers. commun., 1997; N). The age for the Tual andesitic lahar (19.5 Ma) is not displayed here.

SD Fig. 12). Ignimbrites are partially welded and devitrified, and interlayed with pyroclastic surge deposits. The ignimbrite and poorly bedded pyroclastic deposits are ash rich and contain abundant white pumice and lithic fragments of porphyritic dacite and basement rocks. The lithic fragments increase in size (>2 m; SD Fig. 13) downward in each individual flow. Unwelded bedded pyroclastics tend to dominate the base of the sequence, whereas ignimbrites dominate upward in the sequence.

The mineralogy of the Cerro Fraile dacitic pyroclastic rocks readily distinguishes it from other volcanic rocks in the Yanacocha district. The Cerro Fraile has coarse and abundant biotite (0.5 cm diam and up to 10 vol %), quartz (up to 9 vol %), and subordinate hornblende (up to 5 vol %), but lacks pyroxene, apatite, and titanite (Fig. 8, Table 3).

Five $^{40}Ar/^{39}Ar$ ages of biotite and plagioclase from the Cerro Fraile pyroclastic rocks range from 15.51 ± 0.05 Ma at Cerro El Fraile (the type locality, Plate I) to 15.15 ± 0.06 Ma at Maqui Maqui Norte (Table A2). Plagioclase and biotite were analyzed for one sample (DN-12) and the plagioclase yielded a reliable plateau age of 15.18 ± 0.14 Ma (98.2% of the total gas released, MSWD = 0.97), whereas the plateau for the biotite was defined by <50 percent and its isochron $^{40}Ar/^{36}Ar$ intercept differed slightly from the atmospheric value. The age range overlaps the youngest $^{40}Ar/^{39}Ar$ age from the underlying Chaupiloma andesite; nonetheless, we interpret the Cerro

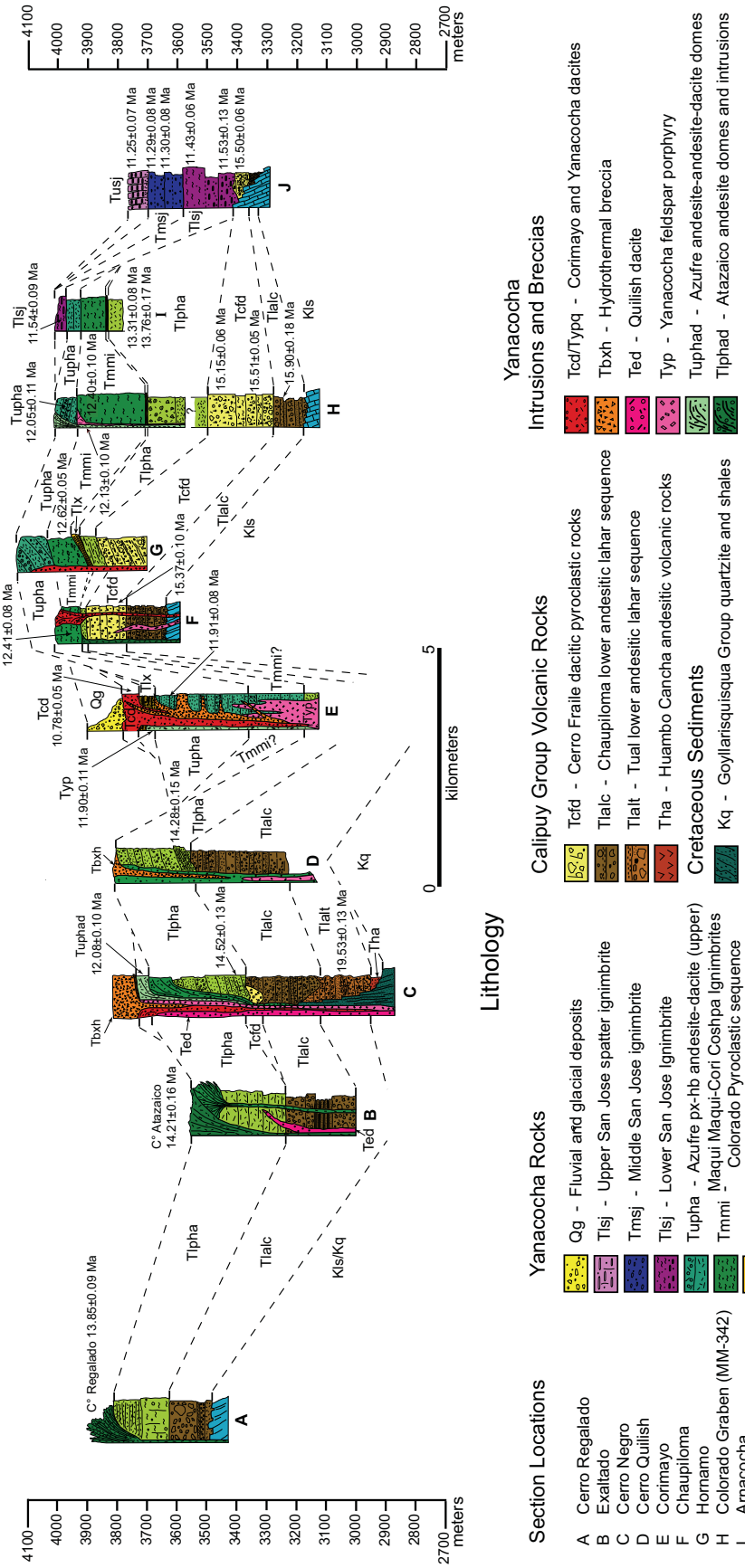

FIG. 7. Fence diagram displaying representative stratigraphic columns of Miocene volcanic rocks together with ages from west (section A) to east (section J) across the Yanacocha district (location line shown in Fig. 3).

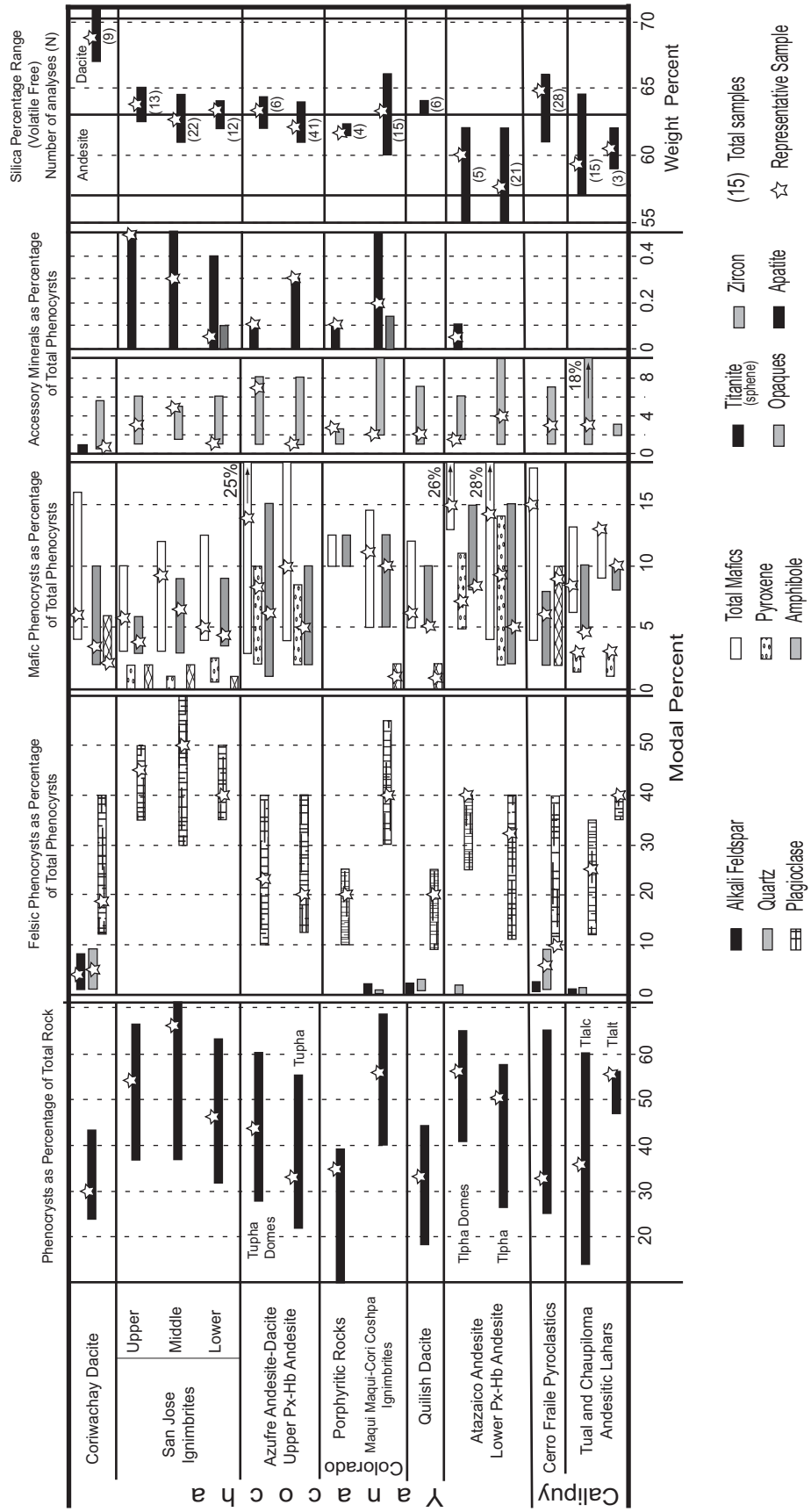

FIG. 8. Modal ranges (vol %) of the phenocryst mineralogy and wt percent SiO_2 for samples of the Calipuy Group volcanic rocks and the Yancocha Volcanics. Individual samples selected to best represent each of the rock units are shown with a white star.

TABLE 4. Thickness and Areal Extent of the Volcanic Rocks in the Yanacocha District

	Rock package	Tual and Chaupiloma Lahars	Cerro Fraile Pyroclastics	Atazaico Andesite	Colorado Pyroclastics	Azufre Andesite	San Jose Ignimbrite	Coriwachay Dacite
	Age (Ma)	19.5–15.9	15.5–15.2	14.5–13.3	12.6–12.4	12.1–11.6	11.6–11.2	10.8–8.4
	Outcrop area/ areal expanse (km²)	88/430	66.3/340+	102.5/340	9.8/89	22/125	136/175	1.2/15
	Locations	Thickness (m)						
Western District	Cerro Regalado	140	?	180	a	a	a	a
	Granja Porcon	230+	?	200–310	a	a	a	a
	Cerro Negro	415	0-55	240–320	a	45	a	a
	Quilish	315	?	250	Northeast Quilish	a	a	a
	Corimayo	?	?	45+	90+	±310	?	0-60 domes
	Encajon	>250	~210	?	>80	a	a	a
	Yanacocha	?	>125	>40	~220	a	a	Intrusions
	Chaupiloma	130+	130	0-20	50-90	a	a	Intrusions
Eastern District	San Jose	?	>90	110	?	80	100+	Intrusions
	Baul	?	?	?	?	≥110	≥60	a
	Chaquicocha	?	>190	170	160	?	?	Intrusions
	Hornamo	?	>135	40	115	125	a	Intrusions
	Maqui Maqui	110+	220	±200	225+	70+	a	a
	Arnacocha	?	?	>50	80+	50	40	a
	Combayo	0-40+	0-50+	a	a	a	350	a

Notes: a = absent from the section, ? = possibly present

Fraile as entirely younger than the Chaupiloma on the basis of field observations that indicate the Cerro Fraile dacite always overlies the Chaupiloma andesite and the two units are not intercalated (see Fig. 4; erosional hiatus 2). Turner (1997) obtained a $^{40}Ar/^{39}Ar$ age of 15.78 ± 0.17 Ma from biotite from a dacitic tuff north of Cerro El Fraile that we include as part of the Cerro Fraile dacitic pyroclastics (Fig. 6).

Yanacocha Volcanics

Volcanic and minor subvolcanic intrusive rocks are divided here into five mappable major units of andesite to rhyolite composition, confined to the Yanacocha district and erupted during a 6 m.y. period, from 14.5 to 8.4 Ma (Figs. 4, 7, 9). The five units from oldest to youngest are the Atazaico Andesite (effusive stage 1), the Colorado Pyroclastics (explosive stage 1), the Azufre Andesite (effusive stage 2), the San Jose Ignimbrite (explosive stage 2), and the Coriwachay Dacite (Longo and Teal, 2005). In total, the volcanic rocks crop out over an area >500 km², display high phenocryst contents, and evolved from spatially and temporally distinct eruptive centers along a 25-km-long northeast-trending corridor (Fig. 3; Tables 3, 4; Plate I).

Atazaico Andesite (Tlpha): Lavas with flow-breccia facies, flow domes, and minor pyroclastic deposits of pyroxene> hornblende andesite (Table 3; SD Figs. 14, 15) accumulated during effusive stage 1 of the Yanacocha Volcanics. They are here named the Atazaico Andesite (Table 3). They attain thicknesses of 320 m in the center of the district and have an areal extent of 340 km² (Figs. 4, 7; Tables 3, 4; Plate I). At the margins of the district, individual lava flows filled paleochannels along an erosional disconformity cut into the Calipuy Group volcanic rocks (see Fig. 4; erosional hiatus 3). The Atazaico Andesite apparently erupted from numerous monogenetic volcanoes and small composite cones around the district, such as Cerro Atazaico (Figs. 3, 5B; Plate I).

The Atazaico Andesite is characterized by abundant phenocrysts of plagioclase and ferromagnesian minerals (Fig. 8; Table 3; SD Fig. 5C). It crops out in two texturally distinct types of lava: (1) fine- to medium-grained plagioclase and hornblende phenocrysts (<2.5 mm long) within a fine-grained pilotaxitic groundmass, and (2) porphyritic with medium-grained phenocrysts (1.0–5.0 mm long). Lavas were intruded and locally overlain by pyroxene andesite flow-domes containing rare quartz phenocrysts and associated with minor amounts of block and ash flows (SD Fig. 16). The domes include the subvertical, flow-foliated andesite at Antibuyoc, Cerro Regalado, Cerro Quilish, and Cerro Negro Oeste (Fig. 3; Plate I). Domes at Quilish are associated with zones of hypogene advanced argillic alteration and hydrothermal breccias.

Lava eruption and subsequent dome building spanned 1.2 m.y. and progressed temporally from southwest to northeast across the district. Lavas to the southwest have ages of 14.52 ± 0.13 to 14.21 ± 0.16 Ma and are overlain by flows from the Cerro Regalado andesitic dome with an age of 13.85 ± 0.09 Ma (Fig. 7A). The two youngest ages in the northeastern part of the district include 13.76±0.17 Ma for an andesitic tuff low in the stratigraphic section and 13.31±0.08 Ma for a stratigraphically higher andesitic lava south of Arnacocha (Figs. 3, 5C-E, 6, 7 Section I). These ages suggest only a minor time gap of ~0.5 m.y. between eruption of the Cerro Fraile Pyroclastics and the Atazaico Andesites (Fig. 6).

Quilish dacitic intrusions (Ted): Numerous early hornblende-biotite dacite porphyry dikes and plugs intrude the Atazaico Andesite and older units in the western district and crop out along the northeast Yanacocha trend for 14 km. They are herein named the Quilish dacitic intrusions (Figs. 4, 7, 9; Plate I). The dacite porphyries contain 30 to 40 percent phenocrysts of plagioclase, hornblende, slightly embayed quartz, sanidine, biotite, and Fe-Ti oxides set in an aplitic (<0.05

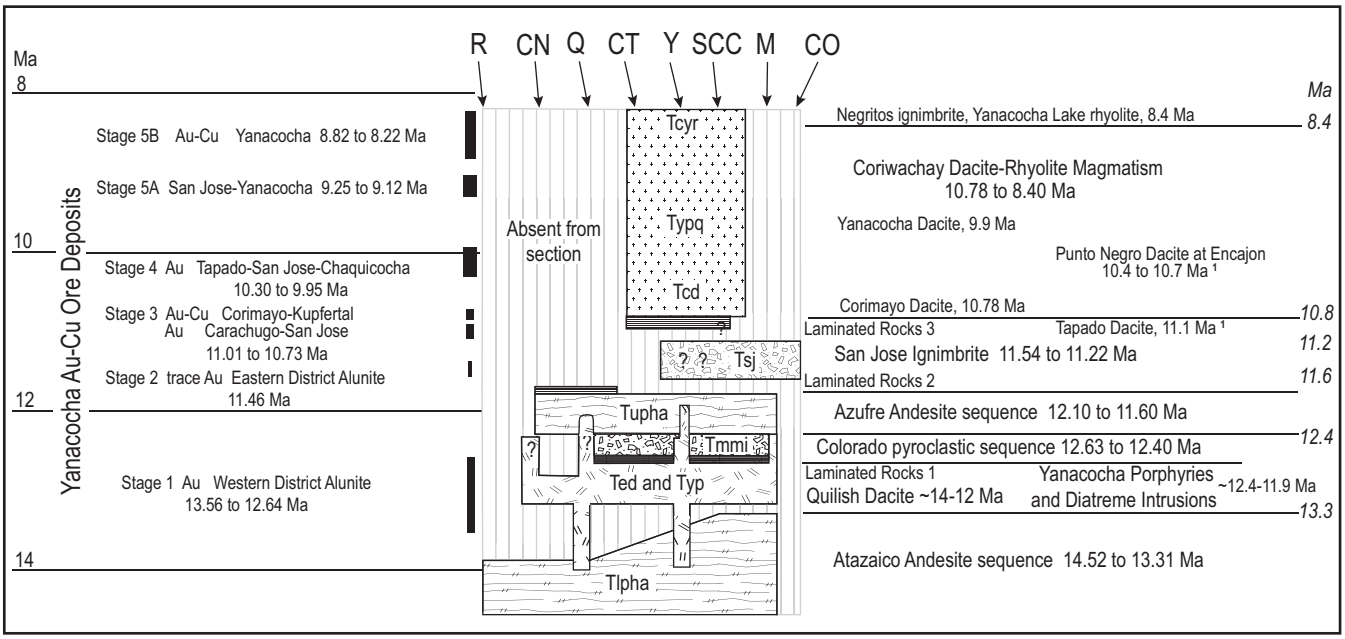

FIG. 9. Composite chronostratigraphic summary that shows the spatial distribution and ages of volcanic units, intrusions, and Au (Cu) deposits in the Yanacocha district. Localities include Cerro Regalado in the west-northwest to Combayo in the east-southeast. Yanacocha district volcanic rocks include: the pyroxene>hornblende Atazaico Andesite (Tlpha), the Maqui Maqui and Cori Cospha ignimbrites of the Colorado Pyroclastics (Tmmi), the Quilish dacite (Ted), Yanacocha porphyry and early diatremes (Typ), hornblende>pyroxene Azufre andesite-dacite (Tupha), San Jose Ignimbrite (Tsj), Corimayo dacite (Tcd), Yanacocha dacitic porphyry plugs and diatreme (Typq), and Yanacocha Lake rhyolitic domes and dikes (Tcyr). Site locations include the following: R = Cerro Regalado, CN = Cerro Negro, CO = Combayo, CT = Corimayo-Tapado, M = Maqui Maqui, Q – Quilish, SCC = San Jose–Carachugo-Chaquicocha, Y = Yanacocha Complex.

mm) quartzofeldspathic groundmass (Fig. 8; Table 3). In the eastern part of the district, several dacite porphyry dikes with hydrothermal andalusite[2] alteration strike northwest and intrude Cretaceous limestone and Chaupiloma andesite in a 2.3-km-long zone near La Sorpresa (Plate I).

In the Quilish area and elsewhere in the district, the dacite intruded lavas of the Atazaico Andesite (14.5–14.2 Ma), but it has not been observed to intrude younger rocks (e.g., Colorado Pyroclastics, 12.6–12.4 Ma). We infer on the basis of stratigraphic relationships that the dacitic intrusions have ages between ~14.2 and ~12.6 Ma, similar to the ~14 to 12 Ma ages for hydrothermal alunites in the western parts of the district.

Colorado Pyroclastics (Tmmi): Andesitic to dacitic ignimbrites, referred to herein as the Colorado Pyroclastics, represent explosive stage 1, and based on available ages, these eruptions began about 0.7 m.y. after the last eruption of the Atazaico Andesite. They crop out in the fault-bounded Colorado graben in the eastern part of the Yanacocha district, and are up to >225 m thick (Figs. 3, 4, 7, 9; Table 4; Plate I). The Colorado Pyroclastics are divided here into three informal members: (1) basal laminated rocks, (2) the Cori Coshpa andesitic ignimbrite member, and (3) the Maqui Maqui dacitic ignimbrite member (Fig. 4). The Colorado Pyroclastics crop out over an area of ~90 km^2 centered on Cerro Yanacocha, which is the likely source of the ignimbrites (Fig. 3; Table 3; Plate I).

Laminated rocks consist of thin-bedded, fine-grained air fall tuff, or reworked tuff, and local medium-bedded lithic tuff with fragments of basement quartzite. They are commonly strongly hydrothermally altered (SD Fig. 17). The thickest sections (20 m) lie at the base of the Colorado Pyroclastics, but laminated rocks are exposed in at least two higher stratigraphic positions where they are associated with gold deposits (Figs. 4, 7, 9). The laminated rocks have <1- to 50-mm-thick beds that are locally crossbedded and consist of chalcedony with local opal and kaolinite. Edwards (2000) interpreted some laminated rocks as water-lain tuffs and surge deposits, and Longo (2000, 2005) interpreted the thinly laminated chalcedony as derived from deposits of colloidal silica that settled from acidic lakes over fumarole vents in volcanic craters.

The Cori Cospha andesite member is the lower of the two ignimbrites. In the type exposures below Cerro Hornamo at Cori Cospha it is 40-60 m thick (Figs. 4, 7, Plate I), is light gray to white, non-welded, and contains 20 to 25 volume percent white pumice of trachyandesitic composition. Lithic fragments include Cretaceous argillite and quartzite as well as porphyritic andesite. Phenocrysts are dominated by plagioclase and include hornblende and biotite, but pyroxene is absent (Fig. 8; Table 3). Biotite yielded an age of 12.63 ± 0.05 Ma (Fig. 6; Table A2).

The Maqui Maqui dacitic ignimbrite member (SD Fig. 18) overlies the Cori Coshpa ignimbrite along a poorly exposed contact, and forms a single cooling unit commonly 90 m thick,

[2]Andalusite is characteristic of relatively high temperature advanced argillic environments in the deeper parts of epithermal systems transitional into porphyry environments. Simmons et al. (2005) and Reyes (1990) report andalusite forms at >250°C in the epithermal environment (>600 m), but its general stability is >360°C.

but up to 230 m thick in the Colorado graben (Fig. 3; Plate I). The Maqui Maqui ignimbrite is dark gray to gray-brown, is moderately welded, has eutaxitic texture, and contains abundant crystals of broken plagioclase as well as both hornblende and biotite. In contrast to the Cori Cospha ignimbrite, the Maqui Maqui ignimbrite has only trace amounts of biotite (Fig. 8; Table 3). It contains minor (<1–2 vol %) accidental fragments of black argillite, quartzite, and porphyritic volcanic rocks <1 to 5 cm in size. Fiamme range from <1 to 10 cm long and have aspect ratios of 6:1.

The Maqui Maqui ignimbrite yields ages of 12.49 ± 0.08 and 12.40 ± 0.10 Ma. A third sample (DN-52, plagioclase) yielded neither acceptable plateau nor isochron ages. These ages are slightly younger at the 95 percent confidence level than the 12.63 ± 0.05 Ma age of the Cori Coshpa ignimbrite. Therefore, the age determinations and the field relationships suggest that the two ignimbrites result from different eruptions (Fig. 6; Table A2).

Yanacocha porphyries and early diatremes (Yp and Cp rocks): Early porphyries and diatreme breccia at Yanacocha include andesite porphyry dikes and plugs, clay-altered diatremes, and coarsely porphyritic lavas. The porphyry intrusions (Yp) have abundant coarse phenocrysts dominated by plagioclase and hornblende, trace biotite and quartz, and pyroxene is trace to absent. They are generally clay altered and hence termed clay porphyry (Cp) by some geologists (Table 3, SD Fig. 19). The compositions and hornblende-rich phenocryst mineralogy of the porphyries are similar to the Maqui Maqui dacitic ignimbrite, and dissimilar to the Atazaico and Azufre Andesites (Fig. 8; Table 3). Volumetrically minor diatreme breccias are spatially associated with the Yanacocha porphyries at Cerro Yanacocha (Rota, 1998; Loayza-Tam, 2002), Carachugo Norte (Myers, 1997; Rota, 1997), and Cerro Pabellon adjacent the Corimayo gold deposit (Barreda and Edwards, 2000) (Figs. 3, 9; Plate I).

Yanacocha porphyries intruded the flow domes at Cerro Negro Oeste and Chaquicocha Norte (E.C. Vicuña, writ. commun., 1997; Velasco et al., 2000), and andesitic lava flows at Corimayo (Gomez, 2002; Longo, 2005). Moreover, the Yanacocha porphyries intruded or occur interbedded with or lie atop ignimbrites with eutaxitic texture at Cerro Yanacocha, Encajon, Carachugo, and Maqui Maqui (Abarca and Harvey, 1997; Myers et al., 1997; Longo, 2005). These ignimbrites are strongly altered, host much of the gold, and have no reliable radiometric ages; therefore, the Yanacocha porphyries provide a minimum age. On this basis, we tentatively assign the altered pyroclastic rocks that are intruded by the Yanacocha porphyries to the Colorado Pyroclastics, although deeper parts of the sections may also include the older Cerro Fraile dacitic pyroclastics.

Three Yanacocha porphyry samples yield ages (12.4–11.9 Ma) that overlap in part with the age range of the Maqui Maqui ignimbrite and the Azufre Andesite (Fig. 6, Table A2). An andesitic lava flow with coarse hornblende (up to 3 mm long), informally called the Yp sill, conformably overlies a eutaxitic-textured ignimbrite above 4,050 m elevation on Cerro Yanacocha and has an age of 12.39 ± 0.12 Ma (YS-370, Table A2). A second sample is a coarsely porphyritic andesitic plug with abundant hornblende phenocrysts (up to 8 mm long) that intruded the Maqui Maqui ignimbrite at Maqui Maqui and has an age of 12.13 ± 0.10 Ma (DN-77). A third sample is an andesitic dike (11.90 ± 0.11 Ma, SLT-2 68 m; Table A2) that intruded Azufre Andesite lava flows at Corimayo (11.91 ± 0.11 Ma, COR-7 178m; Table A2). The dike contains coarse-grained (≤5-mm-long) hornblende phenocrysts but lacks pyroxene so is similar to the phenocryst mineralogy of the Maqui Maqui intrusion (DN-77) and phenocryst textures of Cp dikes. Turner (1997) obtained a $^{40}Ar/^{39}Ar$ age of 12.26±0.12 Ma from hornblende in a biotite-bearing, porphyritic hornblende andesite similar to the Yp sill at Pampa Larga (Fig. 6; Table 3; Plate I). Chiaradia et al. (2009) sampled andesitic intrusions at Quilish and obtained complex U/Pb ages from three zircons from which they interpret a 12.4 Ma age similar to the Colorado Pyroclastics.

Azufre Andesite (Tupha): Lavas, flow-domes, and minor pyroclastic deposits of strongly porphyritic, trachytic-textured, hornblende-pyroxene andesite to dacite, constitute effusive stage 2. These rocks lie atop the Colorado Pyroclastics, or in erosional unconformity atop older units (Fig. 4). Exposures comprise a 125 km^2 area within a 5 to 8 km-wide zone extending ~15 km from Pampa Cerro Negro in the west-southwest to Alta Machay in the east-northeast. Cerro Azufre near the Maqui Maqui mine is the type locality (Fig. 3, Table 3; Plate I). The lavas are up to 310 m thick, flow-layered, and grade locally into blocky autobrecciated horizons a few meters thick (Fig. 4; Table 4). Lavas of Azufre Andesite and the older Atazaico Andesite are difficult to distinguish in the field, on the basis of textures and mineralogy (cf. Fig. 8; Table 3; SD Fig. 20), and are here divided mainly on the basis of $^{40}Ar/^{39}Ar$ age and stratigraphic position. Laminated rocks overlie Azufre lavas at Cerro Negro Este (Fig. 9).

Extrusive domes with feeder dikes (Fig. 5D) are commonly associated with adjacent pyroclastic deposits consisting of block and ash flows that overlie the lavas and occur as isolated exposures. Pyroclastic deposits are relatively more abundant in the Azufre Andesite in comparison to the Atazaico Andesite. The domes have slightly larger and less abundant phenocrysts compared to lavas and typically form equant to slightly elongate bodies (~0.2–2 km^2) characterized by prominent ribs elongate parallel to steeply inclined flow-foliations (SD Fig. 21). Many of the Azufre domes, including those at San Jose, Baul, and Sacsha, are composite in age and formed via dome-building during many eruptive events (Plate I).

Feeder dikes to the domes cut older lavas and pyroclastic rocks (Fig. 7, Sections C, E, F; Plate I). A dense black, porphyritic andesite dike intruded fragmental rocks hosting gold ore and a Colorado-age andesitic lava or the YP sill (YS-370) at Cerro Yanacocha, and is here interpreted a feeder dike to an eroded Azufre dome. The dike has a phenocryst mineralogy with plagioclase, pyroxene, and hornblende in a pilotaxitic groundmass similar to the Azufre Andesite. The center of the black dike is fresh, but the outer margins are altered to kaolinite and dickite adjacent to quartz-alunite altered rock along a distinct contact that was well exposed in the high wall of the Yanacocha Sur mine pit. The black dike has an age of 12.09 ± 0.08 Ma and is assigned to the Azufre Andesite (Table A2). Therefore, it provides a maximum age for the alteration and a minimum age for the pyroclastic rocks that host the gold at Cerro Yanacocha.

Azufre Andesite is bracketed stratigraphically by the Maqui Maqui ignimbrite (12.40 ± 0.10 Ma), and the lower member

of San Jose Ignimbrite (11.54 ± 0.09 Ma), and may overlap in time with Colorado-age Yp porphyry intrusions (see Fig. 6; Table A2, Yanacocha porphyry, 12.4–11.9 Ma; Longo, 2005). A total of eight samples of the Azufre Andesite have ages ranging from 12.09 ± 0.10 to 11.58 ± 0.18 Ma (Turner, 1997, n = 2; Longo, 2005, n = 7; Fig. 6; Tables 3, A2). The age of samples from the western part of the district at Cerro Negro to central parts of the district at Corimayo range from 12.10 to 11.91 Ma, and samples in the east-central part of the district at Cerro Yanacocha to southeastern parts of the district at the Machay dome and the Ocucho dome complex returned ages of 12.09 to 11.68 Ma (Fig. 3; Plate I).

San Jose Ignimbrite (Tsj): Dacitic and andesitic ignimbrites constitute a second stage of pyroclastic volcanism, referred to as explosive stage 2, that postdate the Azufre Andesite and represent the last voluminous eruptions of the Yanacocha Volcanics. The San Jose Ignimbrite consists of three members that were closely followed by eruptions of three or more dome complexes in the east-central part of the district (Figs. 4, 6, 9). The ignimbrites, especially the middle member, contain abundant accidental fragments of quartz-alunite, massive quartz, vuggy quartz, and quartz-sanidine-andalusite (see above footnote 2) altered rock that locally contain up to 350 ppb Au; altered rock fragments indicate at least some advanced argillic alteration and gold mineralization predates the San Jose Ignimbrite (SD Fig. 22). The San Jose Ignimbrite is up to 350 m thick and covers an area of 175 km^2 within a 15-km-wide topographic depression, here named the Otuzco trough, that extends 15 km southward from Cerro Yanacocha to Cajamarca (Figs. 3, 4, 7; Tables 3, 4; Plate I).

Based on $^{40}Ar/^{39}Ar$ ages (Table A2), the lower member (11.46 ± 0.08 Ma) and middle member (11.27 ± 0.05 Ma) may be the products of two temporally distinct eruptions, separated by approximately 0.2 m.y., whereas the ages of the middle and upper members are analytically indistinguishable (~11.3 Ma, see below). Therefore, these middle and upper members could have formed as two temporally distinct eruptions or a single evolving eruption (Fig. 6). Each of the three ignimbrite members is mineralogically and texturally distinct; there are also vertical changes in mineralogy and degree of welding that suggest an origin from several pyroclastic flows. Contacts between members are rarely marked by obvious depositional features such as surge layers, or co-ignimbrite air fall layers (Figs. 5C-E; SD Fig. 23).

The lower member of San Jose Ignimbrite (Tlsj) is the most voluminous, and is extensively exposed in area of 134 km^2. It typically forms a compound cooling unit of three or more hornblende-pyroxene-biotite dacitic ignimbrites, each of which includes a zone of poorly sorted and poorly to non-welded lapilli pumice tuff below an upper densely welded ignimbrite characterized by strongly developed eutaxitic texture. These ignimbrites are crystal rich compared to the juvenile pumice which has sparse phenocrysts (Fig. 8; Table 3). Five $^{40}Ar/^{39}Ar$ ages for the lower member range from 11.54 ± 0.09 to 11.34 ± 0.16 Ma. The last (SJS-79A23.4 wr) has a plateau age making up <50 percent, but a concordant isochron age (Table A2). Thus, the lower member may have erupted as a series of cooling units through a period of ~200,000 years. Since these ages are all within error (Fig. 6, Table A2), an alternative is that they erupted as a single time given by the weighted mean age of 11.46 ± 0.08 Ma (n = 5, MSWD = 2.0).

The middle member of the San Jose Ignimbrite (Tmsj) is a white, non-welded to densely welded, hornblende-biotite andesitic to trachydacitic ignimbrite containing large (1 cm), concentrically zoned hornblendes and lapilli-sized pumice (Table 3). Several internal cooling breaks are recorded by variation upward from non-welded pumiceous ignimbrite to densely welded ignimbrite with fiamme and eutaxitic texture. The ignimbrite crops out from Alta Machay to Cajamarca over an area of ~100 km^2 (Fig. 3; Table 3; Plate I). Basal lithic concentrations are common and may be observed at Machay, where the middle member (11.30 ± 0.09 Ma, CB-74) unconformably overlies the Machay dome of the Azufre Andesite (12.01 ± 0.10 Ma), and nearby in Quebrada Azufre, where the middle member unconformably overlies Atazaico Andesite (Fig. 5C; Table A2; Plate I). These basal accumulations include accidental fragments of previous altered rock (see above) that are boulder size at Machay.

Six $^{40}Ar/^{39}Ar$ ages for the middle member range from 11.30 ± 0.09 to 11.22 ± 0.08 Ma and suggest a short time interval for eruption. Plagioclase and hornblende were analyzed for one sample (CB-38) and both yielded equivalent and acceptable plateau ages (11.27 ± 0.07 and 11.29 ± 0.15 Ma, respectively) with concordant isochron ages (Table A2). The weighted mean age of 11.27 ± 0.05 Ma (n = 5, MSWD = 0.78) is younger than the mean age for the lower member; however, the oldest age of the middle member is indistinguishable from the youngest age from the lower member so it remains unclear whether or not there is significant time interval between the two eruptions.

The upper member of the San Jose Ignimbrite (Tusj) is the most distinctive of the three members, has the smallest volume and surface exposure (16.5 km^2), and ranges in thickness from 10 to 100 m (Figs. 4, 5C, F, 7; Tables 3, 4; Plate I). This simple cooling unit is moderately to densely welded and contains abundant <10 cm- to 50 cm-long, commonly flattened blobs, and subordinate equant sub-angular blocks, of unvesiculated andesite (Fig. 5F; SD Fig. 8C). The flattened blobs are interpreted as spatter, and the deposit is termed a spatter ignimbrite (Longo, 2005; called the Sacsha breccia by Moore, 2002). The clasts are supported by a matrix of glass with ash-sized particles (<2 mm), dominated by broken plagioclase phenocrysts and small blobs and blocks. The upper member displays crude columnar jointing and dips 10°–15° south, away from an apparent vent (Fig. 5C, F). Weathered outcrops have a fluted appearance that is reminiscent of elutriation pipes in which resistant clasts stand in positive relief (Fig. 5F, SD Fig. 24).

The spatter ignimbrite has the most mafic mineralogy of the San Jose Ignimbrite and contains large poikilitic oxyhornblende and abundant green augite similar to the earlier Azufre Andesite, and rare 1 cm size, concentrically zoned hornblende similar to the middle San Jose member (Fig. 8; Table 3). The phenocryst mineralogy of the flattened clasts and the surrounding matrix are similar and both are phenocryst rich (Table 3). The ignimbrite has a weighted mean age of 11.25 ± 0.06 Ma (n = 2, MSWD = 0.027), and is identical to the weighted mean age of the middle member (Table A2). A hornblende separate from sample BS-3 yields a

plateau age (11.50 ± 0.09 Ma) that does not agree with geologic field evidence that it is part of the spatter ignimbrite. Its isochron age (11.30 ± 0.25 Ma), however, agrees with the mean age. This mean age supports two eruption scenarios that are consistent with the stratigraphic relationships; either a single continuous eruption produced both the middle and upper members, or the upper member represents a separate eruption <100,000 years after the middle.

San Jose Ignimbrite both overlies and hosts the San Jose gold deposit where the ignimbrite grades abruptly downward from fresh rock (~30 m depth) to weakly argillic altered rock (~60 m depth) rock, to gold-bearing (5–10 g/t Au) granular and vuggy quartz altered rock with cavities that resemble eutaxitic texture (Plate I; Klein et al., 1997, 1999; Longo, 2005). Before mining operations began at San Jose, siliceous laminated rocks cropped out above the fresh ignimbrite, and a narrow zone, 1 to 2 m wide, of hydrothermal opal and smectite typically marked the transition between the relatively fresh ignimbrite and quartz-rich altered rock (Klein et al., 1997; D.C. Noble, pers. commun., 1997; Sillitoe, 1999). Two diamond drill core samples (SJS-78A-5 m and -79A-20.3 m) of the ignimbrite above the gold deposit yielded ages of 11.43 ± 0.11 to 11.24 ± 0.10 Ma (Fig. 6; Table A2). The ages of these samples are interpreted as the lower and upper members, respectively, of the San Jose Ignimbrite. Local advanced argillic and weaker alteration also cuts both the upper and middle members of the San Jose Ignimbrite southeast of the Ocucho dome. These observations and the presence of gold-bearing hydrothermally altered accidental fragments included within the San Jose Ignimbrite indicate that this ignimbrite both pre- and postdates periods of gold deposition (Fig. 6).

Domes associated with the San Jose Ignimbrite (Tsjd domes): Three low-silica dacitic dome complexes were closely associated in time with the 11.5 to 11.2 Ma San Jose Ignimbrite. These extrusive domes are found at Ocucho (11.68 ± 0.07 and 11.36 ± 0.09 Ma), Chaquicocha Sur (11.28 ± 0.09 Ma), and Alta Machay (11.23 ± 0.07 Ma; Tables 3, A2; Plate I). The composite domes at Chaquicocha Sur, Ocucho, and Alta Machay are part of a 6.5-km-long, northeast trend that also includes the Azufre age San Jose, Baul, and Sacsha domes (Fig. 3; Plate I). The domes are elongated parallel to cm-spaced near-vertical flow banding (SD Fig. 21), were fed by dikes, and show evidence for successive emplacement and growth. Older hydrothermally altered andesitic domes are overlain by fresh domes that post date the San Jose Ignimbrite. The Ocucho dome complex (1.6 km^2) is emplaced into an older dome that was previously altered to kaolinite and opal. The Chaquicocha Sur dome (0.2 km^2) crops out in a glaciated valley and is the root of a formerly larger eroded dome complex. The Alta Machay dome (0.14 km^2) is the least eroded and crops out along the hanging wall of the Sugares fault (Fig. 3; Plate I). Erosional remnants of a pyroclastic deposit crop out on the south side of the dome and contain large blocks (up to 50 cm) of hornblende dacite that lie atop Azufre hornblende-pyroxene andesitic lavas.

The domes are porphyritic to seriate with flow-foliated phenocrysts within a pilotaxitic groundmass. The mineralogy of each dome is similar to a corresponding member of the San Jose Ignimbrite (Fig. 8; Table 3). The Ocucho and Chaquicocha Sur domes are similar to the lower and upper members and contain hornblende and green augite, whereas the Alta Machay dome is similar to the middle member and contains hornblende, but lacks pyroxene. Based on age and phenocryst mineralogy, the Ocucho, Alta Machay, and Chaquicocha Sur domes may occupy the respective vents for the lower, middle, and upper members of the San Jose Ignimbrite (Fig. 3; Plate I).

Coriwachay Dacite: The Coriwachay Dacite includes at least four units of small volume, high-silica, dacitic domes and plugs along with rhyolitic dikes and ignimbrites, that have ages from ~10.8 to 8.4 Ma (Fig 6; Plate I). The principal members are the Corimayo dacitic domes, the Cerro Yanacocha dacite porphyry intrusion, the Yanacocha Lake rhyolitic dike, and the Negritos rhyolitic ignimbrite. Quartz-eye dacite porphyry intrusions, resembling the dacite porphyry intrusion at Cerro Yanacocha, also crop out at Chaquicocha, but intense quartz-alunite and silicic alteration preclude $^{40}Ar/^{39}Ar$ dating. All units of the Coriwachay Dacite have a distinctive phenocryst mineralogy that includes quartz, biotite and hornblende, and accessory titanite (Fig. 8; Table 3; SD Fig. 25). Intrusions and domes have a porphyritic to seriate texture with a glassy to aplitic groundmass and abundant phenocrysts (Table 3; SD Fig. 26).

Corimayo dacite (Tcd): The Corimayo dacite is named for extrusive domes mostly buried beneath the La Quinua gravel deposits at Tapado and Corimayo (Gomez and Klein, 2000; Gomez, 2002), and include the Tapado dacite (U/Pb, zircon, 11.06 ± 0.02 Ma; Chiaradia et al., 2009) and the undated La Quinua dacitic dome (Longo, 2005). These domes, along with similar dacitic domes and intrusions, occupy an ~8 km easterly trend from La Quinua to Chaquicocha Norte. Domes at Corimayo, La Quinua, Punta Negra and Chaquicocha Norte have distinctive flow foliations and are spatially associated with silicified laminated rocks similar to those described in the Colorado Pyroclastics (Figs. 3, 9, Plate I). Dacitic tuffs associated with the domes were found only in drill core at Corimayo (Gomez and Klein, 2000; Gomez, 2002). The Corimayo dacites generally have a higher phenocryst content (up to 43 vol %) compared to other Coriwachay Dacites (Fig. 8; Table 3). The age of biotite from the dome at Corimayo is 10.78 ± 0.05 Ma (Table A2), and is similar to the ages from the Punta Negra dacite at Encajon (U/Pb, zircons, 10.72 ± 0.02 and 10.37 ± 0.02 Ma; $^{40}Ar/^{39}Ar$, biotite, 10.62 ± 0.15 Ma; Chiaradia et al., 2009). Chiaradia et al. (2009) report four ages for their Tapado dacite (U/Pb, zircons, 11.06 ± 0.02, 11.09 ± 0.24, and 11.38 ± 0.25 Ma; $^{40}Ar/^{39}Ar$, hornblende, 11.06 ± 0.67 Ma) and suggest the older zircon ages are antecrysts that reflect an older age inherent to progenitors of the final magma. Therefore, considering the possibility that their accepted age for the Tapado dacite (11.06 ± 0.02 Ma) also reflects the older age of an antecryst, we prefer to accept our $^{40}Ar/^{39}Ar$ age for the Corimayo dacite (10.78 ± 0.05 Ma).

Cerro Yanacocha dacite porphyry and late diatreme (Typq): Intrusions of dacite porphyry crop out at Yanacocha Norte, Yanacocha Oeste, and Chaquicocha along a northwest trend, and are spatially associated with gold ore (Fig. 9; Plate I). Dacite porphyry plugs have a northerly trend through the Cerro Yanacocha deposit, where they are spatially associated

with a large, matrix-supported breccia body containing fragments of the dacite porphyry and referred to as a diatreme. The dacite porphyry intrusions are both unaltered and altered. Altered porphyries have vuggy quartz with halos of advanced argillic alteration, and are cut by hypogene alunite- or alunite-pyrophyllite–cemented open-space breccia that contains covellite-enargite-pyrite assemblages (Loayza-Tam, 2002). Quartz phenocrysts are larger and more abundant, and ferromagnesian minerals less abundant, in the Cerro Yanacocha dacite porphyry compared to the Corimayo dacite (Fig. 8; Table 3; SD Fig. 26). Biotite from the dacite porphyry at Yanacocha Oeste has an age of 9.91±0.04 Ma (Table A2) that is identical to a $^{40}Ar/^{39}Ar$ age from dacitic porphyry at Yanacocha Norte (9.90 ± 0.05 Ma; Turner, 1997).

Yanacocha Lake rhyolitic dikes and plugs (Tcyr): These high-silica dacitic to rhyolitic intrusions are the youngest igneous rocks in the Yanacocha district. They form dikes exposed along a ~4 km northwest trend from Yanacocha Lake, where they intruded clay-altered diatreme breccias (Changanaqui, 1995), to Chaupiloma, where they intruded the Cerro Fraile dacitic pyroclastics (Plate I). The dikes display steeply dipping, commonly contorted, flow foliation. Quartz phenocrysts are smaller and more abundant in the Yanacocha Lake rhyolite compared to the other units of the Coriwachay Dacite (Table 3). Also, the Yanacocha rhyolite is locally spatially associated with diatreme breccias. For example, at Chaupiloma, angular and contorted fragments of the flow-foliated rhyolite occur in a breccia along the dike margin. A biotite from the Yanacocha Lake rhyolitic dike yielded an age of 8.40 ± 0.06 Ma (Turner, 1997), and is similar to another $^{40}Ar/^{39}Ar$ age of biotite (8.59 ± 0.14 Ma) from a rhyolitic intrusion at Yanacocha Oeste (Chiaradia et al., 2009).

Negritos ignimbrite (Tnr): At the Cerros de los Negritos, a single cooling unit of welded rhyolitic ignimbrite forms a ~50-m-thick erosional remnant (~5 km^2) that lies atop dacitic flow domes. The ignimbrite is columnar jointed, pinkish tan to light brown in color, and displays eutaxitic texture (Fig. 3; Tables 3, 4; Plate I; SD Fig. 27). The ignimbrite is crystal-rich, contains a phenocryst assemblage similar to other Coriwachay dacites, and has abundant accidental fragments of argillite, quartzite, porphyritic dacite, and rare granular to vuggy quartz. A sanidine from the Negritos ignimbrite yielded an age of 8.43 ± 0.04 Ma, identical to the age of the Yanacocha Lake rhyolite dike.

The Negritos ignimbrite may have vented near current exposures (Fig. 2) or from 8 km southeast from a fissure that is now occupied by the Chaupiloma and Yanacocha Lake rhyolitic dikes that have the same age as the Negritos ignimbrite.

Revisions to volcanic stratigraphy

Previous geologic mapping first defined most of the undated Cenozoic volcanic rocks in the Yanacocha district as the Calipuy Group, and these rocks were subdivided into the Llama Formation and the overlying Porculla Formation[3] and considered early Tertiary age (Cobbing et al., 1981; Wilson, 1984). The undated dacitic and rhyolitic pyroclastic rocks that overlie the Porculla Formation in the district were previously considered late Miocene and Pliocene age, and named the Huambos Formation (Reyes, 1980; Cobbing et al., 1981; Wilson, 1984). Subsequently, K/Ar and $^{40}Ar/^{39}Ar$ age determinations from pyroclastic units of the Llama Formation and the Huambos Formation in their type areas yielded Eocene ages (Noble et al., 1990).

The new geologic mapping and $^{40}Ar/^{39}Ar$ age determinations from this study significantly revise the volcanic stratigraphy of the Yanacocha district. Volcanic rocks of Eocene and Oligocene age have not been identified at Yanacocha, so previous correlations of local pyroclastic rocks with the Llama Formation (55–44 Ma), the Porculla Formation (~44 Ma), and the Huambos Formation (39–35 Ma, Noble et al., 1990) should be abandoned. Likewise, we have not recognized postmineral volcanic or subvolcanic rocks with late Miocene and Pliocene ages younger than 8 Ma. The pyroclastic rocks mapped as Huambos Formation (Reyes, 1980; Wilson, 1984) and subdivided into the Frailones and Otuzco Members (Turner, 1997) here yield middle Miocene ages of 15.5 to 15.1 and 11.5 to 11.2 Ma and are now assigned to the Cerro Fraile dacitic pyroclastic rocks of the Calipuy Group and the San Jose Ignimbrite of the Yanacocha Volcanics, respectively. Furthermore, the fresh andesitic rocks that were considered to be postmineralization and part of the late Miocene Regalado Volcanics (Turner, 1997) here yield middle Miocene ages from 14.5 to 11.7 Ma and are now assigned to the Atazaico and Azufre Andesites.

The revised stratigraphy now defines the volcanic rocks of the Calipuy Group at Yanacocha as the early Miocene Tual and Chaupiloma sequence of andesitic lahars (20-16 Ma) and the overlying Cerro Fraile dacitic pyroclastic rocks (15.5–15.1 Ma). These rocks can be broadly correlated across the district and underlie the younger Yanacocha Volcanics. The Yanacocha Volcanics are here defined as five units that include in ascending stratigraphic order the Atazaico Andesite, the Colorado Pyroclastics, the Azufre Andesite, the San Jose Ignimbrite, and the Coriwachay Dacite (Fig. 4, 7, Sections E-H). The Atazaico Andesite (14.5–13.3 Ma) is a first sequence of intermediate composition lavas and are intruded by the Quilish dacites (~14.2–12.6 Ma). The younger Colorado Pyroclastics (12.6–12.4 Ma) are here subdivided into three members that include the basal laminated rocks, the Cori Coshpa ignimbrite, and the Maqui Maqui ignimbrite. These rocks are intruded or overlain by the Yanacocha porphyries (12.4–11.9 Ma). The Azufre Andesite (12.1–11.7 Ma) is a second sequence of intermediate composition lavas that are similar to, but younger than, the Atazaico Andesites. Three new members are now defined for the San Jose Ignimbrite (11.5–11.2 Ma) and mapped to source vents occupied by domes of similar age in the east-central part of the district (Figs. 3, 7; Plate I). The Coriwachy Dacites are now recognized as the youngest igneous rocks (10.8–8.4 Ma) at Yanacocha, and are localized to the east-central part of the district.

All these Miocene rocks, and especially the pyroclastic units, host or are associated with gold mineralization at Yanacocha. The Atazaico Andesite and Cerro Frailes pyroclastic rocks host gold in the west part of the district and at depth in the east-central part of the district. The Colorado Pyroclastics

[3] Reyes (1980) first applied the name San Pablo Formation to a sequence of andesitic and dacitic volcanic rocks of the upper Calipuy Group that were subsequently named Porculla Formation by Cobbing et al. (1981).

host much of the gold ore at Maqui Maqui, Cerro Yanacocha, Carachugo and Chaquicocha. The Azufre Andesite also hosts gold mineralization in the east-central part of the district at Chaquicocha, Quecher, and Arnacocha. The San Jose Ignimbrite hosts much of the gold at the San Jose deposit, and the Coriwachay dacites are spatially associated with the gold mineralization from Corimayo to Cerro Yanacocha and Chaquicocha (Fig. 3, Plate I).

Petrology of the Magmas

Each major eruptive and intrusive rock sequence of both the Yanacocha Volcanics and the older Calipuy Group volcanics can be distinguished on the basis of phenocryst mineralogy and abundance as well as major and trace element composition (Figs. 8, 10–12; Tables 3, 5). Effusive eruptions of the Atazaico and Azufre andesites (effusive stages 1 and 2) contain clinopyroxene and high-Al amphibole, whereas explosive eruptions of the Maqui Maqui dacitic ignimbrite of the Colorado Pyroclastics and the dacitic San Jose Ignimbrite (explosive stages 1 and 2) contain biotite, both low- and high-Al amphibole, and local clinopyroxene, sanidine, and titanite (Longo, 2005). Magmatic activity culminated with the Coriwachay high-silica dacitic to rhyolitic domes, intrusions, and ignimbrites that contain low-Al amphibole, biotite, magnetite, titanite, and quartz. On the basis of amphibole barometry, high-Al hornblende crystallized at ~900°C at ~20 km depth from a magma of more mafic composition than the dacites, which contain low-Al hornblende crystallized at ~750° to 800°C from a dacitic upper crustal magma chamber (~5–10 km depth) (Longo, 2005; Chambefort et al., 2008). Therefore, the effusive stage andesites evolved from deep sources, whereas the explosive stages and late Coriwachy dacite are largely evolved in shallow magma chambers. The presence of hornblende throughout the eruptive sequence indicates that melts had high water contents (>4 wt %; Burnham, 1979; Behrens and Gaillard, 2006). The presence of small anhydrite inclusions in high- and low-Al hornblende and pyroxene indicates that the magmas were sulfur rich and sulfate saturated (oxidized) throughout much of their evolution (Chambefort et al., 2008).

Major-element compositions

The combined volcanic and subvolcanic intrusive rocks of the Yanacocha Volcanics range from 57 to 71 wt percent SiO_2, The volcanic rocks dominate igneous rock compositions with <66 wt percent SiO_2 (Fig. 10A-C). Volumetrically minor subvolcanic intrusions range from 55.3 to 70.6 wt percent SiO_2, and include the late Coriwachay Dacites that are the only rocks with >66 wt percent SiO_2 (Figs. 8, 10, 11; Table 3). The Yanacocha Volcanics define a medium- to high-K calc-alkaline suite that ranges from andesite through dacite and rhyolite, and they are distinctly higher in K_2O than the older andesites and dacites of the Calipuy Group (Figs. 10C, 11). Nearly 25 percent of our samples of Yanacocha Volcanics ranging from 60 to 65 wt percent SiO_2 have high total alkali contents and are classified as trachyandesite and trachydacite (Figs. 10C, 11; Tables 3, 5). The K_2O content increases and TiO_2, P_2O_5, MgO and FeO contents decrease with increasing SiO_2 in the Yanacocha Volcanics, similar to other calc-alkaline suites globally (Fig. 10A-D). TiO_2 decreases smoothly with increasing SiO_2, consistent with melt evolution to higher SiO_2 via simple differentiation from a mafic parent magma (Fig. 10B). In contrast, both P_2O_5 and MgO illustrate wide scatter at a given SiO_2 content that is not consistent with simple fractional crystallization of a single mafic parent (Fig. 10A, D).

The Colorado Pyroclastics, Azufre Andesite, and San Jose Ignimbrite have similar compositions that lie along the andesite-dacite boundary and range from 60 to 66 wt percent SiO_2. They are more K_2O rich than the earlier Atazaico Andesite and related Quilish dacitic intrusions (Fig. 11; Table 5). The evolution from the Atazaico Andesite to the Colorado-Azufre-San Jose silicic andesite and low-silica dacite follows a trend of sharply decreasing MgO with increased SiO_2. In contrast, the younger Coriwachay Dacites have significantly greater SiO_2 values and lie along a higher MgO-SiO_2 trajectory (Fig. 10D).

Trace-element compositions

Both Sr and Ba display a large range at a given SiO_2 content (particularly at 60-66 wt %; Figs. 10E, F) and provide evidence for geochemical heterogeneity inconsistent with a single magma source and simple evolution. Strontium increases with SiO_2 content in the pyroxene-bearing rocks from the Atazaico Andesite to compositions of about 62 wt percent SiO_2, and then decreases slightly from 62 to 71 wt percent SiO_2 in the San Jose Ignimbrite and the late Coriwachay Dacite. Barium increases with increasing SiO_2 content, consistent with its generally incompatible behavior in magmas (Korringa and Noble, 1971; Blundy and Wood, 1991).

Chondrite-normalized rare earth element (REE) data for the Yanacocha Volcanics define a consistent inclined pattern, with light REE enrichment (10–100 times chondrite), a relatively flat pattern of heavy REE (2–20 times chondrite), and a lack of any Eu anomaly (Fig. 12). These patterns are characteristic of many andesitic to dacitic volcanic and hypabyssal plutonic rocks associated with porphyry copper and epithermal gold deposits in the Andes and elsewhere (e.g., Gustafson, 1979; Chiaradia et al., 2004). Within the Yanacocha Volcanics, the REE abundances vary by a factor of 2 to 5, with the highest concentrations observed in the Atazaico Andesite and the lowest concentrations in the late evolved Coriwachay Dacite. The light REEs show a slightly smaller range than the heavy REEs, as evidenced by more steeply inclined patterns of the Coriwachay Dacite.

Discussion of magmatic evolution

The compositional evolution of magmas through time at Yanacocha reflects complex processes that include deep mafic source magmas and crustal assimilation combined with crystal fractionation and differentation in both deep and shallow magma reservoirs (see also Chiaradia et al., 2009). Hydrous, sulfate-rich, relatively mafic andesite to basalt likely differentiated in deep magma chambers and conduits (Chambefort et al., 2008), whereas shallow dacitic magma chambers evolved by both crystal fractionation of mafic magma and mixing with crystal melts. The latter processes produced the late Coriwachay high-silica dacite and rhyolite that are temporally associated with most of the gold ores.

Figure 13 illustrates the key fractionation and mixing processes. Deep-sourced hydrous basaltic andesite magmas apparently fractionated garnet and amphibole to produce the

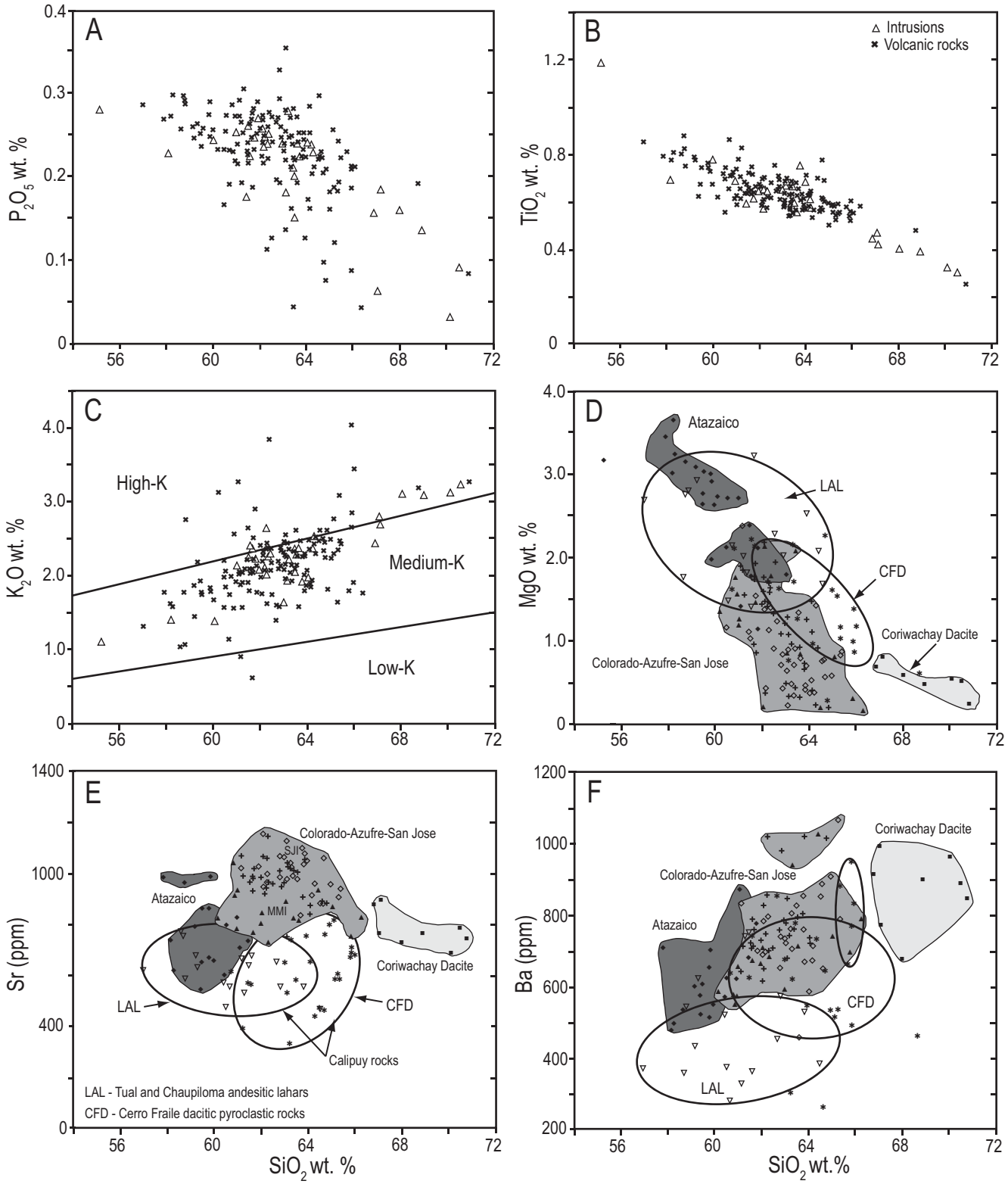

FIG. 10. Selected silica variation diagrams (SiO_2, wt %) for the Calipuy Group volcanic rocks and Yanacocha Volcanics (n = 184): (A) vs. P_2O_5 (wt %); (B) vs. TiO_2 (wt %); (C) vs. K_2O (wt %), illustrating overlapping compositions of volcanic versus intrusive rocks. (D) vs. MgO (wt %); (E) vs. Sr (ppm); (F) vs. Ba (ppm), illustrating lower Ba content of the Calipuy Group (LAL – Tual-Chaupiloma andesitic lahars and CFD – Cerro Fraile dacitic pyroclastics) in comparison with the Yanacocha Volcanics.

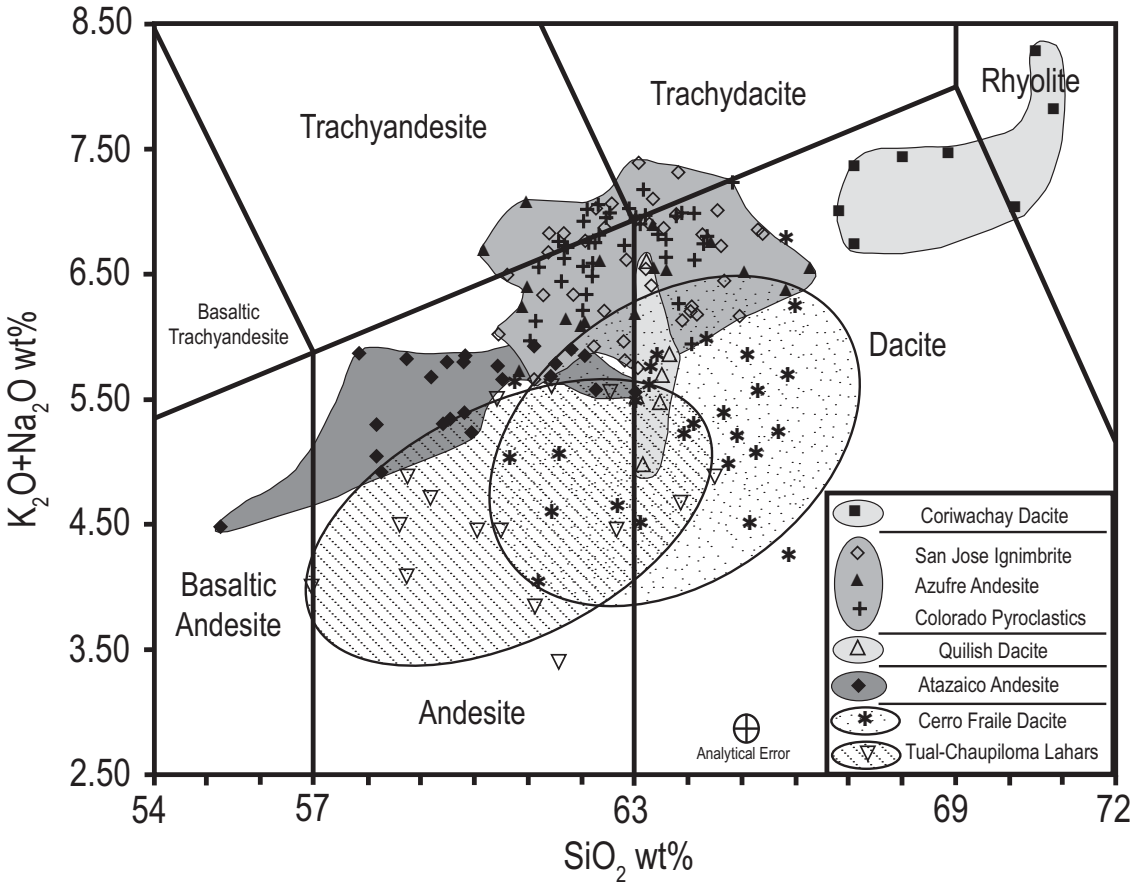

FIG. 11. Total alkali (K_2O plus Na_2O, wt %) versus silica (SiO_2, wt %) diagram (after Le Bas et al., 1986; Best, 2003) for all samples (N = 184) of the Calipuy Group volcanic rocks and the Yanacocha Volcanics from this study. The diagram shows the compositional variation in the Calipuy Group volcanic rocks (Tual-Chaupiloma lahars, Cerro Fraile dacite) and Yanacocha Volcanics (Atazaico Andesite, Colorado Pyroclastics, Azufre Andesite, San Jose Ignimbrite, and Coriwachay Dacite); units in the legend are placed in stratigraphic order. The compositional fields of the Colorado, Azufre, and San Jose units overlap and are plotted as a single field centered on the andesite-dacite boundary.

adakite-like trend of decreasing Y and increasing Sr/Y observed in the Atazaico and Azufre Andesites (Defant and Drummond, 1990). This Y versus Sr/Y trend (Fig 13A) is commonly observed in porphyry copper or other magmas derived from a deep source area where garnet is typically stable (>35 km, i.e., >12 kbars pressure) and preferentially incorporates Y (Chiaradia et al., 2004; Johnson, 1998). Crystal fractionation of garnet, high-Al amphibole, and pyroxene in deep magma conduits would have also reduced the heavy REE content as observed during magma evolution (Kay and Mpodozis, 2001; Figs. 10B, D, 12). This differentiation trend is also characterized by an increase of Sr as a result of the absence of sodic plagioclase, which strongly incorporates Sr but is destabilized under high water-pressure conditions (>2 kbars; Singer et al., 1995). Therefore, much of the differentiation from basaltic andesite to silicic andesite or low-silica dacite occurred via crystal fractionation in deep conduits or magma chambers at >35 to 7 km depth.

The second major process involves assimilation of crustal rock to produce rhyolitic melts that mix with deep-sourced magmas. Such assimilation and mixing may have occurred in both the deep and shallow magma chambers. The elevated content of Ba (500–1,100 ppm) and K_2O (1–3.5 wt %) are both greater than what can be produced by simple crystal fractionation from a basaltic parent, and therefore require crustal sources. The great range of Ba at given SiO_2 content is consistent with assimilation of heterogeneous crustal compositions. Chiaradia et al. (2009) presented isotopic data that indicate an increased component of crustal-derived material in the more silicic and younger magmas at Yanacocha. Figure 13B illustrates the approximate path on a SiO_2 versus MgO diagram produced by crystal fractionation of mafic silicates in deep magmas from a parent Atazaico Andesite with 58 wt percent SiO_2. Although some magma compositions follow this trend, many compositions between 60 and 64 wt percent SiO_2 lie along mixing lines between low-silica parent and high silica differentiates. A mixing hypothesis also explains the presence of both high-Al and low-Al amphiboles in the Colorado Pyroclastics and the San Jose Ignimbrite.

Much of the magma differentiation took place in shallow magma chambers. The mineral assemblage of sodic plagioclase, low-Al hornblende, biotite, pyroxene, Fe-Ti oxides, and titanite in the low-silica dacitic San Jose Ignimbrite provide evidence for shallow crystallization (~750°–800°C and 1.5–2

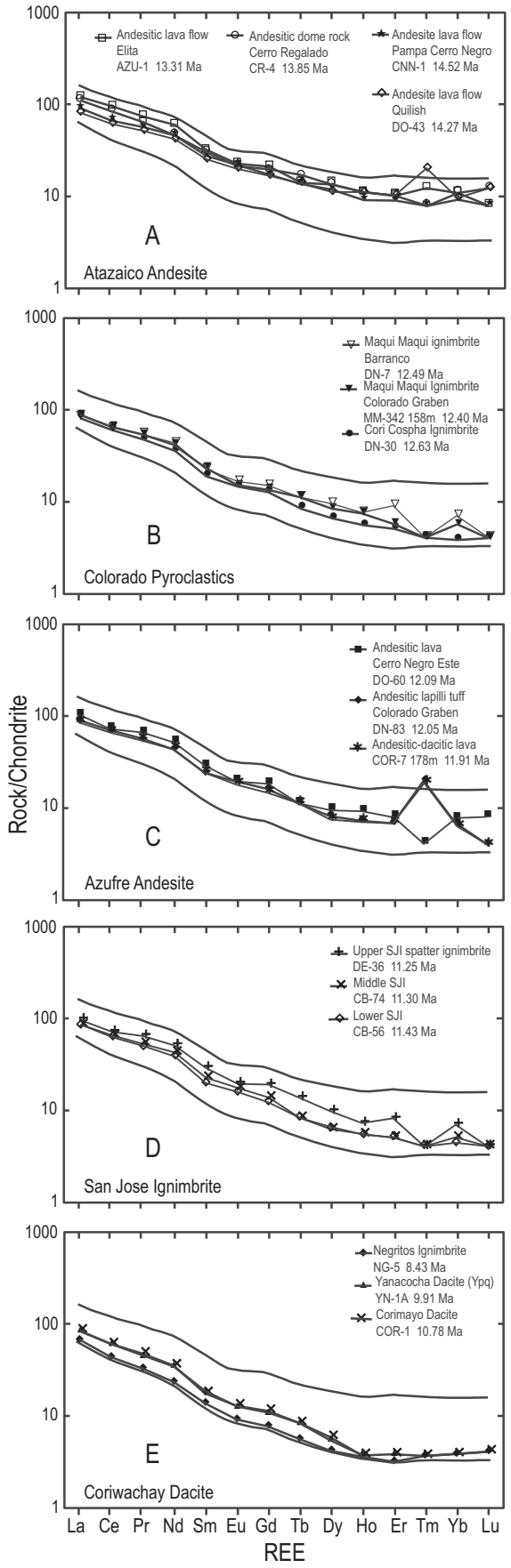

kbars; Chambefort et al., 2008). The decrease of Sr content with increase of SiO_2 to more than 62 wt. percent is consistent with crystallization of plagioclase (Fig. 10E). The lack of an attendant Eu anomaly suggests the magma was oxidized (Weill and Drake, 1973). The decrease in abundance of middle and heavy REE for the San Jose Ignimbrite supports the hypothesis that magmatic evolution involved fractional crystallization of hornblende, titanite, and apatite minerals preferentially enriched in middle and heavy REE (Fig. 12). We conclude that complex processes that include periodic input of a basaltic andesite or low-silica andesite parent magma combined with assimilation-fractional crystallization and magma mixing can produce the observed diversity of high-silica andesite and low-silica dacite (DePaolo, 1981).

The silicic magmas of Coriwachay Dacite appear to be mixtures of silica-rich differentiates or crustal melts (>70 wt % SiO_2) with silicic andesite and low-silica dacite (~62–63 wt % SiO_2) on the basis of the SiO_2 versus MgO plot (Fig. 13B). The Coriwachay Dacites have MgO contents that are too high to be produced by simple crystal fractionation, and therefore require periodical recharge by more mafic melt.

These late Coriwachay dacites and rhyolites are volumetrically minor, but are associated with the bulk of the gold, copper, and sulfur introduction. They are characterized by the highest contents of incompatible elements such as K and Ba, and the lowest middle and heavy REE contents of all the Yanacocha magmas (Figs. 10–12). These REE compositions are consistent with fractional cystallization of low-Al hornblende, titanite, and apatite together with plagioclase in a shallow magma chamber similar to andesite-dacite of the San Jose Ignimbrite. The crystal-rich nature of the late Coriwachay Dacite is consistent with derivation from one or more crystallizing fluid-saturated granitoid magma chambers (e.g., Burnham, 1979; Dilles, 1987) that we hypothesize was periodically recharged by small amounts of deep-sourced and more mafic magma over a period of 2 to 3 m.y.

The Yanacocha magmas were strongly oxidized at NNO +1.5 to +2 based on Fe-Ti oxide geothermometry and the assemblage magnetite + titanite + quartz (Wones, 1989; Longo, 2005; Ghiorso and Evans, 2008). Under these oxidized conditions, little reduced sulfur was present in the melt and magmatic Fe- and Cu-Fe sulfides were only formed in the trace amounts observed (Brennecka, 2005). Therefore, copper and likely gold behaved in the magmas as incompatible elements, similar to Ba (Dilles, 1987; Dilles and Proffett, 1995). The increase of Ba with increased SiO_2 content provides a proxy that is consistent with enrichment of copper and possibly gold in the youngest dacitic-rhyolitic magmas. Thus, we propose that water-, chlorine-, and sulfur-rich fluids separated from the crystallizing silicic magmas and removed magmatic copper

FIG. 12. Rare earth element (REE) patterns normalized to chondrite (Sun and McDonough, 1989) for representative samples of the five main units of the Yanacocha Volcanics, from oldest to youngest: A) Atazaico Andesite, B) Colorado Pyroclastics, C) Azufre Andesite, D) San Jose Ignimbrite, and E) Coriwachay Dacite. The solid black lines outline the field for all the samples in A through E. Note the decrease in REE abundance from oldest to youngest.

TABLE 5. Representative Whole-Rock Chemical Analyses of Igneous Rocks

	Tual andesitic lahar CC-18	Chaupiloma andesitic lahar DN-84	Cerro Fraile Pyroclastics Frailes-1	Atazaico Andesite CNN-1	Quilish Dacite DO-4	Azufre Andesite CHQS-2	Colorado Pyroclastics Maqui Maqui ignimbrite DN-7	Lower San Jose Ignimbrite CB-56	Coriwachay Dacite Cerro Yanacocha YN-1A
Wt %									
SiO_2	61.18	59.33	64.96	61.48	63.50	63.07	63.07	63.86	68.09
TiO_2	0.82	0.62	0.50	0.67	0.58	0.59	0.58	0.56	0.40
Al_2O_3	20.02	18.90	17.17	17.67	17.27	18.09	18.21	18.87	16.72
Fe_2O_3	5.45	5.54	5.24	5.61	5.48	4.31	4.47	3.88	2.55
MnO	0.08	0.08	0.11	0.10	0.18	0.06	0.10	0.03	0.05
MgO	2.01	0.43	1.60	2.38	1.71	1.28	0.85	0.47	0.58
CaO	6.26	8.55	4.89	5.98	5.27	5.28	6.15	4.54	3.85
Na_2O	2.92	4.01	2.72	3.81	3.33	4.60	4.05	5.05	4.33
K_2O	0.90	2.16	2.48	1.89	2.37	2.28	2.14	2.27	3.10
P_2O_5	0.25	0.26	0.16	0.24	0.21	0.23	0.22	0.25	0.16
ppm									
Ba	327	624	959	681	569	776	591	758	677
Co	6.5	9.3	9.5	13.0	9	7.5	8.0	6.7	3.5
Cr	50	70	nd	nd	nd	nd	nd	40.0	nd
Cs	1.7	2.8	2.2	0.9	2.9	1.0	1.8	10.3	7.6
Cu	35	17	20	25	<5	<5	20	13	<5
Ga	22	21	20	21	18	23	22	25	23
Hf	3	4	3	3	2	3	3	3	3
Mo	8	3	nd	nd	nd	nd	nd	2	nd
Nb	7	7	7	4	4	5	6	5	4
Ni	10	<5	15	15	<5	<5	5	6	<5
Pb	10	10	20	30	<5	10	5	13	25
Rb	41.6	62.4	76.8	50	69	50.8	58.2	69.9	80
Sn	2	1	1	<1	<1	<1	1	1	<1
Sr	667	632	612	737	497	888	888	1035	729
Ta	0.5	0.5	0.5	<0.5	<5	<0.5	<0.5	<0.5	<0.5
Th	5	6	5	4	6	6	5	5	7
Tl	<0.5	<0.5	<0.5	0.5	<0.5	<0.5	<0.5	<1	<0.5
U	1.5	1.6	4	1.5	2	1.5	1.5	1.8	2.5
V	160	111	85	135	115	10	80	107	10
W	3	1	1	<1	<1	<1	3	1	<1
Y	43	14.2	11.5	15	13.5	8	13	8.1	5
Zn	65	80	65	70	45	75	60	99	215
Zr	122	114	102.5	116.5	79	126	131.5	112.5	111.5
La	25	19.2	18.5	21	19.5	24.5	20.5	20.7	20
Ce	36.5	38	35	41.5	36	48.5	37.5	39.9	37.5
Pr	5.3	4.5	4.1	5.2	4.5	5.8	5	4.8	4.2
Nd	20	17.8	16	21	16.5	21.5	19.5	18	15.5
Sm	4.8	3.2	3.2	4.0	3.3	3.9	3.3	3	2.7
Eu	1.4	1.1	0.7	1.2	0.8	1	0.9	0.9	0.7
Gd	4.9	3.1	2.7	3.4	3.1	3.0	2.9	2.4	2.1
Tb	0.8	0.5	0.4	0.5	0.4	0.4	0.4	0.3	0.3
Dy	5.8	2.6	2.3	2.9	2.2	2.2	2.3	1.6	1.3
Ho	1.3	0.5	0.4	0.5	0.5	0.3	0.4	0.3	0.2
Er	4.3	1.4	1.3	1.4	1.3	1.0	1.4	0.8	0.6
Tm	0.7	0.2	0.1	0.2	0.2	0.1	0.1	0.1	0.1
Yb	4.6	1.3	1.3	1.5	1.2	1.0	1.1	0.7	0.6
Lu	0.9	0.2	0.2	0.2	0.2	0.1	0.1	0.1	0.1
Sr/Y	15.5	44.5	53.2	49.1	36.8	111.0	68.3	127.8	145.8
Ce/Yb	7.9	29.2	26.9	27.7	30.0	48.5	34.1	57.0	62.5

Analyses normalized 100% volatile-free composition

and gold to form ore fluids (Burnham, 1979; Dilles, 1987; Simon et al., 2005, 2006).

Age of Hydrothermal Alteration

Hydrothermal alteration that is associated with the gold deposits covers >100 km^2 and consists of massive and vuggy quartz, and several advanced argillic assemblages containing alunite, pyrophyllite, diaspore, dickite, and kaolinite plus quartz and pyrite (Plate I). Hydrothermal alunite is present in several of the high-sulfidation gold deposits (Fig. 14). As discussed above, the age of alunite at any given deposit provides an estimate of the maximum age of the gold mineralization at that deposit.

Twenty $^{40}Ar/^{39}Ar$ age determinations on hypogene alunite and one on hydrothermal biotite define five stages of hydrothermal activity, from 13.6 to 8.2 Ma, associated with gold

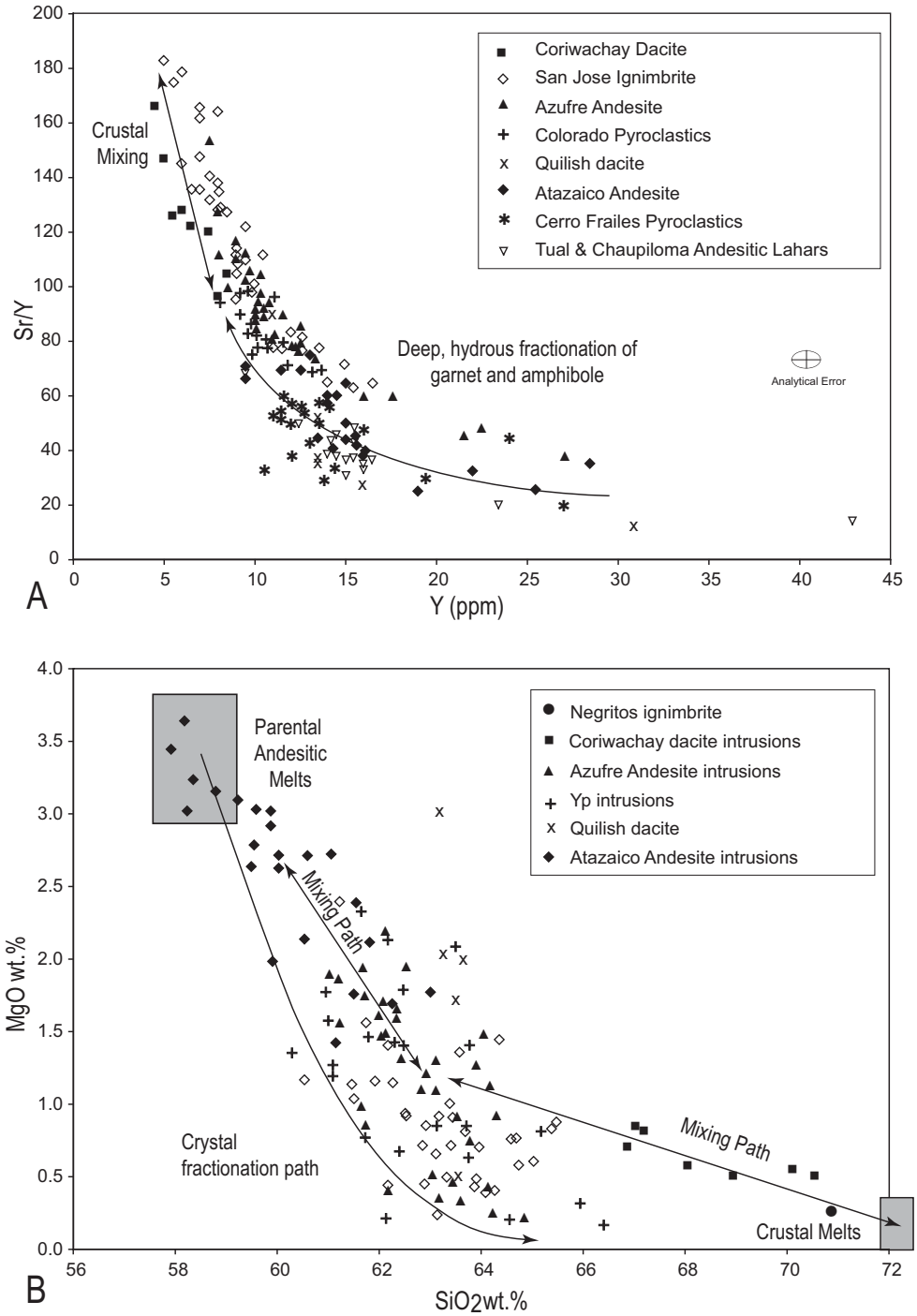

FIG. 13. Trace and major element diagrams illustrating crystal fractionation versus mixing of mafic and silicic melts. A. Y vs. Sr/Y, illustrating the fractional crystallization (amphibole, garnet, pyroxene) path in deep hydrous magmas for the Calipuy Group and early Yanacocha Volcanics, versus late Yanacocha Volcanics mixing trends. B. SiO_2 versus MgO illustrating early crystal fractionation, and intermediate and late stage mixing paths with parental magma compositions. Note high MgO contents of Coriwachay Dacites require admixture of a mafic magma component. Symbols as in A. B also highlights the location of intrusions.

deposits in the Yanacocha district (Figs. 6, 9; Table A2; Longo, 2005; Longo and Teal, 2005). The ages of these 21 altered samples are plotted versus distance along a pseudo-section 15 km long, from Cerro Negro Oeste in the southwest to Cerro Sugares at Maqui Maqui in the northeast (Fig. 14; Plate I). These data indicate that hydrothermal activity began in the southwest at Cerro Negro and Quilish, and then migrated concurrently with magmatism to the eastern parts of the district where it became widespread. By ~9.25 Ma hydrothermal activity became centered exclusively at Cerro Yanacocha (Fig. 14).

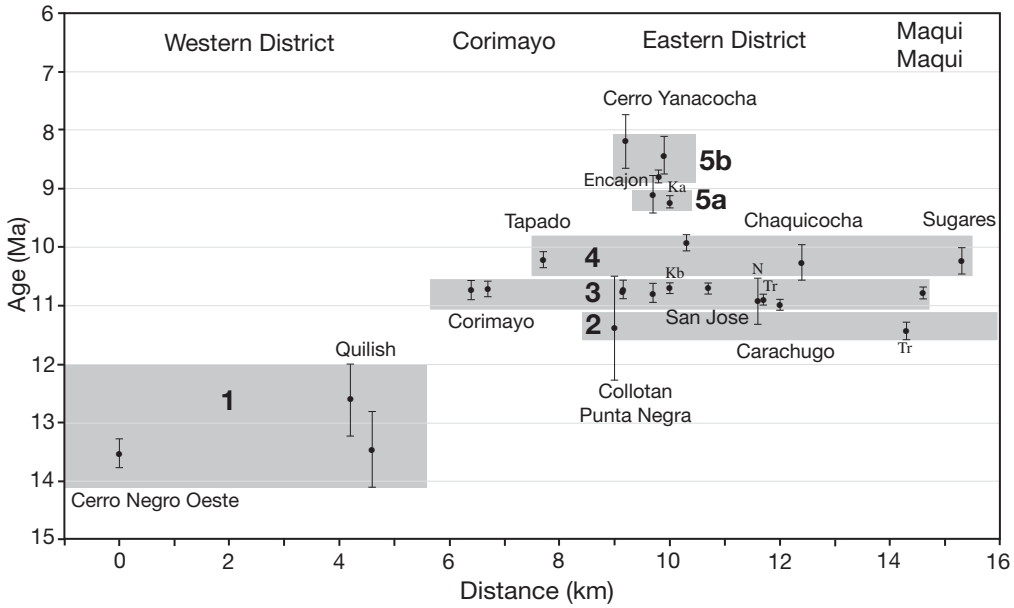

FIG. 14. $^{40}Ar/^{39}Ar$ ages for 21 samples of hydrothermal alunite and biotite plotted versus distance along a 16-km southwest-northeast transect from Cerro Negro Oeste to Maqui Maqui in the northeast (Fig. 9; Plate I). These ages define five general stages of hydrothermal activity, which indicate an early northeastward temporal migration, followed by a late focus, at ~9.25 Ma, at Cerro Yanacocha: stage 1 ~14.2–12.0 Ma, stage 2 ~11.5–11.2 Ma, stage 3 ~11.0–10.7 Ma, stage 4 ~10.3–9.95 Ma, stage 5 ~9.25–8.22 Ma. Ka = Kupfertal alunite, Kb = Kupfertal biotite; N = Noble, pers. commun. (1997), Tr = Turner (1997).

Hydrothermal stage 1 alunite has been found only in the gold deposits at Cerro Negro Oeste (13.56 ± 0.24 Ma) and nearby at Quilish (n = 2, 13.48 ± 0.64 and 12.64 ± 0.61 Ma), both in the southwest. Subsequent Stage 2 hydrothermal activity was apparently widespread in the eastern part of the Yanacocha district at ~11.5 Ma, consistent with eastward migration of hydrothermal activity that traced the progression of volcanism through time across the district. Stage 2 alunite occurs at Cerro Collotan, at Cerro Yanacocha (CLL-1, 11.41 ± 0.89 Ma), and in a zone of advanced argillic alteration with only trace (<100 ppb) gold at Cerro Azufre, adjacent to the Maqui Maqui gold deposit (11.46 ± 0.15 Ma; Turner, 1997; Fig. 14; Plate I). Widespread stage 2 alteration here is interpreted to include extensive and largely barren massive and vuggy quartz crosscut by later sulfide-gold veins, heterolithic breccia, and alunite veins in the Cerro Yanacocha area (Harvey et al., 1999; Longo, 2000, 2005; Loayza-Tam, 2002). The gold-bearing and strongly hydrothermally altered accidental fragments present in the 11.5 to 11.2 Ma San Jose Ignimbrite are inferred to have formed in stage 2.

After eruption of the San Jose Ignimbrite, hydrothermal stage 3 alunite was widely generated along a ~10-km-long northeasterly trending zone from Corimayo to Maqui Maqui (Figs. 9, 14; Plate I). Hydrothermal activity occurred at Corimayo-Tapado, Cerro Yanacocha, Carachugo and Maqui Maqui from ~11.0 to 10.7 Ma on the basis of seven alunite ages and one hydrothermal biotite age, the latter from the underlying Kupfertal porphyry deposit.[4] Hydrothermal biotite at Kupfertal, collected from a depth of 571 m in core hole DDH KUP-3, has an age of 10.73 ± 0.05 Ma (Table A3). Outcrops of quartz-alunite-pyrophyllite–altered andesite cut by quartz-pyrite-enargite-covellite stockwork veinlets with >0.5 g/t Au and up to 1.0 wt percent Cu occur directly above the dated hydrothermal biotite sample. The age of igneous biotite (10.78 ± 0.05 Ma) from the Corimayo dacite dome is similar to the ages of hypogene alunites (10.75 ± 0.16 Ma) from younger cross-cutting veins and breccia (~4 km west of Kupertal), and is similar to the Punta Negra dacite (10.72 ± 0.02 Ma; Chiaradia et al., 2009) at Encajon (~1 km west of Kupfertal) that is crosscut by advanced argillic alteration with alunite (10.81 ± 0.16 Ma; Table A3, Fig. 3, Plate I). Therefore, the $^{40}Ar/^{39}Ar$ ages from six alunites and the hydrothermal biotite age from the Kupfertal porphyry are analytically indistinguishable and have a weighted mean of 10.75 ± 0.04 Ma, and support a single widespread event associated with the 10.75 to 10.72 Ma Corimayo and Encajon dacites (Figs. 6, 14). Nonetheless, one stage 3 alunite age of 11.01 ± 0.09 Ma from veins that crosscut the San Jose Ignimbrite at Cerro Baul is analytically older (Fig. 6), but similar to the ~11.1 Ma age of a dacite at Tapado (Chiaradia et al., 2009). Similar $^{40}Ar/^{39}Ar$ ages for alunites were obtained at nearby Carachugo Sur (10.92 ± 0.09 Ma, Turner, 1997; 10.95 ± 0.40 Ma, Noble, pers. commun., 1997).

A period between ~10.75 and ~10.25 Ma (Figs. 6, 9) lacks hydrothermal ages, and is followed by widespread stage 4 alunite ages that range from 10.3 to 9.9 Ma (n = 4) in the eastern part of the district. Here, alunite is associated with gold mineralization that occurs along a ~4-km-long east-west trend from Chaquicocha to Tapado and a further ~7 km northeast of Tapado at Sugares (Fig. 14; Plate I). The three

[4] The Kupfertal porphyry deposit lies between the San Jose deposit and the Encajon-Cerro Yanacocha deposits ~400 m below the bottom of a deeply incised glacial valley with 300 meters of vertical relief (see Fig. 3; Plate I).

alunite ages from the Chaquicocha and Tapado deposits, and Sugares (Leach, 1999) near the Maqui Maqui deposit, are analytically indistinguishable, and have a weighted mean age of 10.25 ± 0.11 Ma. Alunite from an outcropping zone of quartz-alunite alteration adjacent to the San Jose Sur deposit has an age of 9.95 ± 0.14 Ma (Table A3) that is ~0.8 m.y. younger than the 10.73 Ma age of hydrothermal biotite from the Kupfertal porphyry.

Stage 5 alunites are samples of hydrothermal breccias with alunite cement associated with the central zone of gold deposits at Cerro Yanacocha, ~500 m to 1 km north of the youngest stage 4 alunite at San Jose (Plate I; Table A3). Five ages range from 9.2 to 8.2 Ma and three have relatively large analytical uncertainties (Figs. 6, 14). These alunite ages imply two substages at ~9.2 and ~8.8 Ma that follow an apparent gap in hydrothermal activity from ~9.9 to ~9.3 Ma (Figs. 6, 9, 14). The five alunites are permissive and do not require two substages; however, two substages are supported by geologic evidence for multiple hydrothermal veins and breccias that postdate the Cerro Yanacocha dacite porphyry (9.91 Ma). At Encajon and Cerro Yanacocha, veins cut earlier veins, and breccias contain fragments of both earlier breccia and veins (Abarca and Harvey, 1997; Loayza-Tam, 2002).

Temporal relationship of porphyry-style and epithermal alteration at Yanacocha

Based on previous work by P. Mitchell (writ. commun., 2000), R.H. Sillitoe (writ. commun., 2000), Pinto (2002), and Gustafson et al. (2004), a spatial relationship was proposed for porphyry- and epithermal-style alteration at Kupfertal, Yanacocha Norte, Maqui Maqui, La Zanja, Tantahuatay, Perol and Hualamachay (Figs 1, 2). These authors suggested that hypogene advanced argillic alteration and high-sulfidation gold ores overlie and grade downward to deeper porphyry-style biotite alteration with Cu-Fe sulfides. Alteration grades downward from vuggy and massive quartz to a gray quartz-rich rock with irregular white patches of alunite and pyrophyllite that replace the quartz matrix and grade into worm-shaped clots and discontinuous veinlets (Klein et al., 1999; Hedenquist, pers. commun., 2000; Pinto, 2002), termed patchy and wormy texture alteration (also termed *gusano*; Gustafson et al., 2004). A transition from patchy and deeper wormy texture alteration to A-type quartz veins occurs from ~90- to 150-m depth at Kupfertal (Gustafson et al., 2004). The wormy quartz-pyrophyllite-alunite overlies sericitic (muscovite) alteration, which in turn overlies deeper biotite-bearing potassic alteration containing pyrite, chalcopyrite, and bornite.

The $^{40}Ar/^{39}Ar$ age determinations provide temporal-spatial constraints on the transition from the shallower epithermal environment to the deeper porphyry system at Kupfertal. These constraints are plausible despite minor complications that include the overprint of younger quartz-alunite alteration and possible fault offsets. The age of the deep porphyry-style biotite alteration at Kupfertal (10.73 ± 0.05 Ma) is the same as the widespread stage 3 magmatic-hydrothermal alunites located ~4 km west at Corimayo, ~1 km northwest at Punta Negra in Encajon, and 0.8 km south of Kupfertal from a sample of Yanacocha porphyry (Yp) ~50 m below the San Jose Sur deposit (stage 3; Figs. 6, 14; Table A3). These data indicate that shallow epithermal quartz-alunite alteration was contemporaneous but ~1 to 4 km distal to the deeper Kupfertal Cu-Au-bearing hydrothermal biotite alteration; similar to the distribution of quartz-alunite alteration at Lepanto, Philippines, which occurs up to 4 km from the causative Far Southeast porphyry (Hedenquist et al., 1998).

The two alunite samples closest to the Kupfertal porphyry yield much younger ages that indicate they were not formed from the same porphyry hydrothermal event. Alunite from the San Jose Sur deposit that is topographically above and ~500 m south of Kupfertal has an age of 9.95 ± 0.14 Ma, and patchy alunite that formed directly above the Kupfertal porphyry has an age of 9.25 ± 0.10 Ma; ~0.8 and ~1.5 m.y. younger than the porphyry-style biotite alteration at Kupfertal, respectively. These two younger alunites apparently developed in stages 4 and 5, respectively. The biotite and alunite ages near Kupfertal are consistent with observations throughout the east-central part of the Yanacocha district that suggest at least three distinct hydrothermal vein and breccia events with alunite ages of 11.1–10.7, 10.3–9.9, and ~9.2–8.2 Ma were associated with emplacement of the 11.1–10.78, 9.91, and 8.43 Ma domes and porphyry intrusions of the Coriwachay Dacites. We hypothesize that there were separate pulses of hydrothermal fluids that accompanied each of several Coriwachay porphyry intrusions emplaced episodically over a period of ~2.4 Ma.

Temporal and Spatial Evolution of Magmas and Ores

The temporal and spatial evolution of the Yanacocha district is summarized in a series of six time panel maps that show volcanic rock units and ages, alunite ages, and gold ore occurrences to illustrate the relationships between igneous and hydrothermal events (Fig. 15).

Atazaico Andesite, intrusions of Quilish dacite, and stage 1 alunite

An andesitic volcanic field with an areal extent of ~340 km^2 and average thickness of 80 m first developed, and locally erupted from north-northwest trending vents. Pyroxene-hornblende andesitic lavas erupted from numerous monogenetic volcanoes and small composite cones in the western parts of the district, such as Cerro Atazaico and Cerro Negro Oeste (14.5–14.2 Ma; Fig. 15A). Eruption was followed by dome-building and minor pyroclastic ejection of quartz-bearing pyroxene andesite at Cerro Regalado (13.9 Ma), Quilish, and Cerro Negro Oeste. Volcanism progressed eastward to form the Chaupiloma trend and the Chugares volcano (13.7–13.3 Ma).

The Quilish dacitic porphyry plugs and dikes postdate and intrude the lavas of the Atazaico Andesite and are spatially associated with hydrothermal centers in the western district at Los Pinos, Exaltado, and Quilish. The dacites here are associated with hydrothermal activity that formed stage 1 alunite (~13.6–12.6 Ma) and associated gold ore at Cerro Negro and Quilish. A few of these dacites also crop out in the eastern district.

Colorado Pyroclastics

The Colorado Pyroclastics represent the first eruptions from the east part of the district near the Maqui Maqui dome and Cerro Yanacocha. The latter area is here proposed to constitute

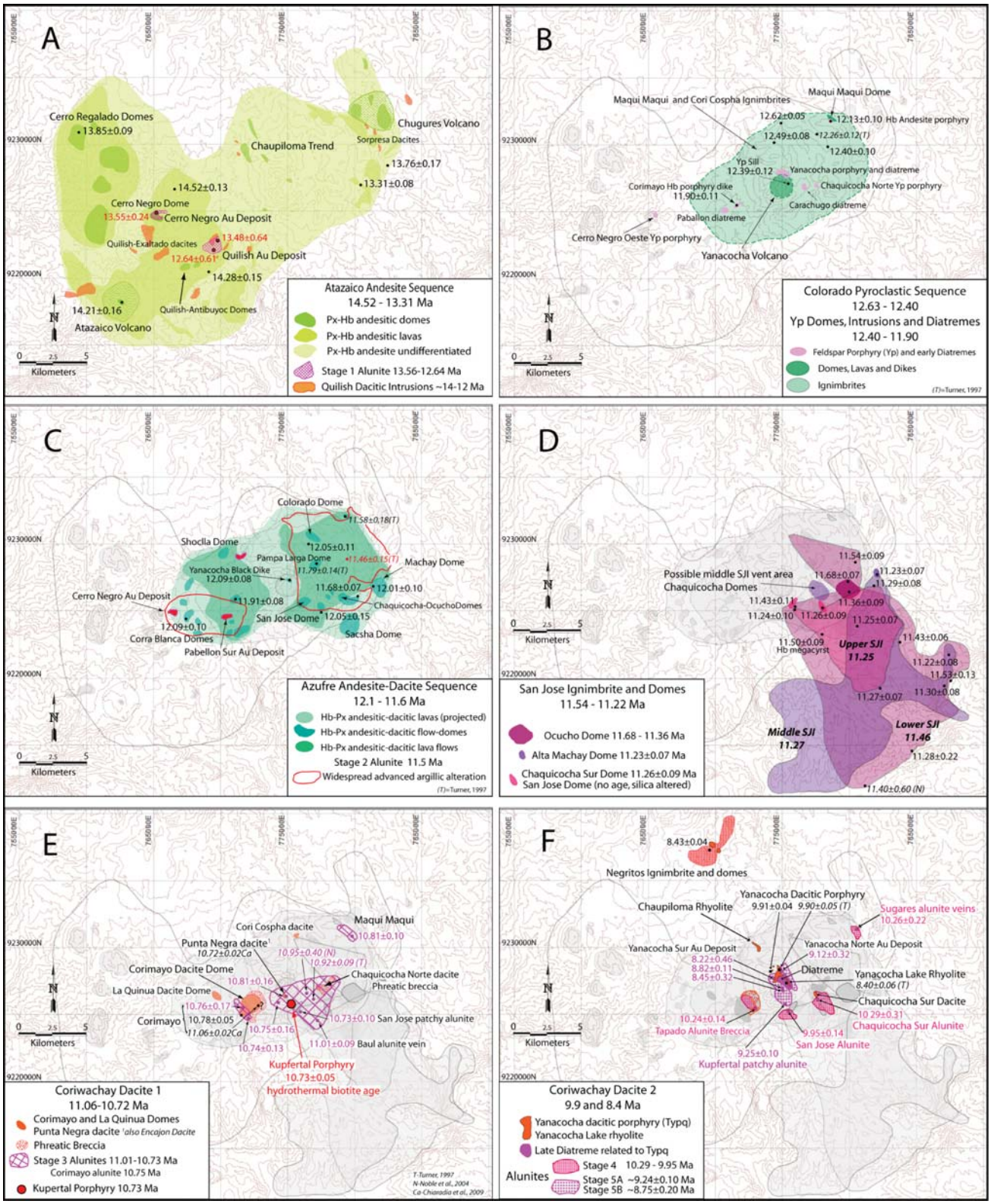

FIG. 15. District plan map model summarizing the temporal and spatial evolution of the Yanacocha Volcanics, alteration zones, and gold ores through time from time A to F. (A) The Atazaico Andesite volcanic sequence, (B) The Colorado Pyroclastic sequence, (C) The Azufre andesite-dacite sequence, (D) San Jose Ignimbrite and domes. The lower member likely erupted from a vent later filled by the Ocucho dome and flow. The middle member and upper member likely erupted from vents filled by domes of similar age at Alta Machay, Chaquicocha Sur, or San Jose. (E) Coriwachay Dacite-phase 1: Corimayo and other dacites; F) Coriwachay Dacite-phase 2, including the Yanacocha dacite porphyry and Yanacocha Lake rhyolitic dikes associated with late diatremes and the bulk of the gold ores.

the composite Yanacocha volcano and center of magmatic activity for a ~4 m.y. period from 12.4 to 8.4 Ma (Fig. 15B). The Colorado Pyroclastics sequence includes the Cori Coshpa and Maqui Maqui hornblende ± biotite ignimbrites of andesite, trachyandesite, and dacite composition, with ages of 12.6 and 12.4 Ma, respectively. Small volumes of associated and slightly younger porphyritic hornblende andesitic sills and dikes, plugs, domes, and lavas (Yanacocha porphyries) have ages from 12.4 to 11.9 Ma. Also, we propose that most diatremes developed during this period (i.e., Pabellon, Carachugo Norte, and Yanacocha, or YBX1 of Loayza-Tam, 2002). Exposures suggest that the Colorado Pyroclastics originally covered ~90 km² with an average thickness of 100 m. Although no alunite alteration related to gold mineralization is identified for this time interval, laminated tuffaceous rocks intercalated with ignimbrites are locally strongly hydrothermally altered.

Azufre Andesite and stage 2 alunite

The Azufre Andesite represents a renewal of effusive pyroxene-hornblende andesitic volcanism erupted between ~12.1 and 11.6 Ma from a series of monogenetic vents and domes of silicic andesite to low-silica dacite. Lavas originally covered an area of ~120 to 125 km² centered on the Yanacocha volcano. Multiple vent complexes produced a series of coalescing domes (i.e., the Corra Blanca domes at Cerro Negro, Shoclla dome at Tatiana, and the San Jose, Chaquicocha, Sacsha, and Machay domes; Fig. 15C), lavas, and minor pyroclastic deposits that covered areas >60 km². These eruptions were similar to large coulee-style lavas, such as the Chao dacite (~90 km² and up to 300 m thick) in northern Chile (Guest and Sanchez, 1969).

Stage 2 alunite formation is inferred, based on geologic arguments presented above, to have produced widespread alteration both in the western district at Cerro Negro Este and Pabellon Sur (15 km²) and in a larger 42 km² area to the east, north, and west of the San Jose gold deposit in the eastern district (Fig. 15C). The alunite alteration is spatially associated with, and likely closely followed, eruption of the Azufre Andesite domes. Two overlapping ages of stage 2 include 11.41 ± 0.89 Ma from a patchy quartz-alunite at Collotan adjacent Cerro Yanacocha (this study), and 11.46 ± 0.15 Ma from an alunite at Cerro Azufre in the eastern district (Turner, 1997). Large tabular bodies of massive hydrothermal quartz in this area obliterated original rock textures, contain 30 to 350 ppb Au, and may represent the earliest stage of gold mineralization in the east (Harvey et al., 1999; Longo, 2000).

San Jose Ignimbrite and associated domes

The San Jose Ignimbrite consists of hornblende-pyroxene ± biotite dacite and is inferred to postdate the stage 2 advanced argillic alteration in the eastern part of the district, based on accidental fragments of advanced argillic altered rock. The San Jose Ignimbrite consists of three cooling units erupted over a period of ~0.3 m.y. (11.54–11.22 Ma; Table A2). Each cooling unit erupted from a distinct and separate vent area near Chaquicocha, flowed south-southeast, and filled a 175 km² topographic depression called the Otuzco trough (Plate I), where thicknesses range from 40 to 350 m (Fig. 15D). The lower member is apparently older (11.46 ± 0.08 Ma), whereas the middle member (11.27 ± 0.05 Ma) and upper spatter member (11.25 ± 0.06 Ma) are identical in age, and represent either a single eruption or two eruptions separated by only a short time gap (~0.1 m.y. or less)[5]. Post-ignimbrite dome complexes filled three vents at Ocucho (11.36 Ma), Chaquicocha Sur (11.28 Ma), and Alta Machay (11.23 Ma) that likely represent the source of the lower, middle, and upper members. Hydrothermal activity was not associated with the eruptions of the San Jose Ignimbrite, but closely followed.

Coriwachay Dacite and stage 3, 4, and 5 alunite

Corimayo dacite and stage 3 alunite: A series of isolated dacitic domes are aligned along a 5-km zone from Chaquicocha Norte, Corimayo (10.78 Ma), Punta Negra (10.72 Ma; Chiaradia et al., 2009) and La Quinua; the Cori Coshpa dacitic intrusion crops out 2.7 km north (Fig. 15E).

Stage 3 alunites occur as veinlets and in hydrothermal breccia containing gold ore that crosscuts intense quartz-rich alteration along the margins of the Corimayo dome (Gomez, 2002). Stage 3 hydrothermal zones contain alunite with ages of 11.0 to 10.7 Ma and extend widely for 10 km from Corimayo to Maqui Maqui (Fig. 15E). Stage 3 alteration zones contain gold in a ~14 km² area that includes the San Jose, Carachugo, Quecher, and Arnacocha deposits (Fig. 3; Plate I). Northwest-striking fault and fracture zones at Maqui Maqui and Corimayo localized gold deposition. The stage 3 alunites have the same age within analytical uncertainty as hydrothermal biotite (10.73 Ma) in the deep Kupfertal porphyry, up to 4 to 6 km distant (Fig. 15E). We conclude that shallow epithermal gold deposits related to stage 3 alteration formed synchronously with the deeper porphyry-style Cu-Au mineralization during the same magmatic-hydrothermal event.

Cerro Yanacocha dacite porphyry and stage 4 alunite: The Cerro Yanacocha dacite porphyry and associated diatreme (YBX4 subtype 2; Loayza-Tam, 2002) intrudes a Corimayo-style porphyry intrusion (the Punta Negra dacite at Encajon), a Yanacocha (Yp or feldspar) porphyry, early diatreme bodies (YBX1; Loayza-Tam, 2002) and breccias, as well as the previously altered Colorado Pyroclastics at Cerro Yanacocha (Loayza-Tam 2002; Longo, 2005). We include the altered dacite porphyry at Chaquicocha Sur as part of the Cerro Yanacocha intrusions (Longo, 2005). The 9.91 ± 0.04 Ma age of the Cerro Yanacocha dacite porphyry is analytically indistinguishable from each of five ages of stage 4 alunite from the eastern Yanacocha district, which range from 10.29 ± 0.31 to 9.95 ± 0.14 Ma (Figs. 6, 15F).

Yanacocha Lake rhyolitic dikes and stage 5 alunite: The Yanacocha Lake rhyolitic dike (8.40 ± 0.06 Ma; Turner, 1997) and the petrographically similar northwest-striking Chaupiloma dike are the same age and compositionally similar to the Negritos rhyolitic ignimbrite (8.4 Ma) that crops out 8 km to the northwest. These dikes are the youngest intrusions related to the Yanacocha Volcanics, and mark the cessation of

[5] Eruption of the San Jose Ignimbrite may be interpreted from the weighted mean ages for the lower (11.46 ± 0.08 Ma, n=5), the middle (11.27 ± 0.05 Ma, n = 5), and the upper (11.25 ± 0.06 Ma, n = 2) members as two separate eruptions; the lower at ~ 11.46 Ma, and the middle and upper at ~11.25 Ma (see p. 1214). The range 11.54–11.22 Ma (Table A2) for eruption of San Jose Ignimbrite is found elsewhere in this paper.

magmatism in the Cajamarca structural block (Figs. 1, 2) when flat-slab subduction began in northern Peru (Gutscher et al., 1999).

Stage 5 hydrothermal alunites range from ~9.3 to ~8.2 Ma (Fig. 14) and are broadly spatially and temporally associated with intrusions of Coriwachay Dacite in the Cerro Yanacocha area (Fig. 15F). The $^{40}Ar/^{39}Ar$ ages and the geologic evidence support division of stage 5 into an earlier substage 5A at 9.3 to 9.1 Ma and a later substage 5B at 8.8 to 8.2 Ma, which is temporally associated with the Yanacocha Lake rhyolites.

Rates of Volcanic Eruption and Gold Deposition

Volcanic volumes and eruption rates

The Yanacocha Volcanics have an estimated cumulative erupted magma volume of ~88 km^3, which represents a small- to moderate-sized volcanic center (Table 6). The volumetric eruption rates at Yanacocha are small and of similar magnitude to other multivent stratovolcano fields of dacitic volcanoes (Kudo et al., 2003; Hildreth et al., 2003, 2004; Frey et al., 2004; Siebe et al., 2004; Klemetti and Grunder, 2007; Grunder et al., 2008). Eruptions of Atazaico Andesite began in the west at 14.5 Ma, lasted ~1.2 m.y., and include ~36 km^3 (0.03 km^3/1,000 yr) of pyroxene-hornblende andesitic lavas (Figs. 16, 17; Table 6). Eruptions of the Colorado Pyroclastics began at 12.63 Ma, spanned 0.23 m.y., and include ~12 km^3 (0.05 km^3/1,000 yr) of andesitic and dacitic ignimbrites. Eruptions of the Azufre Andesite began at 12.1 Ma, spanned ~0.4 m.y., and include ~14 km^3 (0.04 km^3/1,000 yr) of andesitic and dacitic lavas and subordinate associated domes and pyroclastic deposits. The San Jose Ignimbrite erupted ~24 km^3 (0.12 km^3/1,000 yr) at ~11.46 Ma (lower member) and ~11.25 Ma (middle and upper members) that filled the Otuzco graben south of Cerro Yanacocha (see footnote 5). Therefore, over a ~3.3 m.y. interval, from 14.5 to 11.2 Ma, eruptions deposited ~88 km^3 of Yanacocha Volcanics (0.027 km^3/1,000 yr) over an area of 500 km^2.

The Coriwachay Dacite magmatism represents a shift to small volumes of more highly oxidized dacite to rhyolite that formed domes and porphyry dikes and plugs in the center of the district. Three brief episodes of felsic magmatism at 10.8, 9.9, and 8.4 Ma span a 2.4 m.y. interval (Fig. 16). The first two episodes included domes of Corimayo dacite and dikes of Cerro Yanacocha dacitic porphyry that have an estimated 0.9 km^3 of magma. The final magmatism at ~8.4 Ma included the Yanacocha Lake rhyolitic dike (~0.1 km^3) and the Negritos rhyolitic ignimbrite (~0.5 km^3). Thus, from ~10.8 to 8.4 Ma, eruption rates decreased to ~0.006 km^3/1,000 yr.

TABLE 6. Estimated Volcanic Eruption Volumes, Ages, and Silica Contents Compared with Contained Gold and Age of Each Mineral Deposit in the Yanacocha District

Rock Sequence	Average thickness (m)	Areal extent (km^2)	Volume (km^3)	Age[1] (Ma)	SiO_2 (wt %)
Atazaico Andesite			36.2	14.5–13.3	60.0
western district	*185*	*157*	*29*	*14.5–13.9*	*60.8*
eastern district	*90*	*80*	*7.2*	*13.7–13.3*	*61.9*
Colorado Pyroclastics	133	89	11.8	12.63–12.4	63.2
Azufre Andesite	113	125	14.1	12.1–11.7	62.4
San Jose Ignimbrite	138	175	24.2	11.46–11.25	63.4
Coriwachay Dacite	100	15	1.5	11.1–8.4	69.2
Total			87.9		

Gold deposits	Au (Moz)[2]	Age (Ma)[1]	
Cerro Negro deposit	1.0	13.6	
Cerro Quilish deposit	6.0	~13.0	Stage 1
District-wide acid-sulfate alteration	0.5	11.5	Stage 2
Carachugo-Chaquicocha Norte	6.0	11.0	
Maqui Maqui-Corimayo-San Jose	6.6	10.75	Stage 3
San Jose Sur-Tapado-Chaquicocha Sur	10.0	10.3	Stage 4
Cerro Yanacocha Complex[3]	25.0	9.3 to 8.2	Stage 5
Total gold	55.1[4]		

[1] Ages from this study, Turner (1997), and Chiaradia et al. (2009)

[2] The gold endowments in millions of ounces (Moz) from each gold deposit are estimates that consider the unpublished and published proven and probable reserves, and indicated and inferred mineral resources, at Yanacocha of L. Leng writ. commun. (1999); D. Hall writ. commun. (2000); and Newmont annual reports, Form 10-K, 1999–2010; these estimates represent a minimum gold endowment for the Yanacocha district, and do not consider the poorly defined resource of the Au-bearing sulfide, or the loss of gold ore from Quaternary glaciation (Cerro Yanacocha-La Quinua, the exception)

[3] Gold (Moz) for the Cerro Yanacocha Complex includes the La Quinua reserve-resource of ~10 Moz

[4] The basis of the estimate for total gold includes total production from ore tonnes mined by 2010 (38.1 Moz), an estimated 6 Moz Au from the Quilish deposit that was removed from the reserve and resource when permits were relinquished in 2002, the 2010 reserve of 10.5 Moz Au, and an estimated 500,000 oz Au deposited during stage 2 alunite

These data were used for Figure 17

Gold deposition rates compared to magmatic silica content

Gold deposition rates may be estimated on the basis of the alunite ages and the total mass of gold deposited for each hydrothermal center (Figs. 16, 17; Table 6). Hydrothermal activity and associated gold deposition increased as eruptive output decreased, and reached a peak during the end stages of magmatism when eruption volumes were at a minimum. Conversely, high rates of eruption appear to have been affiliated with little gold deposition.

Melt SiO_2 contents increased gradually during eruptions of the Atazaico Andesite, peaked at ~12.4 Ma with eruptions of Colorado Pyroclastics, and then decreased slightly with the initial eruptions of Azufre Andesite (Figs. 11, 17). Early Quilish dacitic dikes intruded the Atazaico Andesite in the west parts of the district and are spatially associated with stage 1 alunite and the oldest gold deposits at Quilish and Cerro Negro (~6 Moz). Stage 2 produced widespread quartz-alunite alteration with little associated gold ore (<0.5 Moz Au) after eruption of Azufre Andesite (12.1–11.6 Ma), but prior to the San Jose Ignimbrite (11.5–11.2 Ma). Melt SiO_2 contents increased with time, from andesite to dacite during eruption of Azufre Andesite and the San Jose Ignimbrite (Figs. 11, 17). Stages 1 and 2 were associated with deposition of ~7.5 Moz of gold during this longer period of volcanism (14.5–11.2 Ma) that erupted ~87 km^3 of volcanic rocks over 3.3 m.y. Over 85 percent of the gold ore at Yanacocha was deposited in the last 2.8 m.y. of hydrothermal activity (~11.0–8.2 Ma), during which the final ~2 percent of the total volume of magma was erupted. During stage 3 (11.0–10.7 Ma), gold deposition increased ~12.6 Moz during a period when less than 0.9 km^3 of dacitic domes were erupted. During stage 4 (10.3–ca. 10 Ma),

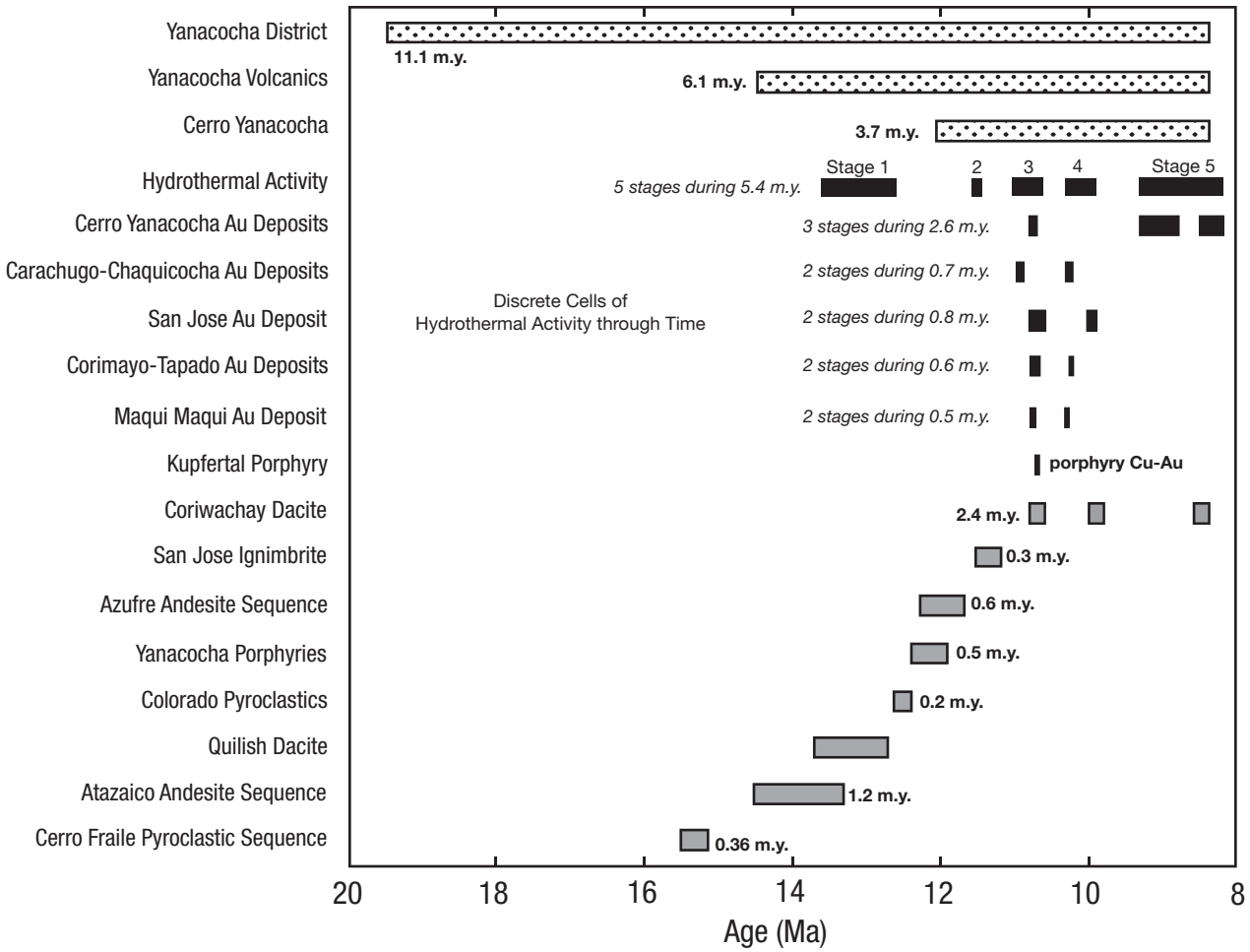

FIG. 16. Bar chart displaying the ages and time spans based on the $^{40}Ar/^{39}Ar$ ages of (A) total magmatism at Yanacocha district (stippled bars); (B) individual igneous rock unit (solid gray bars); and (C) the hydrothermal activity based on alunite stages (solid black bars 1 to 5) and for individual gold deposits (lower small black bars). Note that each stage of gold mineralization is temporally associated with intrusions of either early Quilish Dacite or late Coriwachay Dacite.

~10 Moz of gold was deposited, and during stages 5A and 5B (between 9.4 and 8.2 Ma), 25 Moz of gold ore was deposited—nearly 65 percent of all the gold ore at Yanacocha (Table 6).

Concluding Remarks

Magmatism and ores

Yanacocha is a >50 Moz gold district where gold deposition was temporally and spatially associated with a moderate-sized volcanic field characterized by a low to moderate eruption rate of phenocryst-rich andesitic, dacitic, and sparse rhyolitic lavas and pyroclastic rocks from stratovolcano and dome complexes. Low volumes of erupted magma, and extensive associated hydrothermal alteration, suggest large volumes of magma remained in the crust where they crystallized as plutonic rocks. Similar situations have been observed in crustal sections exposed in tilted and eroded porphyry copper deposits (Dilles, 1987; Stavast et al., 2008). Extensive quartz-alunite alteration in the eastern part of the Yanacocha district was centered on volcanic vent areas during several relatively short and discrete periods lacking volcanism (Figs. 14–17). Volcanic eruptions preceded, and in some cases, postdated the alteration (e.g., eruptions of the San Jose Ignimbrite). Hydrothermal activity occurred as a series of temporally discrete cells, each with a maximum duration of 0.5 to 0.8 m.y., based on ages of alunite (Figs. 6, 9, 16). The compositional diversity of the volcanic rocks and the discrete pulses of hydrothermal activity imply that there was a complex, evolving, and recharging magmatic system at depth.

The volcanic stratigraphy, based on field relations and $^{40}Ar/^{39}Ar$ ages, indicates a magmatic duration of 6.1 m.y. that includes a 5.4 m.y. period of episodic hydrothermal activity (Fig. 16). During this period of 6.1 m.y., magmatism and hydrothermal activity progressed through time from southwest to the northeast across the district. The volcanic eruption rates decreased with time, whereas the volume of hydrothermally altered rock and mass of gold deposited both increased (Fig. 17). The Yanacocha magmas evolved to become more silica-rich and hydrous, and from high to very high oxidation states. High intrusion to volcanic eruption ratios are here inferred to have been associated with the bulk of the gold introduction. This magmatic and hydrothermal record is similar to many porphyry Cu-(Mo-Au) deposits where crystallization

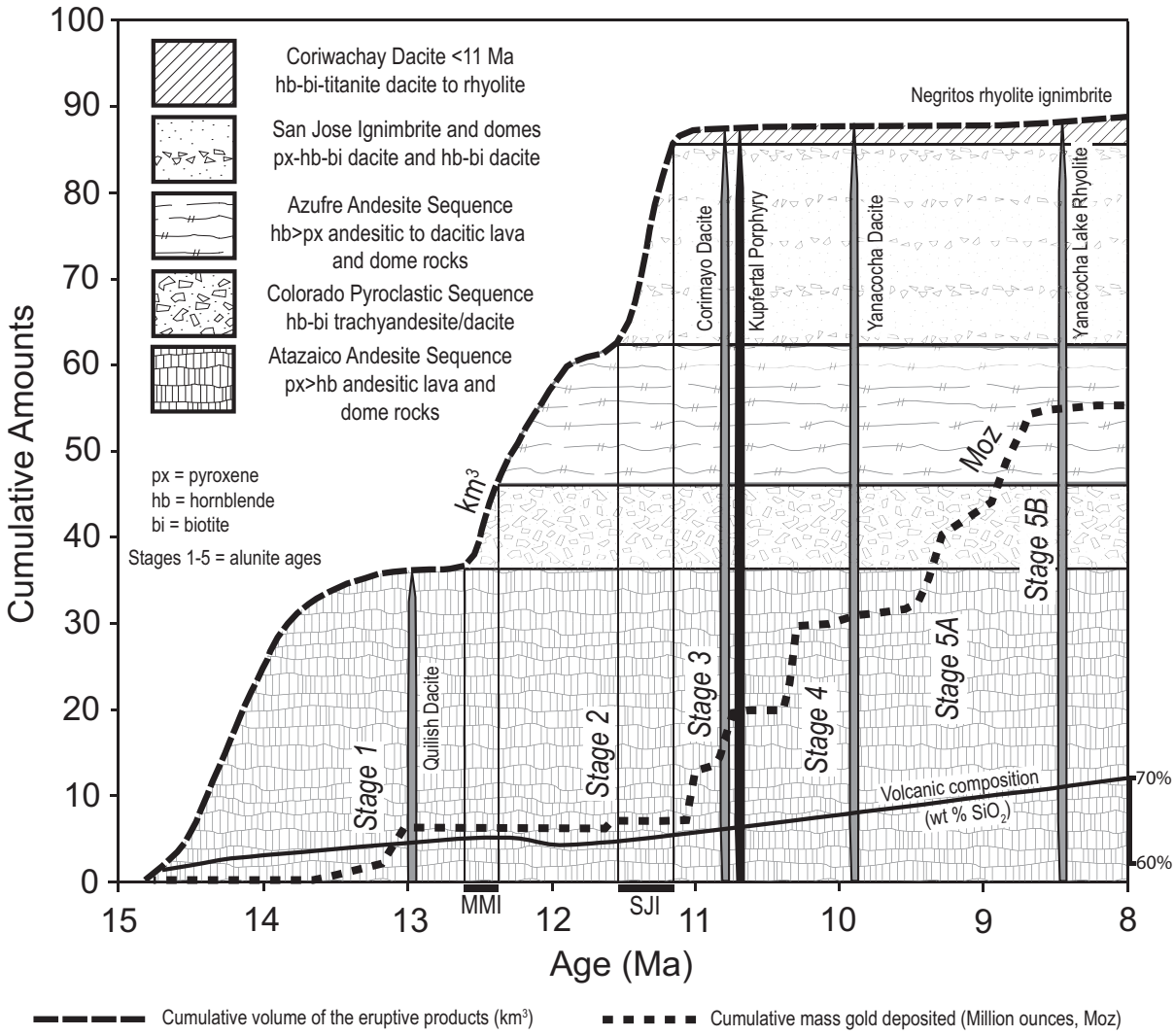

FIG. 17. Cumulative volume (km^3) of the Yanacocha Volcanics, average silica content (wt % SiO_2) of the volcanic rocks, hydrothermal alunite stages 1 through 5, and the cumulative amount of gold deposited (Moz) in the Yanacocha district plotted as a function of age. Both early Quilish dacite and late Coriwachay dacitic to rhyolitic intrusions are gray vertical bands, and the Kupfertal porphyry is a black vertical band (see Table 6 for data)

of late granitoid intrusions and associated porphyry dikes and plugs produce magmatic-hydrothermal fluids and ores (Yerington, Nevada: Dilles, 1987; Bingham, Utah: Keith et al., 1998; El Abra, Chile: Campbell et al., 2006).

We propose that gold deposits similar to Yanacocha are unlikely to form in volcanic centers that experienced only high-volume rates of eruption, or in systems with simple and short-lived magmatic-hydrothermal histories. At Yanacocha and similar magmatic systems associated with quartz-alunite and gold ores (e.g., Goldfield, Ransome, 1909; Summitville, Steven and Ratté, 1960; Nansatsu, Hedenquist et al., 1994), water-rich dacitic magmas crystallized at depth to form plutons which degassed their volatiles to produce hydrothermal solutions. The small volumes of erupted dacites were dominated by thick lavas, domes, and minor pyroclastic deposits; this is consistent with the loss of most volatiles prior to magma eruption. Formation of world-class epithermal gold deposits may be favored in volcanic centers characterized by low eruption rates, compositional diversity, abundant subvolcanic plutons, and several temporally distinct magmatic-hydrothermal pulses that reflect complex evolution of hydrous and sulfur-rich arc magmatism over several million years.

Exploration

Yanacocha demonstrates that world-class high-sulfidation epithermal systems with long-lived volcanic centers and multiple mineralizing events can be partly to entirely concealed by unaltered parts of the host volcanic center. Fresh andesitic rocks previously considered to be postmineralization and part of the late Miocene Regalado Volcanic rocks (Turner, 1997) here yield middle Miocene ages, from 14.5 to 11.6 Ma, and belong to the Atazaico and Azufre Andesites of the Yanacocha Volcanics. They erupted before stage 2 to 5 quartz-alunite alteration and associated gold deposition, and locally these rocks host gold ore. Gold ore has been found below fresh, but

pre-mineral, volcanic rocks at Yanacocha. These outcrops reveal only subtle hints of the deeper hydrothermal system in peripheral alteration assemblages that include low-temperature opal replacement and fracture-filling, clay, or chlorite (i.e., San Jose Sur, Chaquicocha Sur and Quecher gold deposits). By conducting careful and systematic geologic mapping, petrography, geochemistry, and radiometric dating, the explorationist can deduce the stratigraphy of complicated, hydrothermally altered, and faulted volcanic rocks. By knowing the timing, the stratigraphy, and the hypothetical processes for magmatic evolution, the explorationist can construct realistic models and hypotheses for ore formation, and then target potentially hidden orebodies both at Yanacocha and in other districts worldwide.

Acknowledgments

This manuscript results from a Ph.D. dissertation completed at Oregon State University (AAL). We thank Minera Yanacocha, S.R.L. (Newmont Mining Corporation and Compania de Minas Buenaventura) and its management for financial and material support. We thank John Huard and Roger Nielsen for guidance during $^{40}Ar/^{39}Ar$ and electron microprobe analyses. We wish to acknowledge the many geologists who have contributed to the understanding of the volcanic rocks in the Yanacocha district, whose reports and personal communications are referenced herein. We give special thanks to J.W. Hedenquist and J.L. Muntean for their thorough reviews and valuable comments that greatly improved the manuscript, as well as, R.H. Sillitoe, C. Henry, and J. McPhie for their constructive reviews.

REFERENCES

Abarca, D.A. and Harvey, B., 1997, Modelo geologico del proyecto Encajon, *in* Macharé, J., Cánepa, C., and Injoque, J., eds., IX Congreso Peruano de Geología, Resúmenes Extendidos: Sociedad Geológica del Perú, Special Publication 1, Lima, p. 3–7.

Arribas, A., Jr., 1995, Characteristics of high-sulfidation epithermal deposits, and their relation to magmatic fluid: Mineralogical Association of Canada Short Course, v. 23, p. 419–454.

Arribas, A., Jr., Cunningham, C.G., Rytuba, J.J., Rye, R.O., Kelly, W.C., Podwysocki, M.H., McKee, E.H., and Tosdal, R.M., 1995, Geology, geochemistry, fluid inclusions, and isotope geochemistry of the Rodalquilar gold alunite deposit, Spain: Economic Geology, v. 90, p. 795–822.

Barreda, J. and Edwards, J., 2000, Yanacocha district west: Unpublished Minera Yanacocha S.R.L. map set, scale 1:10000, folio YD-29.

Barreda, J., Escalante, J., Bartra, R., Velasco, C., Loayza, C., and Longo, A., 2000, Yanacocha district east: Unpublished Minera Yanacocha S.R.L. map set, scale 1:10000, folio YD-16.

Bartra, R., Leach, B., and Longo, A., 1999, Yanacocha district north: Unpublished Minera Yanacocha S.R.L. map set, scale 1:10000, folio YD-17.

Behrens, H., and Gaillard, F., 2006, Geochemical aspects of melts: volatiles and redox behavior: Elements, v. 2, p. 275–280.

Bell, P.D., Gomez, J.G., Loayza, C.E., Pinto, R.M., 2004, Geology of the gold deposits of the Yanacocha district, northern Peru: PacRim 2004 Congress, Adelaide, South Australia, September 19–22, Australasian Institute of Mining and Metallurgy, Proceedings, p. 105–115.

Benavides, A., and Vidal, C.E., 1999, Exploration and mineral discoveries in Peru: PacRim '99 Congress, Bali, Indonesia, October 10–13, Australasian Institute of Mining and Metallurgy, Proceedings, p. 187–195.

Benavides, V., 1956, Cretaceous system in northern Peru: Bulletin of the American Museum of Natural History, v. 108, p. 355–493.

Benavides-Cacéres, V., 1999, Orogenic evolution of the Peruvian Andes—the Andean cycle: Society of Economic Geologists Special Publication 7, p. 61–108.

Best, M.G., 2003, Igneous and metamorphic petrology, 2nd edition: Oxford, U.K., Blackwell Publishing Company, 729 p.

Blundy, J.D., and Wood, B.J., 1991, Crystal-chemical controls on the partitioning of Sr and Ba between plagioclase feldspar, silicate melts, and hydrothermal solutions: Geochimica et Cosmochimica Acta, v. 55, p. 193–209.

Borredon, E.R., 1982, Etude géologique et metallogenique du district minier de Hualgayoc (Pérou septentrional) à plomb-zinc-cuivre-argent: thèse 3e cycle, Université Pierre et Mari Curie, Paris 6, 287 p.

Brennecka, G.A., 2005, Origin and metal content of magmatic sulfides in Cu-Au mineralizing silicic magmas: Yanacocha, Peru, and Yerington, Nevada: Unpublished M.S. thesis, Corvallis, Oregon, Oregon State University, 49 p.

Burnham, C.W., 1979, Magmas and hydrothermal fluids, *in* Geochemistry of hydrothermal ore deposits, Barnes, H.L., ed.: New York, Wiley, p. 71–136.

Campbell, I.H., Ballard, J.R., Palin, J.M., Allen, C., and Faunes, A., 2006, U-Pb zircon geochronology of granitic rocks from the Chuquicamata-El Abra porphyry copper belt of northern Chile: Excimer laser ablation ICP-MS analysis: Economic Geology, v. 101, p. 1327–1344.

Casselman, M.J., McMillan, W.J., and Newman, K.M., 1995, Highland Valley porphyry copper deposits near Kamloops, British Columbia: A review and update with emphasis on the Valley deposit: Canadian Institute of Mining, Metallurgy and Petroleum, Special Volume 46, p. 161–191.

Chambefort, I., Dilles, J.H., and Kent, J.R., 2008, Anhydrite-bearing andesite and dacite as a source for sulfur in magmatic-hydrothermal mineral deposits, Geology, v. 36, p. 719–722.

Chambefort, I., Dilles, J.H., and Longo, A.A., in press, Amphibole geochemistry of the Yanacocha Volcanics, Peru: Evidence for diverse sources of magmatic volatiles related to gold ores: Journal of Petrology.

Changanaqui, M.B., 1995, Yanacocha Norte project: Unpublished company report, Minera Yanacocha, S.A., 20 p.

Chiaradia, M., Fontbote, L., and Paladines, A., 2004, Metal sources in mineral deposits and crustal rocks of Ecuador (1° N-4° S); a lead isotope synthesis: Economic Geology, v. 99, p. 1085-1106.

Chiaradia, M., Merino, D., and Spikings, R., 2009, Rapid transition to long-lived deep crustal magmatic maturation and the formation of giant porphyry-related mineralization (Yanacocha, Peru): Earth and Planetary Science Letters, v. 288, p. 505–515.

Cobbing, E.J., Pitcher, W.S., Wilson, J.J., Baldock, J.W., Taylor, W.P., McCourt, W.J., and Snelling, N.J., 1981, The geology of the Western Cordillera of northern Peru: Institute of Geological Sciences, London, Overseas Memoir 5, 143 p.

Coleman, D.S., Gray, W., and Glazner, A.F., 2004, Rethinking the emplacement and evolution of zoned plutons: Geochronologic evidence for incremental assembly of the Tuolumne Intrusive Suite, California: Geology, v. 32, no. 5, p. 433–436.

Dalyrymple, G.B., and Lanphere, M.A., 1974, $^{40}Ar/^{39}Ar$ age spectra of some undisturbed terrestrial samples: Geochimica et Cosmochimica Acta, v. 38, p. 715–738.

Davies, C.R., 2002, Tectono-magmatic evolution of the Cajamarca mining district, northern Peru: Unpublished Ph.D. dissertation, Queensland, Australia, James Cook University, 191 p.

Davies, C.R., and Williams, P.J., 2005, The El Galeno and Michiquillay porphyry Cu–Au-Mo deposits: Geological descriptions and comparison of Miocene porphyry systems in the Cajamarca district, northern Peru: Mineralium Deposita, v. 40, p. 598–616.

Davies, A.G.S., Cooke, D.R., Gemmell, J.B., and Simpson, K.A., 2008, Diatreme Breccias at the Kelian gold mine, Kalimantan, Indonesia: Precursors to epithermal gold mineralization: Economic Geology, v. 103, p. 689–716.

Deen, J.A., Rye, R.O., Munoz, J.L., and Drexler, J.W., 1994, The magmatic hydrothermal system at Julcani, Peru: Evidence from fluid inclusions and hydrogen and oxygen isotopes: Economic Geology, v. 89, p. 1924–1938.

Defant, M.J., and Drummond, M.S., 1990, Subducted lithosphere-derived andesite and dacite rocks in young volcanic arc settings: Nature, v. 347, p. 662–665.

DePaolo, D.J., 1981, Trace element and isotopic effects of combined wallrock assimilation and fractional crystallization: Earth and Planetary Science Letters, v. 53, p.189–202.

Diaz, N., Jiménez, C., and Alva, C., 1997, Estudio geoquímica de orientación del deposito pórfido de cobre La Granja, *in* Macharé, J., Cánepa, C., and Injoque, J., eds., IX Congreso Peruano de Geología, Resúmenes Extendidos [Extended Abstracts]: Sociedad Geológica del Perú, Special Publication 1, p. 25–30.

Dilles, J.H., 1987, Petrology of the Yerington batholith, Nevada: Evidence for evolution of porphyry copper ore fluids: Economic Geology, v. 82, p. 1750-1789.

Dilles, J.H., and Proffett, J.M., 1995, Metallogenesis of the Yerington batholith, Nevada: *in,* Pierce, F.W., and Bolm, J.G., eds., Porphyry copper deposits of the American Cordillera: Arizona Geological Society Digest 20, p. 306–315.

Duncan, R.A., Hooper, P.R., Rehacek, J., Marsh, J.S., and Duncan, A.R., 1997, The timing and duration of the Karoo igneous event, southern Gondwana: Journal of Geophysical Research, v. 102, no. B8, p. 18,127–18,138.

Edwards, J., 2000, Yanacocha west district geologic interpretation and implications for exploration: Unpublished Minera Yanacocha S.R.L. memorandum, 5 August, 22 p.

Escalante, J. and Longo, A., 2000, The Cerro Quilish and Antibuyoc project: Unpublished Minera Yanacocha S.R.L. map set, scale 1:5000, folio CQ-09.

Escalante, J., Bartra, R., and Longo, A., 2000, The Arnacocha project, surface and subsurface geology, geochemistry, and RVC drill data: Unpublished Minera Yanacocha S.R.L. map set, scale 1:5000, folio ARN-01.

Frey, H.M., Lange, R.A., Hall, C.M., and Delgado-Granados, H., 2004, Magma eruption rates constrained by $^{40}Ar/^{39}Ar$ chronology and GIS for the Ceboruco-San Pedro volcanic field, western Mexico: Geological Society of America Bulletin, v. 116, p. 259–276.

Ghiorso and Evans, 2008, Thermodynamics of rhombohedral oxide solid solutions and a revision of the Fe-Ti two-oxide geothermometer and oxygen-barometer: American Journal of Science, v. 308, no. 9, p. 957–1039.

Goldie, M.K., 2000, A geophysical case history of the Yanacocha gold district, northern Peru: Society of Exploration Geophysicists, Calgary 2000, SEG, Extended Abstracts, v. 19, p. 750–753.

——2002, Self-potentials associated with the Yanacocha high-sulfidation gold deposit in Peru: Geophysics, v. 67, no. 3, p. 684–689.

Gomez, J.G., and Klein, T., 2000, Corimayo folio: Unpublished Minera Yanacocha S.R.L. map set, scale 1:2500, folio COR-02.

Gomez, J.G., 2002, Corimayo, deposito aurifero de alta ley en un sistema epitermal tipo acido sulfato. Distrito minero de Yanacocha, Cajamarca, Peru: Unpublished Ingeniero Geólogo de Perú thesis, Lima, Peru, Universidad Nacional Mayor de San Marcos, p. 69–75.

Grunder, A.G., Klemetti, E.W., Feeley, T.C., McKee, C.M., 2008, Eleven million years of arc volcanism at the Aucanquilcha volcanic cluster, northern Chilean Andes: Implications for the life span and emplacement of plutons: Transactions of the Royal Society of Edinburgh: Earth Sciences, v. 97, p. 415–436.

Guest, J.E. and Sanchez, R.A., 1969, A large dacitic lava flow in northern Chile: Bulletin of Volcanology, v. 33, p. 778–790.

Gustafson, L.B., 1979, Porphyry copper deposits and calc-alkaline volcanism, *in* McElhinny, M.W., ed., The Earth: its origin, structure, and evolution: Academic Press, London, p. 427–468.

Gustafson, L.B., Vidal, C.E., Pinto, R., Noble, D.C., 2004, Porphyry-epithermal transition, Cajamarca Region, northern Peru: Society of Economic Geologists, Special Publication 11, p. 279–300.

Gutscher, M-A., Olivet, J.L., Aslanian, D., Eissen, J.P., and Maury, R., 1999, The "lost Inca Plateau": cause of flat subduction beneath Perú?: Earth and Planetary Science Letters, v. 171, p. 335–341.

Harvey, B., Myers, S., and Klein, T., 1999, Yanacocha Gold District, Northern Peru: PacRim '99 Congress, Bali, Indonesia, October 10–13, Australasian Institute of Mining and Metallurgy, Proceedings, p. 445–459.

Hedenquist, J.W., Matsuhisa, Y., Izawa, E., White, N.C., Giggenbach, W.F., Aoki, M., 1994, Geology, geochemistry, and origin of high-sulfidation Cu-Au mineralization in the Nansatsu District, Japan: Economic Geology, v. 89, p. 1–30.

Hedenquist, J.W., Arribas, A., Jr., and Reynolds, T.J., 1998, Evolution of an intrusive-centered hydrothermal system: Far Southwest-Lepanto porphyry and epithermal Cu-Au deposits, Philippines: Economic Geology, v. 93, p. 373–404.

Hildreth, W., Fierstein, J., Lanphere, M., 2003, Eruptive history and geochronology of the Mount Baker volcanic field, Washington: Geological Society of America Bulletin, v. 115, no. 6, p.729–764.

Hildreth, W., Fierstein, J., Siems, D.F., Budhan, J.R., Ruiz, J., 2004, Rear-arc vs. arc-front volcanoes in the Katmai reach of the Alaska Peninsula: A critical appraisal of across-arc compositional variation: Contributions of Mineralogy and Petrology, v. 147, p. 243–275.

James, J., 1998, Geology, alteration, and mineralization of the Cerro Corona porphyry copper-gold deposit, Cajamarca Province, Peru: Unpublished master's thesis, British Columbia, Canada, University of British Columbia, Vancouver, 249 p.

Johnson, K.T.M., 1998, Experimental determination of partition coefficients for rare earth and high-field-strength elements between clinopyroxene, garnet, and basaltic melt at high pressures: Contributions to Mineralogy and Petrology, v. 133, p. 60–68.

Kay, S.M., and Mpodozis, C., 2001, Central Andean ore deposits linked to evolving shallow subduction systems and thickening crust: GSA Today, v. 11, p. 4–9.

Keith, J.D., Christiansen, E.H., Maughan, D.T., and Waite, K.A., 1998, The role of mafic alkaline magmas in felsic porphyry-Cu and Mo systems: Mineralogical Association of Canada Short Course Series, v. 26, p. 211–244.

Klein, T., Barreda, J., and Harvey, B., 1997, Sur Jose Sur high-sulfidation gold deposit,

Yanacocha district, northern Peru, *in* Macharé, J., Cánepa, C., and Injoque, J., eds., IX Congreso Peruano de Geología, Resúmenes Extendidos [Extended Abstracts]: Sociedad Geológica del Perú, Vol. Especial 1, Lima, p. 57–60.

Klein, T., Trujillo, J., and Pinto, R., 1999, Yanacocha district south project – Collotan, Kupertal, and San Jose: Unpublished Minera Yanacocha S.R.L. map set, scale 1:5000, folio YD-14.

Klemetti, E.K., and Grunder, A.L., 2007, Volcanic evolution of Volcán Aucanquilcha, a long-lived, monotonous dacite volcano in the Central Andes of Northern Chile: Bulletin of Volcanology, v. 70, p. 633-650. DO10.1007/s00445-007-0158-x.

Koppers, A.A.P., 2002, ArArCALC – software for $^{40}Ar/^{39}Ar$ age calculations: Computers and Geosciences, v. 7, p. 1-14. (http://earthref.org/tools/ararcalc.htm)

Korringa, M.K., and Noble, D.C., 1971, Distribution of Sr and Ba between natural feldspar and igneous melt: Earth and Planetary Science Letters, v. 11, p. 147–151.

Kudo, T., Okuno, M., and Nakamura, T., 2003, Eruptive history of the Kita-Hakkoda volcanic group during the last 6000 years, northeast Japan: Journal of the Geological Society of Japan, v. 109, no. 3, p. 151–165.

Laughlin, A.W., Damon, P.E., and Watson, B.N., 1968, Potassium-argon data from Toquepala and Michiquillay, Peru: Economic Geology, v. 63, p. 166–168.

Le Bas, M.J., Le Maitre, R.W., Streckeisen, A., and Zanettin, B., 1986, A chemical classification of volcanic rocks based on the total alkali-silica diagram: Journal of Petrology, v. 27, p. 745–750.

Leach, B.E., 1999, Yanacocha district northeast project: Unpublished Minera Yanacocha S.R.L. map set, scale 1:5000, folio YD-12.

Llosa, F.T., Veliz, J.M., and Georgel, J.M.P., 1999, Los Porfidos Au-Cu Minas Congas: Historia del descubrimiento y exploracion entre 1992–1998: Primer Volumen de Monografías de Yacimientos Minerales Peruanos, Volumen Luis Hochschild Plaut, ProExplo '99, Instituto de Ingenieros de Minas del Perú, p. 177–195.

Loayza-Tam, C.E., 2002, Geologic study of the Cerro Yanacocha gold-silver deposit, Yanacocha district, northern Peru: Unpublished master's thesis, Reno, Nevada, University of Nevada, Reno, 94 p.

Longo, A.A., 2000, The San Jose-Carachugo-Chaquicocha gold trend, Yanacocha District, northern Peru, *in* Cluer, J.K., Price, J.G., Struhsacker, E.M., Hardyman, R.F., and Morris, C.L., eds., Geology and Ore Deposits 2000, The Great Basin and Beyond: Geological Society of Nevada Symposium Proceedings, Reno/Sparks, Nevada, May 15–18, 2000, v. 1, p. 201–220.

Longo, A.A., 2005, Evolution of volcanism and hydrothermal activity in the Yanacocha mining district, northern Perú: Unpublished Ph.D. dissertation, Corvallis, Oregon State University, 469 p.

Longo, A.A., and Teal, L.B., 2005, A summary of the volcanic stratigraphy and the geochronology of magmatism and hydrothermal activity in the Yanacocha gold district, northern Peru, *in* Rhoden, H.N., Steininger, R.C., and Vikre, P.G., eds., Geological Society of Nevada Symposium 2005; Window to the World: Reno, Nevada, May 2005, Proceedings, v. 2, p. 797–808.

Lorenz, V., 1986, On the growth of maars and diatremes and its relevance to the formation of tuff rings: Bulletin of Volcanology, v. 48, p. 265–274.

MacFarlane, A.W., Prol-Ledesma, R.M., and Conrad, M.E., 1994, Isotope and fluid inclusion studies of geologicical and hydrothermal processes, northern Peru: International Geology Review, v. 36, p. 645–677.

Mallette, P.M., Rojas, R.E., and Guttierrez, A.R., 2004, Geology, mineralization, and genesis of the La Quinua gold deposit, Yanacocha district, northern Peru: Society of Economic Geology, Special Publication 11, p. 301–312.

Marsh, T.M., Einaudi, M.T., and McWilliams, M., 1997, $^{40}Ar/^{39}Ar$ geochronology of the Cu-Au and Au-Ag mineralization in the Portrerillos District, Chile: Economic Geology, v. 92, p. 784–806.

McDougall, I., and Harrison, T. M., 1999, Geochronology and thermochronology by the $^{40}Ar/^{39}Ar$ method: Oxford University Press, New York, 269 p.

McKee E.H., and Noble, D.C., 1982, Miocene volcanism and deformation in the western Cordillera and high plateaus of south-central Peru: Geological Society of America Bulletin, v. 93, p. 657–662.
Megard F., 1984, The Andean orogenic period and its major structures in central and northern Peru: Journal of the Geological Society [London], v. 141, p. 893–900.
Melgar, J., Quispe, J., Rutti, M., Teal, L., 2000, La Sorpresa project: Unpublished Minera Yanacocha S.R.L. map set, scale 1:2000, folio SOR-02.
Moore, S., 2002, Sacsha Breccia: Welded pyroclastic fall deposit: Unpublished Minera Yanacocha S.R.L. memorandum, October 13, p. 1–8.
Myers, S., 1997, Carachugo project: Unpublished Minera Yanacocha S.R.L. map set, scale 1:2000, folio CHG-01.
Myers, S., and Williams, C., 2000, Geologic evolution of the Yanacocha district high sulfidation gold system, northern Peru [abs.], *in* Cluer, J.K., Price, J.G., Struhsacker, E.M., Hardyman, R.F., and Morris, C.L., eds., Geology and Ore Deposits 2000, The Great Basin and Beyond: Geological Society of Nevada Symposium Proceedings, Reno/Sparks, Nevada, May 15–18, 2000, v. 1, p. 235.
Myers, S., Changanaqui, M., Bond, R., Aguirre, C., and Mallette, P., 1997, Geology of the Carachugo deposits, Yanacocha district, *in* Vidal, C., Noble, D., Harvey, B., eds., Guidebook of the Yanacocha district, Cajamarca Province, Peru: IX Peruvian Geological Congress Fieldtrip, August 3–10, p. 26–38.
Noble, D.C., McKee, E.H., Farrar, E., and Petersen, U., 1974, Episodic Cenozoic volcanism and tectonism in the Andes of Peru: Earth and Planetary Science Letters, v. 21, p. 213–220.
Noble, D.C., McKee, E.H., Mourier, T., and Megard, F., 1990, Cenozoic stratigraphy, magmatic activity, compressive deformation, and uplift in northern Peru: Geological Society of America Bulletin, v. 102, no. 8, p. 1105–1113.
Noble, D.C. and McKee, E.H., 1999, The Miocene Belt of Central and Northern Perú: Society of Economic Geologists Special Publication 7, p. 155–193.
Noble, D.C., Vidal, C.E., Perelló, J., and Rodríguez, O.P., 2004, Space-time relationships of some porphyry Cu-Au, epithermal Au, and other magmatic-related mineral deposits in northern Perú: Society of Economic Geology, Special Publication 11, p. 313–318.
Petford, N., and Atherton, M.P., 1995, Cretaceous-Tertiary volcanism and syn-subduction crustal extension in northern central Peru: Geological Society [London] Special Publication 81, p. 233–248.
Pinto, R.M., 2002, Transición de un sistema de alta sulfuración a un sistema porfiritico de alto nivel en Kupfertal, Distrito Minero de Yanacocha, Cajamarca, Perú: Unpublished thesis, Ingeniero Geólogo de Perú, Universidad Nacional Mayor de San Marcos, 46 p.
Quiroz, A., 1997, El corridor estructural Chicama-Yanacocha y su importancia en la metalogenia del norte del Perú, *in* Macharé, J., Cánepa, C., and Injoque, J., eds., IX Congreso Peruano de Geología, Resúmenes Extendidos [Extended Abstracts], Sociedad Geológica del Perú, Vol. Especial 1 [Special Publication 1), Lima, p. 149–154.
Ransome, F.L., 1907, The association of alunite with gold in the Goldfield district, Nevada: Economic Geology, v. 2, p. 667–692.
——1909, Geology and ore deposits of Goldfield, Nevada: U.S. Geological Survey, Professional Paper 66, 258 p.
Renne, P.R., Swisher, C.C., Deino, A.L., Karner, D.B., Owens, T.L., and DePaulo, D.J., 1998, Intercalibration of standards, absolute ages and uncertainties in $^{40}Ar/^{39}Ar$ dating: Chemical Geology, v. 145, p. 117–152.
Reyes, A.G., 1990, Petrology of Philippine geothermal systems and the application of alteration mineralogy to their assessment: Journal of Volcanology and Geothermal Research, v. 43, p. 279–309.
Reyes, L.R., 1980, Geología de los Cuadrángulos de Cajamarca, San Marcos y Cajabamba: Instituto Geológico Minero y Metalúrgico, Lima, Boletín 31 series A, 71 p.
Rota, J., 1997, Carachugo geologic model March 97: Unpublished Newmont Mining Corporation company report, 10 June, 55 p.
——1998, Yanacocha geologic model: Unpublished Newmont Mining Corporation company report, 5 May, 63 p.
Rye, R.O, Bethke, P.M., and Wasserman, M.D., 1992, The stable isoptope geochemistry of acid sulfate alteration: Economic Geology, v. 87, p. 225–262.
Siebe, C., Rodriguez-Lara, V., Schaaf, P., Abrams, M., 2004, Radiocarbon ages of Holocene Pelado, Guespalapa, and Chichinautzin scoria cones, south of Mexico city: Implications for archaeology and future hazards: Bulletin of Volcanology, v. 66, p. 203-225.
Sillitoe, R.H., 1985, Ore-related breccias in volcanoplutonic arcs: Economic Geology, v. 80, p. 1467–1514.
——1993, Epithermal models: Genetic types, geometrical controls and shallow features, in Kirkham, R.V., et al, eds., Mineral Deposit Modelling: Geological Association of Canada Special Paper 40, p.403–417.
——1999, Styles of high-sulphidation gold, silver and copper mineralisation in porphyry and epithermal environments: PacRim '99 Congress, Bali, Indonesia, October 10–13, Australian Institute of Mining and Metallurgy, Proceedings, p. 29–44.
Simmons, S.F., White, N.C., and John, D.A., 2005, Geological characteristics of epithermal precious and base metal deposits: Economic Geology 100th Anniversary Volume, p. 485–522.
Simon, A.C., Frank, M.R., Pettke, T., Candela, P.A., Piccoli, P.M., and Heinrich, C.A., 2005, Gold partitioning in vapor-brine-melt systems: Geochimica et Cosmochimica Acta, v. 69, p. 3321–3335.
Simon, A.C., Pettke, T., Candela, P.A., Piccoli, P.M., and Heinrich, C.A., 2006, Copper partitioning at magmatic conditions: Geochimica et Cosmochimica Acta, v. 70, p. 5583–5600.
Singer, B.S., Dungan, M.A., and Layne, G.D., 1995, Textures and Sr, Ba, Mg, Fe, K, and Ti compositional profiles in volcanic plagioclase: clues to the dynamics of calc-alkaline magma chambers: American Mineralogist, v. 80, p. 776–798.
Stavast, W.J.A., Butler, R.F., Seedorff, E., Barton, M.D., and Ferguson, C.A., 2008, Tertiary tilting and dismemberment of the Laramide arc and related hydrothermal systems, Sierrita Mountains, Arizona: Economic Geology, v. 103, pp. 629–636.
Steven, T.A. and Ratté, J.C., 1960, Geology and ore deposits of the Summitville district, San Juan Mountains, Colorado: U.S. Geological Survey Professional Paper, no. 958, p. 1–9.
Stoffregen, R.E., 1987, Genesis of acid-sulfate alteration and Au-Cu-Ag mineralization at Summitville: Economic Geology, v. 82, p. 1575–1591.
Sun, S.S., and McDonough, W.F., 1989, Chemical and isotopic systematics of ocean basalts: implications for mantle composition and process: Geological Society [London], Special Publication, v. 42, p. 313–345.
Teal, L., Harvey, B., Williams, C., and Goldie, M., 2002, Geologic overview of the Yanacocha district, northern Peru [extended abst.], *in* Marsh, E.E., Goldfarb, R.J., and Day, W.C., eds., Global exploration 2002: Integrated methods for discovery: Denver, Colorado, Society of Economic Geologists, Abstracts, p. 43–44.
Teal, L.B. and Benavides, A., 2010, History and geologic overview of the Yanacocha mining district, Cajamarca, Peru: Economic Geology, p. 1173–1190.
Turner, S.J., 1997, The Yanacocha epithermal gold deposits, northern Peru: high-sulfidation mineralization in a flow-dome setting: Unpublished Ph.D. thesis, Golden, Colorado, Colorado School of Mines, 341 p.
Turner, S.J., 1999, Settings and styles of high-sulfidation gold deposits in the Cajamarca region, northern Peru: PacRim '99, Bali, Indonesia, October 10–13, Australian Institute of Mining and Metallurgy, Proceedings, p. 461–468.
Velasco, C., Loayza, C., Rutti, M., Bartra, R., Escalante, J., and Longo, A., 2000, The Chaquicocha Project: Surface and subsurface geology, geochemistry, and diamond drill core data from 1997-2000: Unpublished Minera Yanacocha S.R.L. map set, scale 1:2000, folios CHQ-03, CHQ-08, and QUE-01.
Weill, D.F., and Drake, M.J., 1973, Europium anomaly in plagioclase feldspar: experimental results and semiquantitative model: Science, v. 180, no. 4090, p. 1059–1060.
Williams, C.L., and Vicuña, E.C., 2000, La Quinua deposit, Peru, *in* Cluer, J.K., Price, J.G., Struhsacker, E.M., Hardyman, R.F., and Morris, C.L., eds., Geology and Ore Deposits 2000, The Great Basin and Beyond, Geological Society of Nevada Symposium Proceedings, Reno/Sparks, Nevada, May 15–18, 2000, v. 2, p. 1173–1176.
Wilson, J., 1984, Geología de los Cuadrángulos de Jayanca, Incahuasi, Cutervo, Chiclayo, Chongoyape, Chota, Celendín, Pacasmayo y Chepeen: Instituto Geológico Minero y Metalúrgico, Lima, Boletín 38 serie A, 104 p.
Wones, D.R., 1989, Significance of the assemblage titanite+magnetite+quartz in granitic rocks: American Mineralogist, v. 74, p. 744–749.

List of Illustrations and Tables

Plate I. Geologic map of the Yanacocha district. The inset Index Map of

Acknowledgments notes contributions to areas 1-8 are by the following: [1]Bartra et al. (1999), [2]Barreda and Edwards (2000), [3]Klein et al. (1999), [4]Barreda et al. (2000), [4]Velasco et al. (2000), [5]Escalante and Longo (2000), [6]Myers (1997), [7]Rota (1998), [8]Melgar et al. (2000), [9]Escalante et al. (2000).

APPENDIX 1
Geochronology

Analytical methods and criteria for interpretation of crystallization ages

The $^{40}Ar/^{39}Ar$ ages reported in this study were determined in the noble gas mass spectrometry laboratory of the College of Oceanic and Atmospheric Sciences at Oregon State University. Samples, either whole-rock disks or mineral separates wrapped in Cu foil and loaded in evacuated silica vials, were irradiated for 6 hours in the Oregon State University TRIGA Reactor. The neutron flux (J) was monitored with Fish Creek Tuff biotite standard (FCT-3), with an age of 28.03 ± 0.12 Ma (Renne et al., 1998), placed at regular intervals in the silica tubes, and the error in J is generally within 0.5%.

Samples were heated incrementally using a 10W CO_2 laser (mineral separates) or a double vacuum resistance furnace with thermocouple temperature control (whole rocks and mineral separates). The isotopic composition of Ar released at each step was measured using a MAP-215/50 mass spectrometer in peak-hopping mode. Step ages are displayed as age spectra and isochrons (App. Figs. A1–A4). A plateau age is the mean of three or more contiguous and concordant step ages, weighted by the inverse of the variance (McDougall and Harrison, 1999). The mean square of weighted deviations (MSWD) is an F-statistic that compares the variability of step ages about the mean with the individual step variances. A value less than about 2.5 indicates that the step ages are true samples of a common plateau age. We also calculated an isochron age from the slope of the linear regression of $^{40}Ar/^{36}Ar$ vs. $^{39}Ar/^{36}Ar$ compositions for the same steps that comprise the plateau age. This calculation makes no assumption about the initial $^{40}Ar/^{36}Ar$ composition of the rock or mineral, and so can be used to assess the significance of non-atmospheric initial Ar. From samples for which plateau and isochron ages are the same, within analytical uncertainty, and for which the $^{40}Ar/^{36}Ar$ isochron intercept is indistinguishable from the atmospheric value (295.5), we conclude that the plateau age is a robust (statistically significant) estimate of the crystallization age (Dalyrymple and

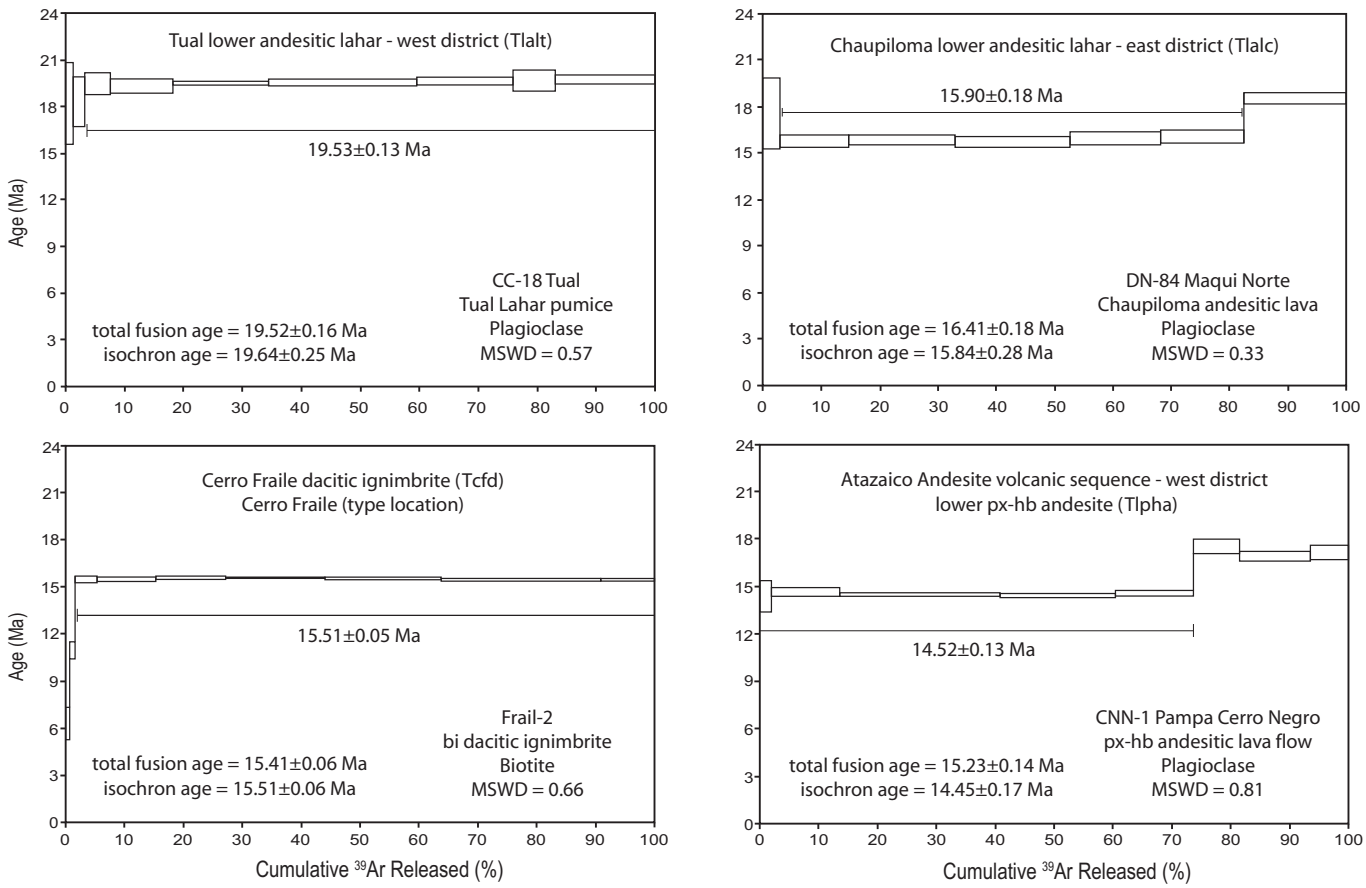

FIG. A1. $^{40}Ar/^{39}Ar$ age spectra for representative samples of the Calipuy Group volcanics and the Atazaico Andesite from the lower Yanacocha Volcanics in the western district. Each heating step is represented by a horizontal rectangle whose height is ± 2σ uncertainty of the step age. Each spectrum yields a robust weighted mean plateau age with a ±2σ uncertainty given by the standard error of the mean. Other data reported includes the total fusion and isochron ages, the mean standard weighted deviate (MSWD), and the sample type as whole rock or mineral. (A) CC-18, plagioclase of pumice from a Tual andesitic lahar; (B) DN-84, plagioclase, Chaupiloma andesitic lava flow intercalated between lahars; (C) Frail-2, biotite, Cerro Fraile dacitic ignimbrite, type locality; (D) CNN-1, plagioclase, Atazaico Andesitic lava flow north of Cerro Negro.

Lanphere, 1974; Duncan et al., 1997; McDougall and Harrison, 1999).

The $^{40}Ar/^{39}Ar$ ages were calculated with ArArCALC v2.2 software from Koppers (2002) and the ages are reported within the limits of a 2σ error (95% confidence interval). The mass spectrometer was scanned through each isotope mass of argon (^{36}Ar, ^{37}Ar, ^{38}Ar, ^{39}Ar and ^{40}Ar) in five passes, and a regression curve fitted to each mass to enable calculation of isotopic ratios at the inlet time of the argon gas.

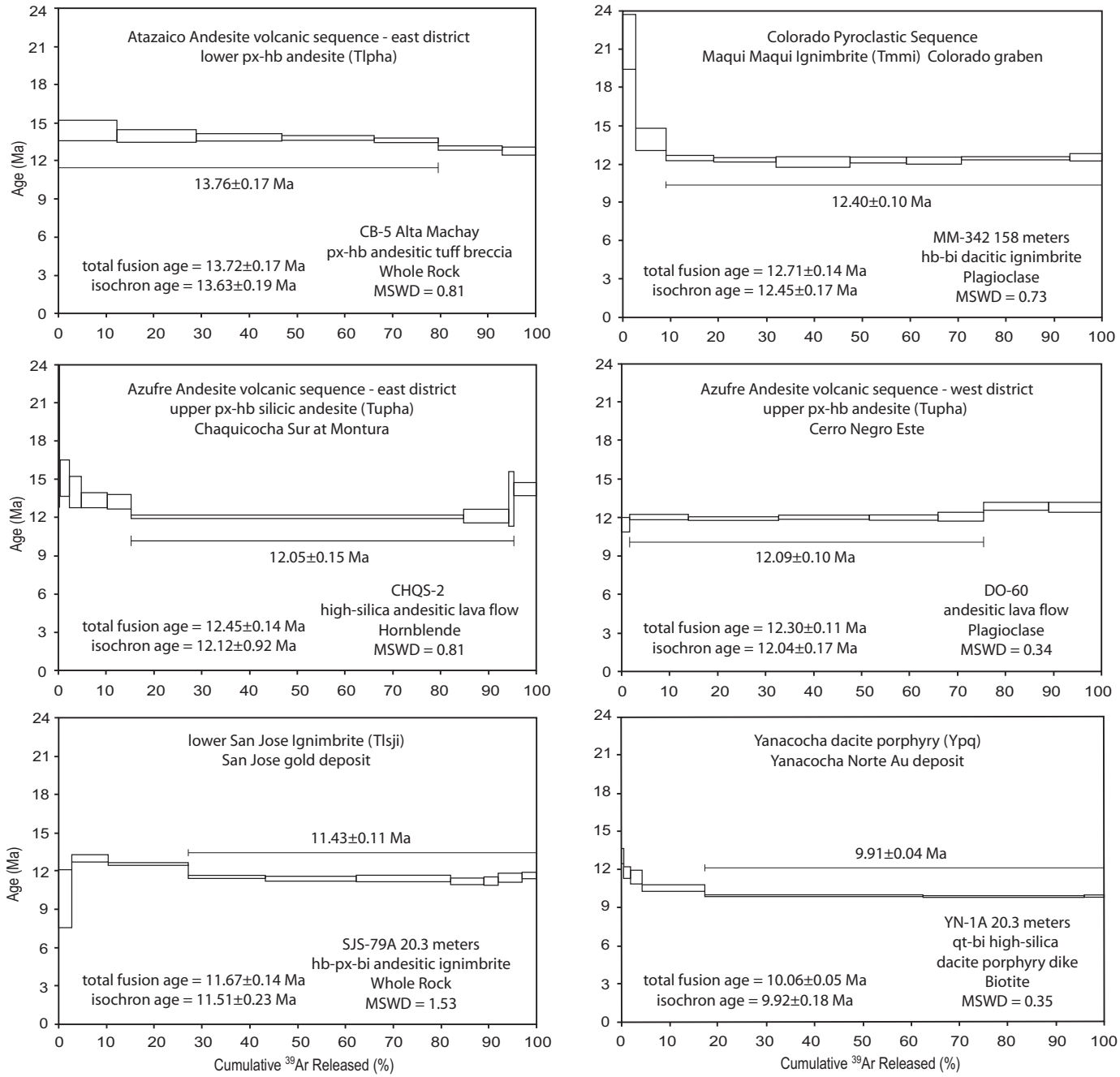

FIG. A2. $^{40}Ar/^{39}Ar$ age spectra for samples, upper part of the Yanacocha Volcanics. Each spectra yields a robust weighted mean plateau age. (A) CB-5, whole rock, Atazaico andesitic tuff-breccia from the eastern part of the district; (B) MM-342, plagioclase, Maqui Maqui ignimbrite from the hanging wall of the Maqui Maqui gold deposit; (C) CHQS-2, hornblende, Azufre andesitic lava flow at Chaquicocha Sur; (D) DO-60, plagioclase, Azufre andesitic lava flow at Cerro Negro Este; (E) SJS-79A at 20.3 m, whole rock, lower San Jose Ignimbrite atop the San Jose gold deposit; (F) YN-1A at 20.3 m, biotite, Yanacocha dacitic porphyry from Cerro Yanacocha.

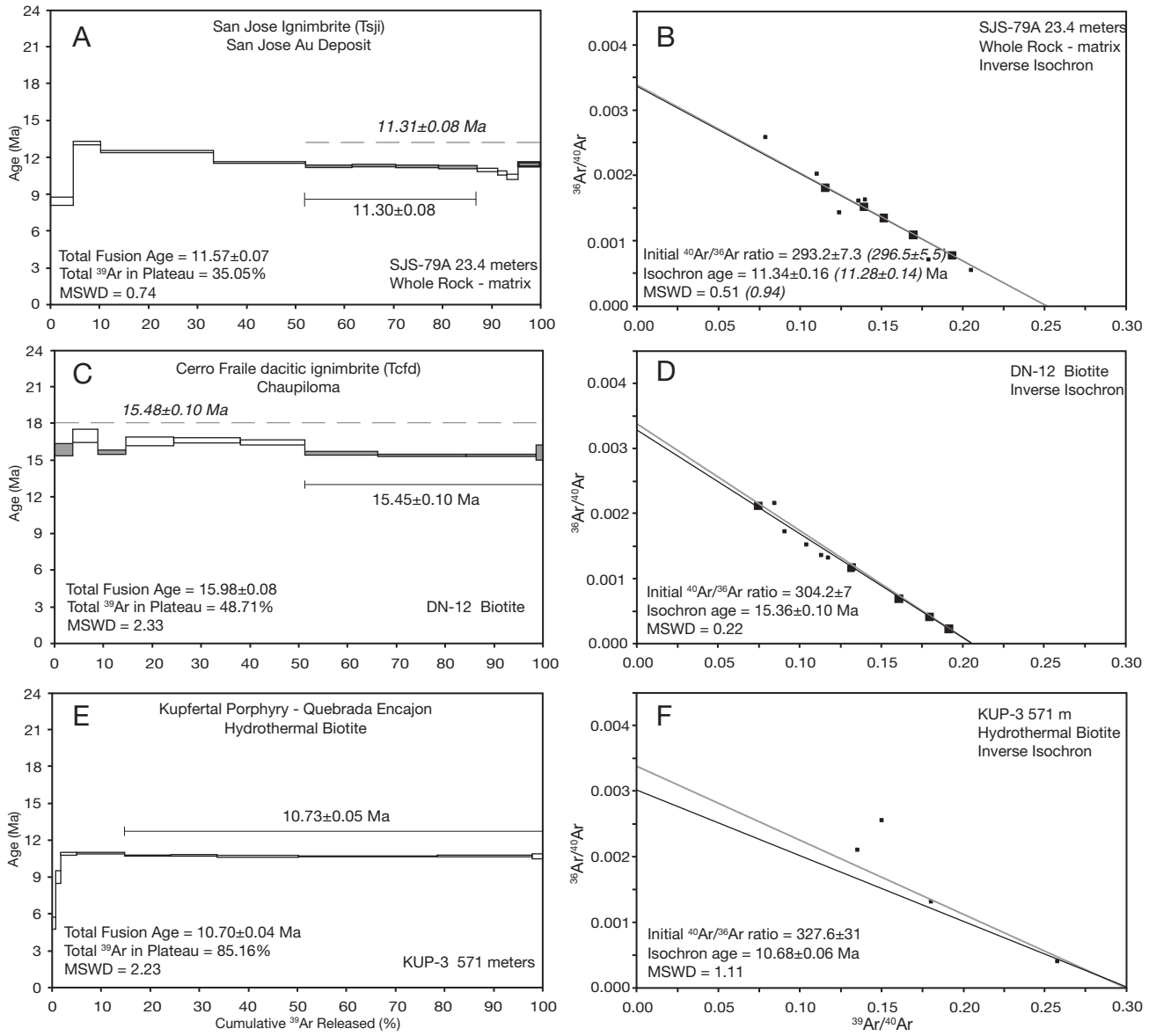

FIG. A3. $^{40}Ar/^{39}Ar$ age spectra and inverse isochron diagrams for three samples that do not meet all the criteria for a robust age interpretation. The age spectra for SJS-79A 23.4 wr (A) and DN-12 biotite (C) are defined by less than 50 percent of the total $^{39}Ar_K$ released, but are concordant with their respective isochron ages (B, D). Both samples yield a robust isochron age that is accepted as the interpreted age for the sample. Additional heating steps (shaded gray), separated by unrelated steps, are congruent with the plateau and bring the total $^{39}Ar_K$ released to 50 percent. A sample hydrothermal biotite (E) collected from the Kupfertal porphyry has an isochron (F) that yields a $^{40}Ar/^{39}Ar$ intercept that differs slightly from the 295.5 atmospheric value, and the robust weighted mean plateau age (E) is accepted as the interpreted age.

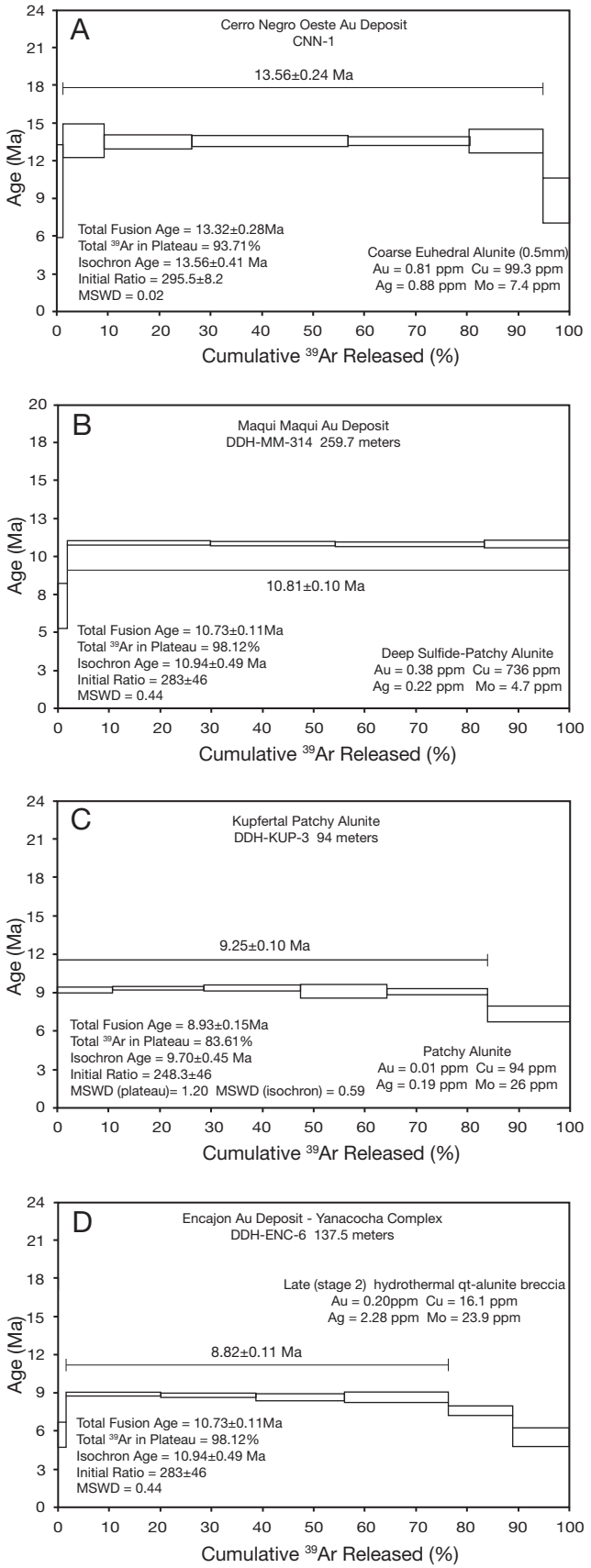

FIG. A4. Experimental $^{40}Ar/^{39}Ar$ data plotted as age spectra for select alunite samples across the Yanacocha district. Each spectra yields a robust weighted mean plateau age, similar to spectra in Figures A1 and A2. (A) CNN-1, Cerro Negro Oeste gold deposit; (B) DDH-MM-314 at 259.7 m, Maqui Maqui gold deposit; (C) DDH-KUP-3 at 94 m, Kupfertal Au (Cu) porphyry; (D) DDH-ENC-6 at 137.5 m, Encajon gold deposit. The gold assays are listed in Table A3.

TABLE A1. Sources of Ages for Late Cenozoic Igneous Rocks and Hydrothermal Minerals in the Yanacocha District, Northern Peru (numbered sources correspond to Fig. 2)

Location	Age (Ma)	Reference
Ages of igneous rocks on map (Fig. 2)		
Llama Formation	54.8–44.2	Noble et al., 1990[1]
Michiquillay	46.4	Laughlin et al., 1968
Picota Diorite	43.6	Laughlin et al., 1968
	42.03±0.46	T. Thompson, writ. commun., 2002[9]
Huambos Formation	39 to 35	Noble et al., 1990[1]
Chala Sequence	23.2	Noble et al., 1990[1]
Michiquillay	20.02±0.15	Noble et al., 2004 (late intramineral intrusion)
	19.77±0.05	Davies and Williams, 2005[13]
Misacocha	20.8	Llosa et al., 1999[10]
El Galeno	17.5±0.3	Davies and Williams, 2005[13]
	16.53±0.13	
Minas Congas district	17.3–15.9	A. Chauvet and L. Bailly, writ. commun., 2001
Amaro stock	17.3	T. Thompson, writ. commun., 2002[9]
Cerro Corona	14.4	James, 1998[3]
Cerro Hualgayoc	14.3	Borredon, 1992[5]
	9.1	Macfarlane et al., 1994[4]
Yanacocha	15.8	Turner, 1997; upper Llama Fm.
	11.4	Noble et al., 1990; Otuzco tuff
	12.3–8.4	Turner, 1997
	12.4–8.6	Chiaradia et al., 2009; four porphyritic intrusions
	19.5–8.4	Longo, 2005; this study[8]
Tantahuatay	13.2–8.3	D. Prihar, writ. commun., 1998[6] Noble and McKee, 1999[7]
La Zanja	11.91±0.06	Noble et al., 2004[11]
Negritos-like rhyolitic ignimbrite	8.2	Sample 90-13; Noble et al., 1990
Ages of ores for deposits on map (Fig. 2)		
Michiquillay	20.6	Laughlin et al., 1968
	20.1	D.C. Noble, pers. commun., 2002
Minas Congas		
Cerro Cocañes	16.06±0.11	Gustafson et al., 2004[12]
Perol	15.8±0.09	Gustafson et al., 2004[12]
Chalhuagón	15.58±0.12	Gustafson et al., 2004[12]
	15.35±0.12	D.C. Noble, pers. commun., 2002
La Zanja	15.61±0.12	Noble et al., 2004[11]
La Granja	13.8±0.4	Diaz et al., 1997[2]
Cerro Corona	13.5	Macfarlane et al., 1994[4]
Tantahuatay	13.3 – 11.0	D. Prihar, writ. commun., 1998[6]
Yanacocha	11.5–10.9	Turner, 1997
Yanacocha	13.6 – 8.2	Longo, 2005; This study

TABLE A2. Summary of $^{40}Ar/^{39}Ar$ Age Determinations

Experiment no.	Name and location	Material	Total fusion age (Ma) ±2σ	Plateau age (Ma)				Isochron age (Ma)			Ma preferred age ±2σ
				Plateau age ±2σ	No. of steps Plateau/total	%^{39}Ar in plateau	MSWD	Isochron age ±2σ	Initial $^{40}Ar/^{36}Ar$ ±2σ	MSWD	
Calipuy Group Volcanics											
Tual-Chaupiloma Lahar Sequence											
02C951	CC-18 Tlalt Tual	Plagioclase	19.52±0.16	**19.53±0.13**	7/9	96.69	0.57	19.64±0.25	289±33	0.56	19.53±0.13
03C3724	DN-84 Tlalc Maqui Maqui Norte	Plagioclase	16.41±0.18	**15.90±0.18**	5/7	79.59	0.33	15.84±0.28	299±13	0.34	15.90±0.18
02C1238	DE-18 Tlalc C° Collotan	Hornblende	15.12±0.25	**15.41±0.36**	4/10	51.76	0.72	15.02±0.76	300±7	0.34	15.41±0.36
				12.24±0.46	4/10	34.35	2.84	11.76±2.51	302±38	4.00	
Cerro Fraile Pyroclastics											
02C1112	Frail-2 Cerro Fraile	Biotite	15.41±0.06	**15.51±0.05**	7/10	98.33	0.66	15.51±0.06	294±4	0.71	15.51±0.05
02C1191	CB-35 Combayo	Biotite	15.51±0.06	**15.50±0.06**	3/10	82.48	0.14	15.51±0.14	293±46	0.27	15.50±0.06
03C2722	DN-12	Biotite	15.98±0.08	15.45±0.10	5/11	48.71	2.33	15.36±0.10	304±7	0.22	No age
	Error plateau	*Case 2*		*15.48±0.10*	*7/11*	*58.27*	*2.65*	15.38±0.09	303±4	0.47	
	Chaupiloma										
03C3672	DN-12 Chaupiloma	Plagioclase	15.37±0.16	**15.18±0.14**	7/8	98.22	0.97	15.02±0.22	305±11	0.46	15.18±0.14
03C3654	DN-71 Maqui Norte	Biotite	15.06±0.07	**15.15±0.06**	7/9	93.53	1.12	15.08±0.09	309±14	0.54	15.15±0.06
Atazaico Andesite											
Western district											
03C2388	CNN-1 Lava Pampa Cerro Negro	Plagioclase	15.23±0.14	**14.52±0.13**	5/8	73.57	0.81	14.45±0.17	311±25	0.50	14.52±0.13
03C2316	DO-43 Lava Quilish	Plagioclase	14.79±0.14	**14.27±0.16**	5/8	68.16	1.67	14.09±0.21	315±18	0.48	14.27±0.16
03C2494	C° Atazaico Lava	Plagioclase	14.87±0.15	**14.21±0.16**	6/7	69.31	1.30	14.10±0.20	313±29	0.88	14.21±0.16
03C3530	CR-4 Dome Cerro Regalado	Plagioclase	13.87±0.09	**13.85±0.09**	7/8	99.29	0.28	13.83±0.13	302±30	0.25	13.85±0.09
Eastern District											
02C858	CB-5 Tuff Alta Machay	Whole rock	13.72±0.17	**13.76±0.17**	5/7	79.55	1.61	13.63±0.19	300±4	0.60	13.76±0.17
02C923	AZU-1 Lava Elita-Azufre	Plagioclase	13.36±0.08	**13.31±0.08**	6/9	85.19	1.18	13.21±0.18	311±25	0.91	13.31±0.08
Colorado Pyroclastics											
02C1227	DN-30 Cori Coshpa Ign Hornamo	Biotite	12.59±0.05	**12.63±0.05**	6/10	96.66	0.57	12.59±0.07	303±13	0.38	12.63±0.05
02C960	DN-7 Maqui Maqui Ign Barranco	Plagioclase	12.56±0.11	**12.49±0.08**	7/9	97.30	1.13	12.50±0.10	295±5	1.25	12.49±0.08
03C2333	MM-342 158m Maqui Maqui Ign Maqui Maqui	Plagioclase	12.71±0.14	**12.40±0.10**	7/9	90.95	0.73	12.45±0.17	293±7	0.77	12.40±0.10

TABLE A2. *(Cont.)*

Experiment no.	Name and location	Material	Total fusion age (Ma) ±2σ	Plateau age (Ma)				Isochron age (Ma)			Ma preferred age ±2σ
				Plateau age ±2σ	No. of steps Plateau/total	%^{39}Ar in plateau	MSWD	Isochron age ±2σ	Initial ^{40}Ar/^{36}Ar ±2σ	MSWD	
Colorado Pyroclastics *(continued)*											
03C3641	DN-52 Maqui Maqui Ign Maqui Norte	Plagioclase	35.86±0.19	30.62±11.61	4/7	61.44	>5000	**13.12±3.41**	1904±278	9.02	13.12±3.41
Yanacocha Porphyries (Yp and Cp)											
03C3547	YS-370 46-48m Lava flow CerroYanacocha	Plagioclase	12.75±0.13	**12.39±0.12**	5/8	68.10	1.02	12.33±0.14	303±10	0.65	12.39±0.12
			12.50±0.13	12.05±0.12	5/8	68.93	0.28	12.01±0.14	299±9	0.17	
03C2616	DN-77 Maqui Norte Int	Hornblende	12.19±0.11	**12.13±0.10**	5/8	95.78	0.94	12.09±0.17	300±18	0.82	12.13±0.10
03C2704	SLT-2 Dike Corimayo-Pabellon	Hornblende	11.95±0.13	**11.90±0.11**	8/8	100.00	0.63	11.84±0.13	303±11	0.46	11.90±0.11
Azufre Andesite											
Western District											
03C3585	DO-60 Cerro Negro Este	Plagioclase	12.30±0.11	**12.09±0.10**	5/8	73.81	0.34	12.04±0.17	306±31	0.25	12.09±0.10
03C2370	COR-7 178 m Corimayo Lava	Plagioclase	12.16±0.07	**11.91±0.08**	6/8	78.11	1.24	11.86±0.10	302±8	0.84	11.91±0.08
Eastern District											
02C1087	YSBD Black Dike Yanacocha Sur	Whole rock	12.11±0.08	**12.09±0.08**	4/7	84.04	0.51	12.04±0.54	299±32	0.74	12.09±0.08
02C969	CHQS-2 Lava Chaq Sur	Hornblende	12.45±0.14	**12.05±0.15**	3/9	80.20	0.81	12.12±0.92	291±54	0.88	12.05±0.15
03C3610	DN-83 Tuff Colorado Graben	Plagioclase	12.54±0.13	**12.05±0.11**	5/8	61.26	1.01	12.01±0.16	300±13	1.20	12.05±0.11
03C2526	CB-65 Machay Dome	Plagioclase	12.52±0.10	**12.01±0.10**	6/8	66.15	1.25	11.83±0.24	303±10	0.88	12.01±0.10
02C932	AZU-2 Ocucho Dome	Plagioclase	11.71±0.08	**11.68±0.07**	6/8	94.71	0.97	11.65±0.07	302±6	0.16	11.68±0.07
San Jose Domes											
03C2297	DE-2 Ocucho Dome Sur	Plagioclase	11.73±0.09	**11.36±0.09**	5/8	75.98	1.13	11.30±0.11	316±20	0.00	11.36±0.09
03C3576	CHQS-1 Chaquicocha Sur Dome - SJI	Plagioclase	11.30±0.09	**11.28±0.09**	6/8	89.59	1.14	11.22±0.11	298±21	0.54	11.28±0.09
03C3561	CB-3 Alta Machay Dome - SJI	Plagioclase	11.39±0.08	**11.23±0.07**	4/8	71.72	1.09	11.15±0.13	315±24	0.29	11.23±0.07

TABLE A2. *(Cont.)*

Experiment no.	Name and location	Material	Total fusion age (Ma) ±2σ	Plateau age (Ma)				Isochron age (Ma)			Ma preferred age ±2σ
				Plateau age ±2σ	No. of steps Plateau/total	%^{39}Ar in plateau	MSWD	Isochron age ±2σ	Initial ^{40}Ar/^{36}Ar ±2σ	MSWD	
San Jose Ignimbrite											
Lower Member											
03C2405	CB-44 Arnacocha	Plagioclase	11.86±0.09	**11.54±0.09**	5/8	72.53	0.86	11.51±0.12	298±6	0.95	11.54±0.09
03C3624	VC-4 Basal SJI Combayo	Plagioclase	12.66±0.42	**11.53±0.13**	4/8	60.60	0.44	11.47±0.22	301±18	0.45	11.53±0.13
03C2423	CB-56 Que Azufre Combayo	Plagioclase	11.55±0.06	**11.43±0.06**	6/9	78.69	1.54	11.37±0.10	307±16	1.22	11.43±0.06
02C1009	SJS-79A20.3m San Jose	Whole rock	11.67±0.12	**11.43±0.11**	7/10	72.81	1.50	11.51±0.23	294±4	1.62	11.43±0.11
02C1020	SJS-79A23.4m San Jose	Whole rock	11.57±0.07	11.30±0.08	4/12	35.05	0.48	**11.34±0.16**	293±7	0.51	11.34±0.16
			11.57±0.07	11.31±0.08	5/12	39.60	0.74	11.28±0.14	297±6	0.94	
Middle Member											
03C2580	CB-74 Ign contact to Machay dome	Plagioclase	11.58±0.11	**11.30±0.09**	5/8	73.41	0.81	11.14±0.24	319±33	0.28	11.30±0.09
02C896	CB-38 La Masma Ign	Plagioclase	11.45±0.07	**11.27±0.07**	5/9	59.57	0.83	11.15±0.19	345±76	0.30	
02C1249	6 km S of Paquerumi 4 km S of DE-36	Hornblende	11.19±0.17	**11.29±0.15**	5/9	97.88	0.24	11.29±0.44	296±18	0.36	11.29±0.15
03C3664	CB-59 Ventanillas Combayo	Plagioclase	11.27±0.09	**11.29±0.08**	7/7	100.00	0.74	11.39±0.17	269±38	0.52	11.29±0.08
02C1180	RC-6 Rio Chonta	Hornblende	11.51±0.27	**11.28±0.22**	4/11	95.70	0.52	11.26±0.40	296±7	0.46	11.28±0.22
03C2476	VC-1 Combayo	Plagioclase	11.55±0.07	**11.22±0.08**	5/8	71.78	0.68	11.22±0.12	326±137	0.49	11.22±0.08
Upper Member-spatter ignimbrite											
02C1098	BS-3 Sacsha Breccia	Hornblende	11.46±0.12	11.50±0.09	9/12	99.27	0.73	**11.30±0.25**	315±23	0.40	11.30±0.25
03C2598	DE-36 Spatter Ign 2 km SE of Paquerumi	Plagioclase	11.33±0.07	**11.25±0.07**	6/8	80.70	0.49	11.23±0.11	302±57	0.52	11.25±0.07
03C3594	SJS-78A 5.0m San Jose	Plagioclase	11.41±0.09	**11.24±0.10**	6/8	93.52	1.57	11.11±0.14	318±21	0.70	11.24±0.10
Coriwachay Dacite domes and intrusions, and Negritos ignimbrite											
02C1170	COR-1 Corimayo Dome	Biotite	10.74±0.04	**10.78±0.05**	6/10	97.63	1.63	10.74±0.05	303±6	0.34	10.78±0.05
02C1216	YN-1A, Yqp dacite Cerro Yanacocha	Biotite	10.06±0.05	**9.91±0.04**	5/10	82.70	0.35	9.92±0.18	294±23	0.47	9.91±0.04
03C2279	NG-5 Negritos Ign	Sanidine	8.48±0.04	**8.43±0.04**	6/8	93.93	2.00	8.48±0.04	339±33	0.49	8.43±0.04

Preferred age, generally the weighted mean plateau age (plateau age), is shown in bold; as noted in the text, the isochron age is used in three cases; C° – Cerro, Ypq - Cerro Yanacocha dacitic porphyry, Ign – ignimbrite

TABLE A3. Summary of $^{40}Ar/^{39}Ar$ Age Determinations on Hypogene Alunite and Biotite

				Plateau age (Ma)				Isochron age (Ma)					
Experiment no.	Name and location	Material	Total fusion age (Ma) ±2σ	Plateau age ±2σ	No. of steps Plateau/ total	$\%^{39}Ar$ in plateau	MSWD	Isochron age ±2σ	Initial $^{40}Ar/^{36}Ar$ ±2σ	MSWD	Ma preferred age ±2σ	$\delta^{34}S_{cdt}$ (‰)	Au[1] (ppm)
Magmatic – hydrothermal alunite and biotite													
02C1300	CN-1 vuggy Cerro Negro Oeste	Coarse Alunite	13.32±0.28	**13.56±0.24**	5/10	93.71	0.02	13.56±0.41	295±8	0.02	13.56±0.24	20.8	0.81
03C2998	CQ-37 110m Quilish Norte	Alunite breccia	13.55±0.69	**13.48±0.64**	5/6	98.91	1.19	11.81±4.24	334±104	1.52	13.48±0.64	25.3	3.2
02C1358	QN-1 vuggy Quilish	Coarse Alunite	13.63±0.95	**12.64±0.61**	5/6	95.65	0.48	11.62±1.72	312±26	0.04	12.64±0.61	21.8	0.5
02C1373	CLL-1 dacite tuff Collotan Angelita	Alunite	11.18±1.49	**11.41±0.89**	5/7	92.50	0.36	11.58±1.94	295±4	0.47	11.41±0.89	18.8	0.03
02C1033	Baul-1 Cerro Baul	Alunite vein	11.03±0.14	**11.01±0.09**	3/4	99.95	0.20	11.02±0.11	295±10	0.40	11.01±0.09	17.9	0.01
02C1312	MM-314 259.7m Maqui Maqui	Alunite Patchy	10.73±0.11	**10.81±0.10**	4/6	98.12	0.44	10.94±0.49	283±46	0.52	10.81±0.10	11.4	0.38
03C3466	PNE-3 45-50m Punta Negra dacite	Alunite	9.94±0.29	**10.81±0.16**	8/9	83.09	0.81	11.16±0.76	282±28	0.85	10.81±0.16	16.8	0.06
03C3490	COR-39 213m Corimayo	Alunite vein	10.44±0.24	**10.76±0.17**	5/8	89.21	1.12	11.01±0.67	291±13	1.27	10.76±0.17	14.5	1.50
03C2976	CLL-2 Collotan Angelita	Alunite vein	9.88±0.14	10.75±0.16	5/7	47.10	0.43	**10.73±0.17**	297±10	0.48	10.73±0.17	19.0	0.02
03C2965	LBQ-40 441.2m Corimayo Sur	Alunite vein	10.43±0.14	**10.74±0.13**	4/8	52.47	0.80	11.28±0.71	258±49	0.22	10.74±0.13	16.5	0.005
03C3478	SJS-1 Yp bottom of San Jose Pit	Alunite	10.67±0.14	**10.73±0.10**	4/7	83.28	0.93	10.61±0.75	305±61	1.33	10.73±0.10	16.4	0.05
02C1363	CS-1 dacite tuff Chaquicocha Sur	Alunite breccia	10.59±0.79	**10.29±0.31**	5/5	100.00	0.25	10.25±0.33	297±3	0.13	10.29±0.31	15.9	0.01
02C1330	MM-46377 Cerro Sugares	Alunite vein	9.99±0.31	**10.26±0.22**	4/6	97.87	0.94	10.29±0.53	295±13	1.56	10.26±0.22	15.9	0.04
03C3512	TAP-169 382m Tapado	Alunite breccia	10.23±0.19	**10.24±0.14**	6/7	98.83	1.16	10.78±0.60	271±26	0.69	10.24±0.14	15.8	0.10
03C2954	SJS-3 andesite[2] lava San Jose Sur	Alunite	9.96±0.14	**9.95±0.14**	6/7	99.37	1.26	9.95±0.30	295±17	1.47	9.95±0.14	20	0.13
03C2987	KUP-3 94m Kupfertal[3]	Alunite patchy	8.93±0.15	**9.25±0.10**	5/7	83.61	1.20	9.70±0.45	248±46	0.59	9.25±0.10	15.9	0.01
02C1339	YN-105 88.7m YBX2 breccia Yanacocha Norte	Alunite breccia	9.18±0.32	**9.12±0.32**	4/4	100.00	0.96	9.18±2.85	287±273	0.21	9.12±0.32	16.0	0.11
03C3502	ENC-6 137.5m at Encajon	Alunite breccia	8.21±0.15	**8.82±0.11**	4/7	74.74	1.06	8.23±0.89	341±69	0.49	8.82±0.11	19.0	0.20
02C1368	YO-1 Encajon Co Yanacocha	Alunite breccia	8.51±0.48	**8.45±0.32**	5/6	99.46	0.37	8.41±0.36	296±3	0.46	8.45±0.32	18.5	0.36
03C2944	YS-219 111.8m Yanacocha	Alunite breccia	7.67±0.51	**8.22±0.46**	5/7	88.92	0.31	8.20±2.65	295±100	0.45	8.22±0.46	no data	0.23
02C1203	KUP-3 571m Kupfertal	Hydrothermal Biotite	10.70±0.04	**10.73±0.05**	6/11	85.16	2.23	10.68±0.06	328±31	1.11	10.73±0.05		0.50

Preferred age, generally the weighted mean plateau age (plateau age), is shown in bold; as noted in the text, the isochron age is used in one case

[1] Whole-rock Au assay

[2] SJS-3 was collected from an outcrop of quartz-alunite altered porphyritic rock on the high ridge near the San Jose Sur deposit; the sample is located ~210 m above the collar elevation of DDH KUP-3

[3] DDH KUP-3 (collar elev ~3800 m, azimuth N45E, –70º angle) contained both the deep Kupfertal hydrothermal biotite (~537 m vertical depth) and shallow patchy alunite (~88 m vertical depth); vertical depth estimates may be complicated by fault offsets; the patchy alunite sample KUP-3 94 m is from an elevation of 3712 m and is ~450 vertical meters above the Kupfertal hydrothermal biotite (KUP-3 571 m) from the same hole; KUP-3 571 m is from an elevation of ~3250 m; assay of the 0.5 m interval sampled for the biotite age is 0.5 g/t Au, 0.3% Cu